Novel Methodology Integrating Experimental ADME and Physicochemical Data for Rational Lead Optimization Using Selected Clinical Compounds

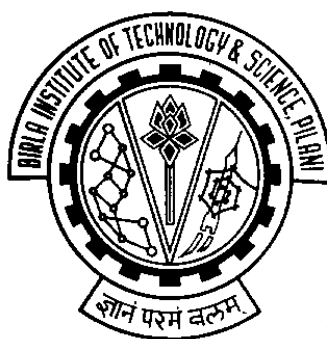## THESIS

Submitted in partial fulfillment

of the requirements for the degree of

DOCTOR OF PHILOSOPHY

by

BIJU BENJAMIN

Under the Supervision of

Dr. Nuggehally R. Srinivas

BIRLA INSTITUTE OF TECHNOLOGY AND SCIENCE PILANI (RAJASTHAN) INDIA
2012

BIRLA INSTITUTE OF TECHNOLOGY AND SCIENCE
PILANI (RAJASTHAN)

CERTIFICATE

This is to certify that the thesis entitled **'Novel Methodology Integrating Experimental ADME and Physicochemical Data for Rational Lead Optimization Using Selected Clinical Compounds'** which is submitted for award of Ph.D Degree of the Institute, embodies original work done by him under my supervision.

Signature in full of the Supervisor:

Name in capital block letters   : Dr. NUGGEHALLY R. SRINIVAS

Designation   : Chief Operating Officer,
Vanthys Pharmaceutical Development Pvt. Ltd.
96, Industrial Suburb, 2nd stage, Yeshwanthpur, Bangalore, 560022

Date:

ACKNOWLEDGEMENTS

BIJU BENJAMIN

ABSTRACT

The development of novel ways of investigating drug like properties of new chemical entities (NCEs) has been a topic of great interest for researchers. Identification of the ideal blend of properties that can result in druggability and efficacy, enabling a clinical proof concept (POC) is the most significant step in the translatability of discovery research programs. Besides the promising and/or differentiating biological dose-response relationship which is a must, the pharmacokinetic parameters play equally important role in influencing the therapeutic response or toxicity of an NCE. There are numerous techniques available to evaluate individual drug-like properties for a chemical entity. However, the profile of an NCE in a dynamic *in vivo* system, which influences its therapeutic or toxic effects, is a result of the composite functions of its various physicochemical and pharmacokinetic properties. This implies the need to understand the collective influence of various properties, and how variations can be made in them to alter the *in vivo* profile to enhance efficacy and reduce adverse effects. An early identification of these factors is vital to a successful and time efficient lead optimization process. Most of the efforts in this direction continue to rely on empirical quantitative structure activity relationship (QSAR) based approaches or focus on individual properties perceived to improve pharmacokinetic-pharmacodynamic (PK-PD) relationships, without a mechanistic evaluation of their combined effect. Therefore, there exists a research gap in the development of a new methodology to effectively integrate various physicochemical as well as absorption, distribution, metabolism and excretion (ADME) properties of an NCE and rationally choose relevant properties for optimization. This methodology should be able to link various compound properties mechanistically with the *in vivo* PK profile and identify critical properties contributing to a favorable pharmacokinetic profile with a suitable analytical approach. Physiological based pharmacokinetic (PBPK) models are of great interest in this context as they involve a mechanistic approach of integrating the individual NCE properties with physiological parameters to predict human *in vivo* profile, enabling comparison with a desired Target Product Profile (TPP). Additionally, with the infleunce of various properties on the *in vivo* profile of an NCE, it would require a multivariate analytical approach to assess the interplay of these properties and to identify critical properties for lead optimization. In the current research, described in this thesis, a retrospective analysis of 13 clinically proven drugs has been utilized to develop a methodology

and achieve these objectives. Various physicochemical and ADME screening data generated experimentally for these compounds have been integrated using PBPK models to predict key PK parameters of absorption, distribution and clearance. These parameters were utilized to simulate human oral concentration-time profile using a one compartment PK model and were compared with clinical reports for their accuracy. Further, a multivariate approach has been applied using partial least square (PLS) regression to identify the trends in the prediction data and unambiguously evaluate the key physicochemical and ADME properties that influence PK parameters along with their relative contribution allowing their prioritization in lead optimization. The utility of this approach was illustrated with hypothetical examples indicating the changes in concentration-time profiles due to variations made on individual properties as well as their correlation with efficacy. As an outcome of the new methodology developed from of this research, key physicochemical or ADME properties influencing the *in vivo* profile of an NCE can be rationally identified and rank ordered, which further can be optimized by modification of the chemical scaffold. The results of the various modifications on human PK profile can be prior assessed by generating ADME and physicochemical data of the modified series, which can be substituted in the PBPK models to simulate human PK profile. To improve the assessments, and understand variability that could be expected in clinic, evaluations of possible deviations from the predicted profile due to transporter interactions, induction, biliary secretion or entero-hepatic recycling, metabolic enzyme polymorphism etc. could also be performed. The improved profile can be correlated with; known PK-PD relationships or be used to extrapolate them from animal efficacy models, compared with other critical parameters of toxicity and chemistry manufacturing and control (CMC), to select the best candidate for clinical development.

TABLE OF CONTENTS

Section		Contents	Page no.
		Certificate	ii
		Acknowledgements	iii
		Abstract	iv
		Table of Contents	vi
		List of Tables	ix
		List of Figures	xii
		List of Abbreviations and Symbols	xiii
1.0		**Literature Survey**	
	1.1	Introduction	2
	1.2	Human Oral Drug Absorption	3
	1.3	Human Tissue Distribution	16
	1.4	Human Drug Elimination	27
	1.5	Partial Least Square Regression and Its Role in Current Research	34
	1.6	Compounds Used in Current Research	40
	1.7	Therapeutic Areas of Selected Compounds in the Current Research: Overview	42
2.0		**Research Gap**	
	2.1	Parameter Integration in Drug Discovery : Research Gap	52
	2.2	Key Research Gaps Identified	56

5.0   Results and Discussion

LIST OF TABLES

LIST OF FIGURES

LIST OF ABBREVIATIONS AND SYMBOLS

AUC : Area under curve

CL_{int} : Intrinsic clearance

Cmax : Maximum plasma concentration after *in vivo* dosing

CMC : Chemistry manufacturing and control

COPD : Chronic obstructive pulmonary disease

DASH : DPP IV activity and/or structural homologue

DM : Diabetes mellitus

DPP IV : Dipeptidyl peptidase IV

FFA : Free fatty acid

GI : Gastro intestinal

HIV : Human immunodeficiency virus

HPLC : High performance liquid chromatography

IND : Investigational new drug

IU : International units

K_a : Absorption rate constant

K_{el} : Terminal elimination rate constant

LC-MS : Liquid chromatography tandem mass spectrometry

MAD : Maximum absorbable dose

MDR : Multi drug resistance

MDCK : Madin-Darby Canine Kidney cell line

NADPH : Nicotinamide adenine dinucleotide phosphate

NCE : New chemical entity

NRS : NADPH regenerating solution

Papp : Apparent permeability

PAMPA : Parallel artificial membrane permeability assay

PBPK model : Physiological based pharmacokinetic model

PBS : Phosphate buffered saline

PDE4 : Phosphodiesterase 4

P-gp : P-glycoprotein

PhRMA   : Pharmaceutical Research and Manufacturers Association of America

PK-PD   : Pharmacokinetic-pharmacodynamic relationship

PLS   : Partial least square

PPAR γ   : Peroxisome proliferator-activated receptor γ

QSAR   : Quantitative structure activity relationship

RBC   : Red blood cells

RNA   : Ribonucleic acid

SAR   : Structure activity relationship

TPP   : Target product profile

Tmax   : Time to reach maximum concentration after *in vivo* dosing

TZD   : Thiazolidinedione

V_d : Volume of distribution

V_{ss} : Volume of distribution at steady state

1.0. LITERATURE SURVEY

1.1. Introduction

Pharmacokinetic properties play an important role in the successful development of a clinical candidate and unfavorable PK attributes could contribute significantly to attrition of compounds in clinical development [1]. This has made the selection of an NCE having optimal PK properties as one of the key factors determining its success in development. Evaluation of PK properties in preclinical species as well as *in vitro* assays to predict human PK has thus become a very important area of research. Efforts have been made in developing various models like allometric scaling, compartmental models etc. Though these models are widely used, they lack integration of natural physiological characteristics into their framework and therefore are not representative of ideal *in vivo* conditions. Physiological based pharmacokinetic (PBPK) models relate the physicochemical and ADME properties of a test compound with physiological parameters like tissue and organ size and volumes, lipid partitioning, metabolic pathways, blood flow etc. and provide a mathematical model that can closely mimic the *in vivo* situation. PBPK models were also one of the earliest reported models in scientific literature with the work of Teorell [2] in 1937, on an integrated approach to whole body physiologically based modeling of pharmacokinetics. PBPK models provide numerous advantages in terms of accommodating the variations in physiological factors with species, age, disease state etc, allowing a reliable prediction of *in vivo* data in humans. An added advantage of this technique is its potential for utilization in drug discovery, where there are limitations to conduct extensive *in vivo* experimentation considering compound availability, volume of effort, time and cost. The major drawbacks perceived with these models were the extensive computational steps, lack of reliable physiological data as well as numerous experimental data inputs required. With the advent of faster computing systems, standardized physiological parameters published in literature, newer high throughput *in vitro* screening assays as well as sensitive bioanalysis techniques, these requirements are no longer a limitation. The development of a physiological model requires the initial mathematical description of the relevant compartments that undertake the key processes determining the exposure, partitioning and biotransformation of the test compound. This is followed by a buildup of relationships using mass balance or differential equations. This can be followed by simulation or prediction of relevant PK parameters with the use of various measured input data. A combination approach is also feasible with physiological model derived human PK

parameters are employed in a compartmental model (for e.g. one compartment PK model with first order absorption) to simulate human oral or *intravenous* concentration-time profile [3]. In many cases the simulations could also be validated using an animal species [4], however due to species specific parameters, the human prediction may vary (for example with interspecies differences in metabolism) and therefore a retrospective analysis of clinically proven compounds as employed in the current research which allows verification of results with published data [3-6], is a meaningful approach to assess their utility. Having a reliable method for prediction of human PK also opens up the possibility of methodically analyzing and identifying the relevant properties to be optimized to produce a lead candidate. This rationale forms the background of current research.

1.2. Human Oral Drug Absorption

The preferred route of administration for a pharmaceutical dosage form is oral due to the flexibility of administering wide range of doses with adaptability of various regimens as well as convenience of self-administration. The absorption of a drug from the gastrointestinal (GI) route is affected by the physiological characteristics as well as the various properties of the drug. The key physiological factors that influence absorption are the absorptive surface area, local pH environment, pH gradient, volumes of fluids, gastric emptying and transit time. Additionally the diurnal variability, expression of transporters, metabolizing enzymes, secretion of bile and presence of food can also influence the drug absorption. The major drug related properties include its solubility in relation to dose, permeability, efflux liability, as well as stability in the GI tract. Having numerous factors influencing absorption also points to the relevance of a physiological based approach to integrate them for reliable prediction of human absorption.

Physiological Parameters Influencing Oral Absorption

The major physiological factor influencing absorption is the absorptive surface area of GI tract. Small intestine with the largest absorptive surface area forms the major site of drug absorption [7]. The small intestine has an average length of about 280 cm with its anatomical segments of duodenum (21 cm), the jejunum (105 cm), and the ileum (156 cm). The diameter of the small intestine ranges from 3-6 cm in the proximal part to 1.5-2.5cm in the distal part [8].

The major modes of absorption are passive diffusion, active transport, and pinocytosis (especially in neonates) [9,10]. The absorption of drugs from GI tract is majorly influenced by absorptive surface area and transit time. The surface area of the human small intestine is greatly enhanced by the presence of fold, villi and microvilli. Large folds are more in duodenum and less in ileum and provide a surface amplification factor of 3 at some areas. The villi present in the intestine have an average height of 800μm and 500μm in the proximal and distal end of the intestine. However, the radius of the villi is constant (50μm) throughout the length of small intestine and density of about 25mm [11,12]. The apical surface of the enterocytes (columnar epithelial cells in intestine) contains numerous microvilli giving the appearance of brush border which greatly increases the absorptive surface area of the enterocyte which is approximated to around 25 fold [8,13]. The plasma exposure profile of orally administered drugs is greatly influenced by the dynamics of gastric emptying rate, and the intestinal transit time [14]. This may be specifically important for such drugs that have a narrow window of absorption from a particular gastrointestinal region. Gastric emptying refers to the time at which ingested food materials leave the stomach. The transit time is the amount of time taken for a bolus of chyme to pass through a region of the alimentary tract. The total transit time through the human pharynx and esophagus is about 6 seconds. The gastric emptying time largely depends on the nature of its contents. In a fasted condition the gastric transit time is about 4h [15]. Generally, meals comprising of various dietary constituents empty from the stomach at varying time with carbohydrate being the faster, protein at an intermediate and fats and lipids being the last to transit [15].The speed of chyme in the human small intestine is 1-4 cm per min [15]. The velocity of transport is faster in the proximal part of the small intestine i.e. duodenum and proximal part of jejunum and decrease as the chyme approaches the ileum. On an average the transit of a bolus of chyme for the small intestine is 3-4h. The transit of human large intestine is considerably slower and depending on the food intake, could range from 2-4 days [15,16].

The other major factor influencing drug absorption is the pH gradient of the GI tract. The mean gastric pH of small intestine is 1.8 [17]. The pH rises towards the distal direction from 5.0 at the pyloric sphincter to 6.0 at the distal end of the duodenum. The jejunum has a mean pH of 6.0 to 7.0 with the pH further rising to about 7.5 at the ileum [8].

The effect of bile is another key physiological factor that affects absorption due to its emulsification property. The average bile salt concentration in the jejunum is approximately

4

3mM in the fasted state and 5-15mM in the fed state and the bile salt/phospholipid ratio is approximately 4:1 [18-20].

Molecular Properties that Influence Oral Absorption

Major molecular properties that influence absorption are the molecular weight, ionization, polar surface area and lipophilicity. The rule of 5 principle proposed by Lipinski evaluates the feasibility of a drug demonstrating pharmacological activity to be orally active (drug-likeness) based on these properties. According to Lipinski's rule, an orally active drug has no more than one violation of the following criteria [21]:

a) Not more than five hydrogen bond donors (nitrogen or oxygen atoms with one or more hydrogen atoms)

b) Not more than ten hydrogen bond acceptors (nitrogen or oxygen atoms)

c) A molecular weight not greater than 500 Daltons

d) An octanol-water partition coefficient (Log P) not greater than 5

Daniel et al. evaluated the relative importance of molecular properties [22] and observed that the reduced molecular flexibility as measured by the number of rotatable bonds and low polar surface area or total hydrogen bond count were good predictors of oral drug bioavailability, independent of molecular weight. Development of a potent and selective drug molecule with high oral bioavailability thus involves a balance of the two aspects of freezing overall molecular shape and functional group presentation compatible with optimal target interaction and clearance mechanisms in the body as well as retaining properties compatible with membrane permeation.

Physiochemical Properties Influencing Drug Absorption

Major physicochemical properties that influence drug absorption are related to its solubility and permeability characteristics [17]. After oral administration, a solid dosage form needs to undergo the process of disintegration and dissolution to be finally available in soluble form. Dissolution is the kinetic process of dissolving a solute in a solvent, and dissolution rate (amount/time) is used to represent the speed of this process. The first step in dissolution is the detachment of a molecule from the solid surface. The second step is the diffusion of the detached molecule across

the diffusion layer adjacent to the solid surface [23]. In most cases rapid saturation is achieved at the solid surface and therefore, the second step determines the dissolution rate (DR). The basic diffusion controlled model was first described by Noyes and Whitney [24] and was later modified by Nernst [25] and Brunner [26].

$$DR = \frac{d\,X_{solid(t)}}{dt} = -\frac{A_{solid(t)} \times D_{drug}}{h_{(t)}} \times \left(S_{bulk} - C_{bulk\,(t)}\right)$$

$$= -\frac{A_{solid(t)} \times D_{drug}}{h_{(t)}} \times \left(S_{bulk} - \frac{X_{solu(t)}}{V_{bulk}}\right)$$

Where $X_{solid(t)}$ is the amount of undissolved solid at time t, $A_{solid(t)}$ is the total solid surface area at time t, $h_{(t)}$ is the thickness of the diffusion layer at time t, D_{drug} is the diffusion coefficient of the drug, $C_{bulk\,(t)}$ is the concentration in the bulk medium at time t, $X_{solu(t)}$ is the dissolved amount in the bulk solution at time t and V_{bulk} is the volume of bulk.

For a drug substance to solubilize, it would require interaction of the solute molecules with the solvent with different, but well defined associations (ionic, hydrogen bonding Van der Waals forces etc.). Once a solid is dispersed in a liquid, it could exist as any of the following [23]

a) Monomer (single molecule surrounded by solvent molecules)

b) Dimer or higher self-aggregate

c) Complexes with larger molecules

d) The micelle included state

e) Nano scale particles (usually termed as nano-suspensions)

Solubility could be defined in quantitative terms as the concentration of solute in a saturated solution at a certain temperature. From a drug discovery perspective, solubility could also be defined as kinetic or equilibrium solubility. Kinetic solubility is the concentration attained after addition of a concentrated sample stock solution (like in DMSO) into an aqueous media. Equilibrium solubility can be defined as the concentration of the compound in a solution which is in contact with an excess amount of the solid compound when the concentration and the solid form do not change over time (in equilibrium) [23].

Solubility may be viewed to be closely related to dissolution, which is a kinetic parameter. Absorption of an orally administered compound in a solid dosage form (tablet or capsule) involves the disintegration of the solid particles followed by the dissolution. Inside the gastrointestinal tract there would exist a dynamic interchange between the dissolved and precipitated stages of the solid drug based on the volume of intestinal fluid as well as the pH microclimate. Once dissolved, the ionization of the dissolved drug, the unstirred water layer, the concentration gradient as well as permeability influence the diffusion of the dissolved compound across the GI epithelium [17, 27]. For poorly soluble drugs the intestinal solubility (S_{int}) can limit the concentration of the compound in the intestinal lumen. If the drug concentration in the lumen is higher (especially compounds that are administered in solutions and/or highly soluble drugs) than the local intestinal solubility (at the particular pH and intestinal fluid volume), the compound may have a tendency to precipitate (if it was previously in dissolved state). This results in low effective concentrations of drug available in dissolved state.

Drug Permeability

Apart from the dissolution rate and solubility of the drug in the intestinal fluid, the absorption of the drug is also related to its permeability coefficient (P) which relates to the rate at which the dissolved drug will cross the intestinal wall to reach the portal blood circulation [28]. Applying Fick's law to the intestinal membrane the flux (passive diffusion per unit area of intestinal wall) of a solute can be assessed as the product of the diffusivity and the concentration gradient of the solute inside the membrane.

$$J_{wall} = P_{wall} \times C$$

Where J denotes flux, P denotes the permeability coefficient and C denotes the maximum concentration in solution. The major driving force for passive permeability is the concentration gradient that exists between the intestinal lumen and the central compartment (blood) that drives the compound to get absorbed (based on Fick's law). However, the main barrier to drug absorption is formed by the intestinal epithelium. Additional barriers include the mucosal layer and the unstirred water layer. Out of the many forms that a drug could exist as in a bio-relevant media, the free monomer state is the most effective for membrane permeation. Generally compounds with poor solubility tend to have high lipophilicity and high membrane permeability. In such cases the effective intestinal membrane permeability is limited by the unstirred water

layer [23]. Amidon et al. [29] demonstrated that when the membrane permeability is limited by unstirred water layer, free monomer drug molecules as well as micelle incorporated drug molecules are effective for permeation across the rate limiting layer.

For effective passive diffusion of an ionizable drug, the molecule needs to be uncharged at the membrane surface. The unionized form of a compound partitions more into the lipids than the ionized form. The proportion of the compound in an unionized stage at any particular pH is described by the of Handerson-Hasselbalch equation (simplified for monoprotic acids or bases) which defines pKa [30, 31] as the pH at which both the ionized and unionized form exist in equal proportion for acids and bases

$$For\ acids\ pK_a = pH + \text{Log}\left(\frac{[HA]}{[A^-]}\right)$$

$$For\ bases\ pK_a = pH + \text{Log}\left(\frac{[BH^+]}{[B]}\right)$$

For diprotic ampholytes

$$pK_{a1} = pH + \text{Log}\left(\frac{[XH_2]}{[XH]}\right)$$

$$pK_{a2} = pH + \text{Log}\left(\frac{[XH]}{[X^-]}\right)$$

For compounds that are ionized at physiologically relevant pH, the lipid partitioning of the ionized species Log D has a greater practical significance. Depending on the pH microclimate at the particular segment of intestine the compound (at a total concentration denoted as C) would thus exist in two distinct soluble forms (ionized and unionized, indicated by i and u, respectively) at various proportions that can be related to the location of the intestine (z) at a defined time (t) [8].

$$C^u(z,t) = f^0(z) \times C(z,t)$$

$$C^i(z,t) = [1 - f^0(z)]C(z,t)$$

f⁰(z) is the neutral fraction, dependent on the pKa of the compound at the pH at location z. The value of f⁰(z) of a compound for a known pH can be can be obtained from the Handerson-Hasselbalch equation [8].

$$f^0(z) = \frac{1}{1 + 10^{\pm(pH(z)-pK_a)}}; \; (+for\; acids\,, -for\; bases)$$

Principal Routes of Passive Diffusion

Paracellular and transcellular diffusion form the principle routes of passive diffusion. Paracellular transport include diffusion with aqueous solution through the pores in the tight junctions joining the intestinal cells (generally Mol. Wt. <200 Daltons). Transcellular diffusion involves permeation through the membrane and is dependent on the lipophilicity as well as charged state of the molecule. The neutral form of a molecule could have a 10^5 fold greater permeability than the charged form across the epithelium [17].

Reasons for Poor Permeability

The causes of poor absorption can be categorized into three types basing on the balance between solubility, dissolution rate and permeability of a drug [23].

a) Dissolution-rate limited oral absorption: The permeation rate is much larger than the dissolution rate, whereby the dissolution becomes the rate limiting step. In this case, the absorbed amount would increase dose proportionately. Absorption would also be enhanced with particle size reduction as it increases the surface area improving dissolution.

b) Permeability limited oral absorption: The permeation is slow and dissolution is fast, resulting in accumulation of dissolved amount in the intestinal fluid. Until the concentration in intestinal fluid approaches the maximum soluble limit for the pH in the intestinal segment, the absorbed amount will increase proportionately with dose. There will be no effect of particle size reduction on absorption.

c) Solubility limited oral absorption: The solubility of the administered drug reaches the maximum possible limit in the intestinal fluid and for increased absorption it would require more of the drug to come into solution. In this case absorption could also be limited due to lower effective permeability, unstirred water layer etc. and the high

dissolution rate has caused the drug to accumulate eventually approaching the maximum solubility limit.

The Biopharmaceutical Classification System (BCS)

The influences of solubility and permeability in drug absorption have been incorporated in the biopharmaceutics classification system proposed by the US Food and Drug Administration (US FDA) as a bioavailability-bioequivalence guideline. The following is a representation of the BCS class

The Biopharmaceutical Classification System

Class 1	Class 2
High permeability	High permeability
High solubility	Low solubility
Class 3	**Class 4**
Low permeability	Low permeability
High solubility	Low solubility

The drugs are classified in BCS [32] based on their solubility and permeability characteristics. The class boundaries of these properties are

a) Solubility: A drug is considered highly soluble if the highest dose strength is soluble in 250mL or less of aqueous media at a pH range of 1 to 7.5.

b) Permeability: A drug is estimated as highly permeable when the extent of absorption in humans is 90% or more of the dose administered based on mass balance or comparison with an *intravenous* dose. Alternatively other techniques capable of predicting human absorption (like *in vitro* cell culture based methods) can be used.

c) Dissolution: An immediate release dosage form is considered rapidly dissolving if no less than 85% of the drug substance dissolve in 30 minutes using USP dissolution apparatus 1 at 100rpm or apparatus 2 at 50rpm in a volume of 900mL or less in 0.1N hydrochloric acid or simulated gastric fluid or pH 4.5 buffer and pH 6.5 buffer or simulated intestinal fluid.

Additional Factors Influencing Drug Absorption

In addition to clearance mediated by the liver enzymes, the drug metabolizing enzymes and transporters present in the intestine could also regulate the extent of absorption of orally administered drugs [33]. The drug metabolizing enzymes include Cytochrome P-450 (CYP) 1A, 2D, 3A as well as phase II enzymes like glucuronyltransferase, N-acetyltransferase (NAT), sulfotransferase, and glutathione S-transferase [34]. Efflux transporters include the P-glycoprotein (or Multidrug resistance protein1-MDR1) and multidrug resistance-associated protein-2. Transporters involved in the absorption of various substrates include bile acid transporters, peptide transporter, monocarboxylic acid transporter organic anion transporter protein, nucleoside transporters etc [35].

Physiological Pharmacokinetic Model Based Prediction of Drug Absorption

The development of a physiological prediction model requires the incorporation of a number of parameters. The physiological parameters such as intestinal length, surface area and volume have been studied and are available in reported literature. A simple absorption model is to define the small intestine as a long tube with a total absorptive surface area of $200m^2$ with an average pH of 6.8 and a total intestinal transit time of 6 hours. The maximum absorbable dose (MAD) can be determined using this model equation with the estimation of absorption rate constant (K_a) using a suitable technique like Caco-2 permeability and assuming negligible first pass metabolism [36].

$$MAD = S \times K_a \times SIWV \times SITT$$

Where SIWV represents small intestinal water volume and SITT denotes small intestinal transit time. K_a is determined by the following relationship, where Pm is the Caco-2 permeability, A is the absorptive surface area and V is the volume of intestinal lumen [37].

$$K_a = P_m \times \frac{A}{V}$$

Another approach to estimate human absorption rate constant for an NCE is to extrapolate from estimated rate constant from rat using the relationship proposed by Yuasa et al. accounting for the interspecies differences in surface area and luminal volume of small intestine between human and rats [38].

$$K_{a\,human} = 0.744 \times K_{a\,rat}$$

Further enhancement of the above approach includes the incorporation of variability in solubility and ionization profiles of a compound at various segments of the GI tract due to the physiological pH gradient. This approach incorporates the variable proportion of ionized and unionized drug in solution as a function of position (segment of intestine) as well as time, considering the different transit times at various intestinal segments. Willmann et al. reported the continuous flow absorption model [8, 39] which represented the concentration of the compound administered orally (C, at an absolute dose D) in the intestinal lumen (at position z and at time t) as

$$C(z,t) = \frac{D\left(1 - f_{abs}(t)\right)}{\pi r_{SI}^2(z)l_{SI}} T_{SI}(z,t)$$

Where $f_{abs}(t)$ is the fraction of the administered drug that has reached the portal blood pool via the intestinal membrane, r is the radius of the intestinal lumen and t denotes the transit time. The subscript SI denotes small intestine. In the continuous flow model, the solubility and pH influenced dissolution or precipitation are assumed to occur at a significantly shorter span of time than intestinal transit or absorption and therefore are not rate limiting. As a consequence, this assumption is not suited for slowly dissolving/precipitating compounds or controlled release formulations [40].

Further, the amount of drug (X) that is absorbed into the portal vein from a small intestinal segment (z+dz) at a small time interval (t+dt) is expressed as a product of permeability and effective concentration in the lumen corrected for the concentration that partitions into the portal circulation, as sum of the ionized and unionized species, derived separately [8].

$$\frac{d^2X_{pv}(z,t)}{dz\,dt} = P_{int}^0\left[C_{lumen}^0(z,t) - \frac{C_{pv}(t)}{K_{lumen}^0}\right]\frac{dA_{eff}(z)}{dz} + P_{int}^i\left[C_{lumen}^i(z,t) - \frac{C_{pv}(t)}{K_{lumen}^i}\right]\frac{dA_{eff}(z)}{dz}$$

Where $P_{int}^{0/i}$ and $K_{lumen}^{0/i}$ are the apparent permeability coefficients of the gut wall and the equilibrium partition coefficients between the portal blood and the gut content for the neutral and ionized species, C_{pv} is the concentration in the portal vein and $dA_{eff}(z)$ is the effective surface area element at intestinal position z. The flow model also applies a realistic approach of having permeability and solubility of ionized and unionized species and uses a ratio (P_{int}^i/P_{int}^0 and S_{int}^i/S_{int}^0). Integration of the previous equation over the length of the intestinal segments yields

the amount absorbed in the respective region at a designated time, while integration with respect to time gives the amount of dose absorbed as a function of position within the small intestine. The continuous flow and absorption model thus derives the fraction dose absorbed (F_a) for a passively absorbed compound undergoing negligible metabolism in gut wall as

$$F_a = \int_{t=0}^{\infty} \int_{z=0}^{L_{int}} \frac{d^2 X_{pv}(z,t)}{dzdt} dzdt / (DOSE \times BW)$$

Another approach proposed by Kimura and Higaki [41] categorized the GI tract to various segments of definite pH and transit times with separate determination of absorption parameters for each, considering the pH gradient and transition times. For any compound significantly ionized at physiologically relevant pH ranges, the ionized as well as unionized species could have different rates of permeation at a particular pH. Kimura and Higaki [41] developed the GI-Transit Absorption Model (GITA) which divides the GI tract into eight segments (stomach, duodenum, upper jejunum, lower jejunum, upper ileum, lower ileum, ceacum and large intestine) with the transit of a non-absorbed drug from one segment to the other assumed to follow a first order kinetics. The availability of the drug (X) at every segment of the intestine and the fraction absorbed at each segment was estimated by Laplace transformation of the following differential functions derived.

$$\frac{dX_s}{dt} = (k_s + ka_s)X_s$$

$$\frac{dX_{i+1}}{dt} = X_i k_i - (k_{i+1} + ka_{i+1})X_{i+1}$$

$$X_{i+1}(s) = \frac{k_i X_i(s)}{s + k_{i+1} + ka_{i+1}}$$

$$fraction\ absorbed\ f_{i+1}(s) = \frac{k_i f_i(s)}{s + k_{i+1} + ka_{i+1}}$$

Where subscript s stands for stomach, i+1 denotes the next segment after intestine (i), K_i is the rate of intestinal transit and K_a is the rate absorption. The inverse Laplace of the above expressions transformed, provide the amount of compound, the absorption rate constants and the fraction absorbed at every segment of intestine.

Usansky et al. [6] proposed the absorption-disposition kinetic model linking gastric emptying, intestinal absorption and plasma disposition. The absorption parameters were predicted from Caco-2 permeability. Assuming that the drug dissolution is not a rate limiting step in drug absorption and absorption from stomach is negligible; differential equations were constructed relating drug concentrations in plasma with intestinal concentration

$$\frac{dX_{pl}}{dt} = K_a X_i F_{FP} - K_{el} X_{pl}$$

Where X_{pl} represents the amount of drug in plasma, X_i the amount in intestine, K_a and K_{el} are the first order rates of absorption and elimination, respectively and F_{FP} is the fraction of the drug that escapes first pass intestinal and hepatic metabolism. The model incorporates the influence of intestinal metabolism and derives the first-order rate constant of absorption K_a as

$$K_a = \frac{P_m S}{V_c} \times \frac{F_{FP} C_i}{C_{pl}}$$

Where V_c is the volume of distribution in well perfused organs assuming that the initial drug distribution is limited by drug diffusion [42], P_m is the drug permeability across intestinal mucosa, S is the absorptive surface area and C is the concentration (amount/mL) of drug in intestine (i) and plasma (pl). Assuming negligible first pass metabolism or an equilibrium condition (where $F_{FP} \times C_i / C_{pl} = 1$), an equilibrium solution for K_a is assumed which is independent of drug concentration changes in the intestine or plasma

$$K_a = \frac{P_m S}{V_c}$$

Usansky et al. [6] also derived the analytical solution for fraction absorbed after oral administration as

$$F_a = \frac{K_{a,eq}}{K_i + K_{a,eq}}$$

Table 1: Summary of Various Physiological Absorption Model Parameters Used in the Research

Segment of GI	Stomach	Duodenum	Jejunum	Ileum	Colon
pH	1.2 – 2.5	5.0 – 6.0	6.0 – 7.0	7.0 – 7.5	> 7.0
Volume (mL)*	600	47	200	181	5770
Effective Surface area (cm^2)*	350	77674	331002	301324	3297
Transit time (min)	15	14	71	114	2160

* the total area of intestine based on Wilman et al,.the effective surface area are derived by divided in proportion to the volume using amplification factors for villi and folds in the intestine as mentioned by Wilman et al. [8]

Various Discovery Stage Screens on Drug Absorption

Measurement of absorption potential is a major first line screen in drug discovery. As the *in vivo* PK profiling of an NCE in pre-clinical species is a time and labor-intensive process, numerous *in vitro* methods have been developed to assess the absorption potential [28]. Compared to the *in vivo* pharmacokinetic profiling which is influenced not just by absorption but also the clearance and entero-hepatic circulation, *in vitro* methods have the advantage of assessing a single parameter (absorption across a membrane or cell layer) thereby enabling the rank ordering of compounds based on a single parameter. Earlier methods of investigating the absorption potential of the compounds included everted gut sac, Ussing chamber or rat intestinal perfusion techniques [28]. With the advancement in combinatorial chemistry and parallel synthesis resulting in expanding compound libraries, newer high throughput methods were developed. Parallel artificial membrane permeability (PAMPA) technique is one such where an artificial immobilized lipid bilayer (e.g. lecithin in dodecane) is prepared on a filter membrane which when sandwiched between two aqueous layers would orient to a structure similar to the fluid mosaic description of the cell membrane [43]. Absorption across these membranes is through passive diffusion governed by the lipid solubility and ionization of the compound driven by the concentration gradient. PAMPA is also a cost effective method to perform and is ideally suitable as a first line high throughput screen.

Madin-Darby Canine Kidney cell line (MDCK) permeability assay is a cell based assay method to estimate intestinal absorption [44]. This cell line is preferred due to the ease of culture and the

rapid doubling time. Once optimized in laboratory culture, MDCK forms monolayer with tight junctions within three days of seeding to a filter trans-well, and therefore could be used very efficiently to screen large number of compounds for passive permeability. Another advantage of using MDCK is the possibility to co-express various transporters (MDRI (P-gp), peptide transporters etc.) in them due to the relatively low constitutive expression and use these for mechanistic studies like assessing if the test compound is liable to active efflux, selective uptake etc.

Colon adenocarcinoma (Caco-2) cell line is the most rugged and reliable cell based system to assess drug absorption [45]. Derived from colon adenocarcinoma cells, Caco-2 form stable monolayer with tight junctions (similar, but reportedly tighter than intestine) expressing polarization, transporter and alkaline phosphatase activity. Many of the common transporters in the intestine including P-gp are expressed in Caco-2 cell lines and they form an excellent assay system for estimation of drug permeability. Compared to other assays, Caco-2 permeability has been the most correlated with intestinal absorption.

1.3. Human Tissue Distribution

Tissue distribution refers to the reversible transfer of drug from the central compartment to the tissues [42]. Definitive information on distribution requires its measurement in various tissues which is practically impossible in humans. However, much useful information on rate and extent of tissue distribution can be made from observations in blood and plasma (especially after *intravenous* dose) and with the estimation of the PK parameter 'volume of distribution' (V_d).

Distribution of drugs can be rate limited by either perfusion or permeability. The distribution may be perfusion rate limited when the tissue membranes present no barrier to distribution. The rate of presentation of drug to the tissue can be expressed as the product of blood flow to the tissue and arterial blood concentration [42]

$$Rate\ of\ presentation = Q\ \times C_a$$

The net rate of uptake by the tissue can be presented as the product of tissue blood flow to the difference in the arterial and venous concentration of the drug in the tissue. The maximal rate of input will be the rate of presentation after which, with no further impedance to movement into the tissue, the emergent venous concentration becomes in equilibrium with the levels in tissue

16

(C_t). Therefore assuming this equilibrium has established, the amount of drug in tissue [42] can be presented by

$$Amount\ of\ drug\ in\ tissue = V_t \times P_{tp} \times C_v$$

Where V_t is the tissue volume, P_{tp} is the equilibrium tissue venous plasma distribution ratio and C_v is the concentration in venous blood/plasma. C_v is also expressed as C_p in the succeeding sections and equations as for pharmacokinetic measurements, the measurements of drug levels are made in venous blood [42]. Further the fractional rate of exit of drug from the tissue can be expressed as

$$k_t = \frac{rate\ of\ exit}{amount\ in\ tissue} = \frac{Q \times C_p}{V_t \times P_{tp} \times C_p}$$

or

$$k_t = \frac{(Q/V_t)}{P_{tp}}$$

Where Q/V_t is the perfusion rate of the tissue. The parameter k_t is a distribution rate constant with units of reciprocal time, analogous to the elimination rate constant [42]. The tissue half-life of the drug could thus be expressed as

$$half - life = \frac{0.693}{k_t} = \frac{0.693 \times P_{tp}}{(Q/V_t)}$$

Thus the drug leaves slowly from tissue that have high affinity for it (P_{tp}) and that are poorly perfused [42].

In a hypothetical case where the arterial concentration is maintained constant with time, the tissue uptake would increase and eventually reach a plateau. In this case the arterial and venous concentration reach similar levels. This mimics the situation of a constant rate infusion of drug [42].

$$C_t = P_{tp}\ C_a[1 - e^{-k_t.t}]$$

A permeability dependent rate limitation in tissue distribution arises for polar drugs diffusing across tightly knit lipoidal membranes. A permeability rate limitation simply decreases the rate of entry of the drug into tissues and hence increases the time to reach distribution equilibrium.

Apparent volume of distribution [42]: The volume of distribution (or being a hypothetical parameter, the apparent volume of distribution) can be defined as the ratio of the total amount of drug in the body to the amount of drug in plasma. For a large volume of distribution the fraction available in plasma is lesser indicating high tissue distribution. Volume of distribution (V_d) can be expressed as

$$V_d = V_p + V_t \times P_{tp}$$

Therefore a higher tissue partitioning for drugs would contribute to the high volume of distribution. Within a tissue, the common binding sites include neutral lipids and phospholipids. Additional binding sites for drugs in the body include partitioning to blood cells and plasma proteins. Plasma proteins include albumin (Mol. Wt. 67000, 35-50g/L), $\alpha_1$acid glycoprotein (Mol. Wt. of 42000, 0.4-1.0g/L), lipoproteins (Mol. Wt. 200,000 to 2,400,000 variable levels) and cortisol binding globulin (Mol. Wt. 53000, 0.03-0.07g/L) [42]. The unbound fraction is therapeutically important and becomes significant with very high protein binding (e.g. protein binding of 99.9% vs. 99.8% has 100% difference in free fraction).

The fraction of drug present in plasma depends on both tissue and plasma binding and considering partition in tissue, the volume of distribution can also be expressed as

$$V_d = V_p + V_{tw} \times \frac{C_{tw}}{C}$$

Where C_{tw}/C denotes the apparent volume of tissue. C is the total concentration.

Physiological Pharmacokinetic Model Based Prediction of Tissue Distribution

Physiological PK model based prediction of tissue distribution is very advantageous tool in drug discovery as it can potentially avoid the tedious experimental determination of these parameters in animals and their extrapolation.

Oie and Tozer [46] estimated the volume of distribution based on fraction unbound in plasma and other physiological parameters. An average value of the fraction unbound in tissues determined for various animal species ($f_{ut\ average}$) using experimentally determined values of volume of distribution and protein binding, was used for estimation of human volume of distribution .

$$f_{ut} = \frac{V_r f_u}{[V_{ss} - V_P - (f_u V_e)] - \left[(1 - f_u)\frac{R_e}{i}V_p\right]}$$

The V_d values in humans at steady state (V_{ss}) were estimated by rearranging the above equation [1].

$$V_{ss} = V_P + [f_{uh} \times V_e] + \left\{[1 - f_{uh}] \times \frac{R_e}{i}V_p\right\} + V_r \times \frac{f_{uh}}{f_{ut\ average}}$$

The parameters V_{ss}, V_p, V_e, f_u, V_r and R_e/i denotes volume of distribution, volume of plasma, extracellular fluid volume, fraction unbound, remainder of fluid volume the ratio of binding proteins in extracellular fluid (except plasma) to binding proteins in plasma, respectively and subscript *h* stands for human.

Poulin and Theil [4, 47, 48] proposed a tissue composition based technique for determination of organ plasma partitioning ratios and determination of volume of distribution. The theoretical background of the equation assumes that at steady state, the tissue plasma partitioning of the compounds can be calculated from the following classical equation

$$P_{tp} = \frac{C_t}{C_p}$$

Where C represents the total concentration in tissue (t) and plasma (p), respectively. Further the above equation is expanded as the ratio of the sum of unbound (u) and bound (b) drug in plasma (p) and tissue (t)

$$P_{tp} = \frac{C_{ut} + C_{bt}}{C_{up} + C_{bp}}$$

Which is further simplified using the fraction unbound (f), as

$$P_{tp} = \left(\frac{C_{ut}}{C_{up}}\right)\left(\frac{f_{up}}{f_{ut}}\right)$$

Further, on a physicochemical basis, the left term unbound concentration ratio in the above equation is considered to be equal to the ratio of drug solubility between tissues and plasma at steady state and independent of drug concentration

$$P_{tp} = \left(\frac{S_t}{S_p}\right)\left(\frac{f_{up}}{f_{ut}}\right)$$

The solubility in tissues and plasma are estimated using the tissue composition based equations [49, 50], which consider tissues as a mixture of proteins, neutral lipids (n) and phospholipids (p). The polar lipids (phospholipids) in tissues have a lipo-hydrophilicity similar to a mixture of 70% (by volume) of water and 30% by volume of neutral lipids. The assumption is made on a rapid homogenous partitioning into the lipid and aqueous fraction of plasma as well as tissues. The ratio of the solubility in various tissues including plasma to the solubility in water brings in the partitioning ratio component. This is represented by the oil to water partitioning ratio (P_{ow}) in case of non-adipose tissue and the vegetable oil to water partitioning ratio (D_{vow}) representing the non-ionized species in case of adipose tissue. The final tissue partitioning equation by Poulin–Theil method [47] is expressed as:

$$P_{tp\ non\ adipose} = \frac{[P_{ow}(V_{NLt} + 0.3V_{PHt})] + [1 \times (V_{Wt} + 0.7V_{PHt})] \times f_{up}}{[P_{ow}(V_{NLp} + 0.3V_{PHp})] + [1 \times (V_{Wp} + 0.7V_{PHp})] \times f_{ut}}$$

$$P_{tp\ adipose} = \frac{[D_{vow}(V_{NLt} + 0.3V_{PHt})] + [1 \times (V_{Wt} + 0.7V_{PHt})] \times f_{up}}{[D_{vow}(V_{NLp} + 0.3V_{PHp})] + [1 \times (V_{Wp} + 0.7V_{PHp})] \times 1}$$

Where V indicates the fractional tissue (t) or plasma (p) volume content of neutral lipids (NL), phospholipids (PH) and water (W). The data on tissue volumes are obtained from published literature [4]. Log P_{vow} can be derived from experimental or predicted data on Log P_{ow} using the following empirical relation [51].

$$Log P_{vow} = 1.115\ Log P_{ow} - 1.35$$

The Log P_{vow} could then be converted to Log D_{vow} using the Handerson-Hasselbalch equations

1) For monoprotic acids

$$Log D_{vow} = Log P_{vow} - Log\ (1 + 10^{pH-pKa})$$

2) For monoprotic base

$$Log D_{vow} = Log P_{vow} - Log\ (1 + 10^{pKa-pH})$$

3) For diprotic acids

$$Log D_{vow} = Log P_{vow} - Log\ (1 + 10^{pH-pKa1+pH-pKa2})$$

4) For diprotic base

$$LogD_{vow} = LogP_{vow} - \text{Log}\,(1 + 10^{pK_a1-pH+pKa2-pH})$$

5) For zwitterionic compounds

$$LogD_{vow} = LogP_{vow} - \text{Log}\,(1 + 10^{-pKa2+pH+pKa1-pH})$$

Where pKa1 is acidic and pKa2 is basic.

6) For neutral compounds

$$LogD_{vow} = 1.115\,LogP_{ow} - 1.35$$

The values of the fraction unbound in tissue (f_{ut}) used in the equations are commonly estimated from experimental data on f_{up} as per the following relation assuming albumin as the main tissue component for binding [5]

$$f_{ut} = \frac{1}{1 + (1 - f_{up})/f_{up})RA}$$

RA indicates the ratio of albumin concentration found in tissue over plasma. For adipose tissue, RA is set to 0, whereas for non-adipose tissue RA is set to 0.5 [4, 5].

Individual plasma tissue partitioning ratios estimated using the above method could be used to estimate the steady state volume distribution using the classical equation [42, 52].

$$Vd = V_p + \sum_{i=1}^{n} P_{t:p}V_t$$

The Poulin-Theil method [4, 47, 48] requires the blood plasma partitioning and vegetable oil water partitioning coefficients as input values. Physiological parameters used are the tissue volumes expressed as fraction of body weight (L/kg), volume of water in tissue, volume of neutral lipids and phospholipids in tissues and volume of extracellular space. Neutral lipids refer to sum of triglycerides, diglycerides, cholesterol and other types of non-polar lipids, Phospholipids represent lipids that contain phosphoric acid esterified at one position of the glycerol molecule (e.g. phosphatidyl choline, phosphatidyl ethanolamine, phosphatidyl serine, sphingomyelin. The reported values of tissue fractions [6, 47] are presented in Table2.

21

Table 2: Human Tissue Composition Data Used for Prediction of Volume of Distribution in the Current Research

Tissue	Fraction of body weight (L/kg)	Volume fraction of wet tissue weight (L/kg)		
		Volume of water	Volume of neutral lipids	Volume of phospholipids
Heart	0.005	0.758	0.012	0.017
Kidney	0.004	0.783	0.021	0.016
Liver	0.026	0.751	0.035	0.025
Lung	0.008	0.811	0.003	0.009
Spleen	0.003	0.788	0.020	0.020
Muscle	0.400	0.760	0.024	0.007
Plasma	0.042	0.945	0.004	0.002
RBC*	0.035	0.603	0.002	0.003
Adipose	0.120	0.180	0.790	0.002
Bone	0.086	0.439	0.074	0.001
Brain	0.020	0.770	0.051	0.057
Gut	0.017	0.718	0.049	0.016
Skin	0.037	0.718	0.028	0.011

*red blood cells

The tissue partitioning equations consider reversible binding of drugs to macromolecules in plasma, which include albumin, globulins and lipoproteins. Fraction unbound in plasma can be assessed experimentally; however in the absence of a direct method of assessment Poulin et al. [4] used the relative concentrations ratios of macromolecules between tissue interstitial fluid and plasma at steady state ($C_{m\ tissue}$/$C_{m\ plasma}$). He postulated that, assuming the binding isotherm of $f_{up} = (1/1+nKa\ C_{m\ plasma})$ and $f_{ut}=1/\ (1+nKa\ C_{m\ tissue})$ to approximate by $1/nKa\ C_{m\ plasma}$ and $1/nKa\ C_{m\ tissue}$, respectively (where n denotes the number of binding sites and Ka the affinity constant), the ratio of f_{up}/f_{ut} approximates the ratio of macromolecules ($C_{m\ tissue}$/$C_{m\ plasma}$). This ratio was approximately found to range between 0.3 to 1 and a median value of 0.5 was proposed [4].

Contrary to the assumptions of similar macromolecular binding in plasma and tissues, Rodgers et al. [53] pointed out that moderate to strong bases that are strongly ionized at physiological pH

preferably interact with tissue acidic phospholipids with electro static interactions. Binding of moderate to strong bases are preferential to $\alpha_1$acid glycoprotein which is largely restricted in plasma. In comparison, acids and very weak bases preferentially bind to albumin and neutrals to lipoproteins present in appreciable quantities in tissue and extracellular water.

Rodgers et al. [53] derived plasma tissue partitioning equations in rat. The equations were based on the assumption of complete solubility of drugs in the intra and extra cellular water and partitioning into the neutral lipids and neutral phospholipids within tissues. Further, in the absence of other specialized mechanisms like active transport or metabolism, for compounds that are sufficiently ionized within tissues (at least one basic pKa$\geq$7, ionized bases and corresponding zwitter ions), electrostatic interactions with acidic phospholipids predominate. For the other drug classes, the predominant association is with extra cellular components, with acids and weakly basic compounds assumed to bind to albumin and neutral drugs to lipoproteins. Based on the above assumptions, Rodgers et al. [53] derived the tissue partitioning equation as

$$P_{tpu} = V_{EW} + \frac{1 + 10^{pKa-pH_{IW}}}{1 + 10^{pKa-pH_p}} V_{IW} + \frac{k_a [AP]_t 10^{pKa-pH_{IW}}}{1 + 10^{pKa-pH_p}} + \frac{P V_{NL} + ((0.3P + 0.7)V_{NP})}{1 + 10^{pKa-pH_p}}$$

Where V denotes the fractional tissue volume content of extracellular water (EW), intracellular water (IW), neutral lipids (NL) and neutral phospholipids (NP). $[AP]_t$ denotes the concentration of acidic phospholipids in tissue. Values of pH$_p$ (pH of plasma) and pH$_{IW}$ are 7.4 and 7.0, respectively. pKa represents the dissociation constant of the monoprotic base where a cut off value of >6.8 was used by Buck et al. [5]. P is the vegetable oil: water partition coefficient, k_a is the association constant of the compound with the acidic phospholipids. Rodgers et al. proposed an approach to determining k_a by estimating it for blood cells (k_{aBC}, BC indicating blood cells) based on blood to plasma concentration ratio, fraction unbound in plasma and the hematocrit and assuming it to be representative of all tissues.

$$k_{aBC} = \left(P_{tpuBC} - \frac{1 + 10^{pKa-pH_{BC}}}{1 + 10^{pKa-pH_p}} V_{IW,BC} - \left(\frac{P.V_{NL,BC} + (0.3P + 0.7)V_{NP,BC}}{1 + 10^{pKa-pH_p}} \right) \right) \times \left(\frac{1 + 10^{pKa-pH_p}}{[AP]_{BC}.10^{pKa-pH_{BC}}} \right)$$

Where

$$P_{tpuBC} = \frac{E{:}P}{f_{up}} \qquad \text{and} \qquad E{:}P = \frac{R_B - (1 - Ht)}{Ht}$$

E: P indicates erythrocyte to plasma ratio, Ht indicates hematocrit and R_B indicates blood to plasma ratio.

The above model predicts the plasma tissue partitioning of the unbound drug (P_{tpu}) with the assumption that only the unbound drug distributes to tissues. For determining the P_{tp} values, the bound and unbound drugs are related by the following expression [53].

$$P_{tp} = \frac{C_t}{C_p} = f_u \ P_{tpu}$$

Berezhkovskiy [52, 54] modified the Poulin-Theil equation by pointing out that the tissue plasma partitioning coefficient is not equal to the ratio of fraction unbound in plasma to tissue if the peripheral exit of drug occurs. The conventional assessment of steady state volume of distribution after and intravenous dose is based on the following relation, which assumes rapid equilibrium of protein and tissue (lipid) binding in plasma.

$$V_{ss} = \frac{D}{AUC} \times MRT$$

Additionally, the equations apply well to a general linear model where drug elimination occurs exclusively from the central compartment, an assumption which is not realistic. To elaborate this fact and to estimate the tissue partitioning coefficients with the account of peripheral elimination, Berezhkovskiy [52] used a multi compartment open mammillary model (with the drug being reversibly transported from the central compartment (plasma) into peripheral compartments). k_t^+ and k_t^- indicate the rate constant of drug transport from plasma to tissue and tissue to plasma, respectively. The rates of possible reactions inside each compartment (binding and dissociation to a lipid or protein) are indicated by k_{tj}^+ and k_{tj}^-. a_{tj} is the quantity of drug either bound to protein or partitioned into lipid, j indicating a protein or lipid to which the drug binds.

The fraction unbound in tissue and plasma were expressed as

$$f_{u\,t} = \frac{C_{u\,t\,ss}}{C_{t\,ss}} = \frac{(A_{tss}/V_{Wt})}{\left[(A_{tss} + \sum a_{tj\,ss})/V_t\right]} = \frac{(V_t/V_{Wt})}{(1 + \sum k_{t\,j}^+/k_{tj}^-)}$$

$$f_{u\,p} = \frac{C_{u\,p\,ss}}{C_{p\,ss}} = \frac{(A_{pss}/V_{Wp})}{\left[(A_{pss} + \sum a_{pj\,ss})/V_p\right]} = \frac{(V_p/V_{Wp})}{(1 + \sum k_{p\,j}^+/k_{pj}^-)}$$

Where u, p, t and ss denotes unbound, plasma, tissue and steady state, respectively. The tissue to plasma partitioning ratio was derived to the following relationship.

$$P_{t;P} = (k_t^+/k_t^- + k_t^{el})\,(f_{up}/f_{ut})\,(V_{Wp}/V_{Wt})$$

Assuming steady state and no peripheral elimination (hypothetical case), the unbound drug concentration in plasma and tissue are equal and elimination from tissue would be zero. This simplifies the above equation to the following form which formed the basis for Poulin-Theil equation as well.

$$P_{tp}^0 = f_{up}/f_{ut}$$

Where the superscript '0' denotes the assumption of steady state and lack of tissue elimination.

However, in case of peripheral drug exit Berezhkovskiy derived the above given tissue partitioning equation as [52]

$$P_{t;P} = P_{tp}^0(k_t^+/k_t^- + k_t^{el})\,(V_{Wp}/V_{Wt}) = P_{tp}^0/(1 + k_t^{el}/k_t^-)$$

The above equation indicates that peripheral elimination leads to the decrease of tissue plasma partition coefficient reducing the steady state volume of distribution as the unbound drug concentration in tissue at steady state becomes less than that in plasma. Also basing on the below derived relation, it was proven that the unbound drug concentration in tissue at steady state becomes less than that in plasma

$$C_{u\,t\,ss} = \frac{C_{u\,p\,ss}}{\left(1 + \dfrac{k_{el\,t}}{k_t^-}\right)}$$

In the above equation, the unbound concentration in tissue at steady state ($C_{u\,t\,ss}$) is related to the unbound concentration in plasma and the elimination rate constant from tissue ($k_{el\,t}$) as well as the transit rate constant from tissue to the central compartment (k_t^-). Berezhkovskiy further derived the relationship between the organ tissue plasma partition coefficient (P_{tp}) and the partition coefficient of non-eliminating organ through the parameters of organ permeability, surface area of plasma tissue boundary and the elimination rate constant. Subsequently the equation for plasma tissue partitioning coefficient (P_{tp}) was developed by expressing f_{up} and f_{ut} through protein binding parameters and drug partition coefficients between different phases in tissues and plasma and further incorporating the tissue partitioning equation [52] as

25

$$P_{tp} = \frac{P_{vow}(V_{NLt} + 0.3V_{PHt}) + 0.7V_{PHt} + \left(\frac{V_{Wt}}{f_{ut}}\right)}{P_{vow}(V_{NLp} + 0.3V_{PHp}) + 0.7V_{PHp} + \left(\frac{V_{Wp}}{f_{up}}\right)}$$

Various methods of estimating tissue distribution

There are numerous methods of estimating tissue distribution. Most common include the conventional tissue excision and experimental estimation of drug levels in tissues by using a suitable sample clean up and analytical technique. This technique is however limited to animal species. Whole body auto radiography is another effective technique that could be used for a detailed tissue distribution profile. The most common procedure [55] is to *intravenously* administer as series of experimental animals with the labeled compound with each animal receiving a single dose. After various intervals the animals are rapidly deep frozen and sagittal microtome sections are taken at different levels through the whole frozen bodies. The sections are freeze dried and pressed against a photographic film. After exposure the section and film are separated and the pattern of the drug distribution will appear on the developed film. The sections may be stained and mounted under cover slips or they may be used in their unstained state as references for the interpretation of autoradiograms.

Microdialysis [56] is a semi invasive focal sampling method based on the use of probes with a semipermeable membrane at the probe tip. The probe is constantly perfused with a physiological solution at a low flow rate of 1-10μL per minute, is implanted into the tissue and substances in the interstitial fluid is dialyzed into the perfusion medium inside the probe. Owing to the small sample volume, there is no substantial biological fluid loss. Sample analysis however requires sensitive methods such as LC-MS/MS. Microdialysis technique provides selective access to the unbound and thus the pharmacologically active drug fraction.

Positron Emission Tomography (PET) [56] is a nuclear imaging technique based on the use of molecules labeled with positron emitting radioisotopes. The emitted positrons pass through tissue and are ultimately annihilated when combined with an electron, resulting in two 51 KeV photons emitted in opposite directions. Detectors are arranged in a ring around the tissue of interest and only triggering events that arrive near simultaneously at diametrically opposite detectors are recorded. The resulting PET images might yield three dimensional information on tissue

distribution of the positron emitting molecules with a spatial resolution of 1 to 5 mm and a maximum temporal resolution of approximately 30 seconds. The most commonly employed PET radionuclides are oxygen-15 (^{15}O), nitrogen-13 (^{13}N), carbon-11 (^{11}C) and fluorine-18 (^{18}F). ^{18}Fluorine is favored as a radioisotope due to its long half-life (about 10 hours), however it would require the drug molecules to contain the fluorine atom in its native structure. Therefore despite the shorter half-life carbon -11 (20.4 minutes) is most widely used.

Magnetic resonance imaging (MRI) [56] uses radiofrequency pulses and magnetic fields to obtain signals from changes in nuclear magnetic moments. Magnetic resonance spectroscopy (MRS), in addition provides a greater degree of molecular characterization. MRS can reveal the spectroscopic profiles of the chemical constituents as well as distinguish between parent drug and metabolites due to the differences in chemical shifts of the resonance signals. A major drawback of this technique is its low sensitivity.

1.4.   Human Drug Elimination

Elimination of drugs occurs by excretion and metabolism. Excretion of drugs can be through bile or through the breath in case of volatile substances, but for many drugs, a major route of excretion is through kidneys. Metabolism is other major mechanism of elimination of drugs from the body. The most common routes of metabolism include oxidation, reduction, hydrolysis (phase I reactions) and conjugation (phase II reactions, e.g. glucuronidation, sulphation, amino-acid conjugation, glutathione conjugation, acetyl conjugation etc.). Liver is the major target organ of metabolism; however drugs are extensively metabolized in other tissues such as kidneys, skin, lungs, blood and gastrointestinal wall.

Cytochrome P450 enzyme system form the major class of enzymes responsible for drug metabolism. There are 57 human genes and more than 59 pseudo genes divided among cytochrome P450 genes and 43 subfamilies [57]. Prominent CYPs involved in phase I drug metabolism include CYP 1A2, 2B6, 2C9, 3C19, 2E, 2D6 and 3A4. Other enzymes involved in drug metabolism are flavin monooxygenases (FMO), alcohol dehydrogenase, esterases, epoxide hydrolase etc.

Inhibition of CYP enzymes by co-administered drugs or food components that are substrates of the same enzyme is an important concept in drug discovery and development and prior

understanding of CYP inhibition by a lead drug candidate is an important requisite to avoid potentially fatal drug interaction in the clinic [58]. Inhibition could also involve mechanism based inhibition with covalent adducts formed by reactive metabolic species generated by CYP metabolism of the drug. Human liver microsomes based inhibition assays using known specific substrates of CYPs are used to assess the inhibition potential of a drug candidate. Ratio of predicted human levels (I) over inhibition constant (Ki) is used as major criteria for predicting the possibility and severity of drug interaction due to inhibition of CYP enzymes [58].

The induction of CYP 450 enzymes by xenobiotics is a major concern in clinical use of a drug due to the enhanced metabolism of drugs and endogenous substrates reducing their plasma levels or elevating metabolites, some of which might be toxic or highly reactive [59]. Induction of CYP enzymes involves de novo RNA and protein synthesis. Most common mechanisms include ligand activation of key receptor transcription factors including pregnane X- receptor (PXR), constitutive androstane receptor (CAR), aryl hydrocarbon receptor (AhR) and others, leading to increased transcription. Human hepatocyte based experiments are commonly used for investigating the CYP induction profiles. Induction of CYP enzymes are assessed using various techniques in cultured human hepatocytes including quantitative mRNA detection by real-time PCR (taqman probes), CYP activity by functional assays involving metabolism of specific chemical substrates and quantitation of CYP protein by western blotting [58].

Pharmacokinetic Parameters Signifying Drug Metabolism

Clearance is an important parameter that describes the elimination of drug from the body. Clearance may be regarded as the volume of blood from which the drug would be removed per unit time. Clearance could also be related as the rate of drug extraction by an organ of elimination relating to the incoming concentration of blood. Clearance can be estimated as a product of volume of distribution and elimination rate constant

$$in\ vivo\ plasm\ clearance\ (CL) = \ V_d \times K_e = \frac{Dose}{AUC}$$

Where AUC denotes the area under plasma concentration-time curve. Clearance is accurately estimated after an *intravenous* dose (avoiding interference of absorption) at low concentration of the substrate (test drug) to avoid saturation of metabolism.

Clearance can be described in terms of the eliminating organ (hepatic, renal and pulmonary). The anatomy of the human body dictates that the clearance of a drug by one organ adds to the clearance of another. This is the consequence of circulation. The plasma clearance estimated based on a concentration-time profile is an additive value including hepatic and renal clearance and also including clearance from other tissues.

Renal Clearance

The renal clearance of a drug excreted by glomerular filtration can be expressed as the product of fraction unbound (f_u) and glomerular filtration rate (GFR) [60].

$$CL_{GFR} = f_u \times GFR$$

The PBPK model on renal clearance proposed by Janku [60] also predicts proportionality of renal drug clearance to glomerular filtration rate. Additionally compounds excreted by tubular secretion, in general exhibits a curvilinear relationship, with the curvature being less pronounced with increasing plasma protein binding of the drug. According to the model, distinct deviation from simple proportionality can be expected only for compounds for which efficient flow-dependent secretion process is not counteracted by extensive binding of the drug to blood constituents.

Biliary excretion and re-absorption of drugs have profound influence on the pharmacokinetics of certain drugs. The threshold molecular weight for drugs to be excreted through bile ranges 500-600 in humans [61]. Once inside the hepatocytes, the compounds can be transported into bile either unchanged or as more hydrophilic metabolites after phase I and/or phase II bio-transformations, or can be excreted into blood by basolateral transport proteins. Modeling or influence of entero-hepatic circulation is not included as part of the current research however the methodology enables the integration of modeling of this phenomenon with future advancement in understanding (also as mentioned in the section on limitations of the current research).

Physiological Pharmacokinetic Model Based Prediction of Metabolic Clearance

A common method is the scale up from liver microsomal intrinsic clearance data to organ level, also known as the *in vitro* half-life approach. The underlying principle bases on the derivation of the integrated Michaelis-Menten equation

$$CL_{u,int} = \frac{V_{max} \times C}{K_m + C}$$

Simplifying the above relation to derive intrinsic clearance (V_{max}/K_m) would require a substrate concentration significantly smaller than K_m which would reduce the above equation neglecting the very low substrate concentration. A low substrate concentration also ensures linear non saturating metabolism and the hepatic intrinsic clearance for the unbound drug ($CL_{u,int}$) per gram of liver is be expressed as [62].

$$CL_{u,int} = \frac{V_{max}}{K_m} = \frac{0.693}{t_{1/2}}$$

The intrinsic clearance can therefore be estimated at a single substrate concentration estimating the first order rate of decay of substrate or the half-life in presence of liver enzymes (microsomes or hepatocytes) which when normalized to the microsomal protein content in the metabolic reaction returns the numerical value of intrinsic clearance.

Following the same principle, when the drug concentration is higher than K_m, it would require the estimation of maximum metabolic rate (V_{max}) and Michaelis-Menten constant (K_m) using multiple incremental concentration of substrate until the rate of metabolism reaches a plateau.

The intrinsic clearance can further be extrapolated to *in vivo* blood clearance using various models and are described in the subsequent section. The clearance relates to the extraction ratio and blood flow (Q) to the eliminating organ as per the following relation. The extraction ratio (E) is a measure of the efficiency of the eliminating organ in eliminating the drug from systemic circulation in a single pass. The extraction ratio could range from 0 to 1 with 1 indicating the complete removal in first pass. The hepatic clearance therefore can be related to extraction ratio (subscript 'h' indicating hepatic) as

$$CL_h = Q\,E_h$$

The venous equilibrium model (well stirred model)

The well stirred model assumes rapid equilibrium inside the eliminating organ. The organ is considered to be of discrete volume and is perfused by homogenous medium (blood) and is connected to the central volume by flow. The hepatic clearance is described by the model as

$$CL_h = \frac{Qf_uCL_{int}}{Q + f_uCL_{int}}$$

Several important variables like binding to macromolecules, erythrocyte partitioning etc. affect the clearance [63]. Incorporation these parameters into the well stirred model give the following expression [5, 64].

$$CL_{H,blood} = \left[\frac{\frac{fu_p}{R_B} \times Q_h \times (\frac{CL_{int\,invivo}}{fu_{inc}})}{Q_h + \left(\frac{CL_{int\,invivo}}{fu_{inc}}\right) \times \frac{fu_p}{R_B}} \right]$$

Where fu_{inc} and fu_p indicates the unbound fraction in microsomal reaction and plasma, respectively and R_B indicates the blood plasma partitioning. Austin et al. [64] reported the following empirical model to estimate fraction unbound in liver microsomes using octanol water partitioning data.

$$f_{u\,microsomes} = \frac{1}{e^{(0.53\,log\,D\,o/_w - 1.42)} + 1}$$

Log $D_{o/w}$ at pH 7.4 can be estimated from Log P using the following relation [65]

$$Log\,D_{7.4} = LogP - \log\left(1 + 10^{(7.4\,A + BpK_a)}\right)$$

Where A=1 and B= -1 for an acidic compound and A= -1 and B=1 for basic compound.

Additional factors that are not currently under purview of the model include transporter activities, effect of enzyme induction etc.

The Sinusoidal Perfusion Model (Parallel Tube Model)

The parallel tube model assumes similar intrinsic clearance and blood flow in parallel for the liver sinusoids, considering them like parallel tubes. A concentration gradient is assumed from the periportal to the centrilobular side of the liver, but no diffusion or dispersion is assumed in the blood flow within the sinusoid. The hepatic clearance based on this model is derived as

$$CL_h = Q(1 - e^{-f_uCL_{int}/Q})$$

Distributed Sinusoidal Perfusion Model

This model extends the parallel tube model with the assumption of variability in the blood flow rate (q) as well as the intrinsic clearance ($CL_{u, int}$) of each sinusoid. The sinusoids in intact liver are divided into 'n' groups with the same ratio of clearance to blood flow ($CL_{u,int} / q$) . The total blood flow and intrinsic clearance are expressed as Q(n) and $CL_{u,int}$(n), respectively and the hepatic clearance (CL_h) is derived as

$$CL_h = Q\{1 - e^{\left(-\frac{f_u CL_{int}}{Q} + \frac{1}{2}\epsilon^2 \left(\frac{f_u CL_{int}}{Q}\right)^2\right)}\}$$

Where ϵ^2 is the variance of $CL_{u,int} / q$ for each sinusoid in the whole liver expressed by the following equation.

$$\epsilon^2 = \Sigma \frac{(CL_{u,int}(n)/CL_{u,int})^2}{\frac{Q(n)}{Q}} - 1$$

Dispersion Model

Roberts and Rowland [66] introduced the dispersion model with the assumption of drug dispersion along the flow path in the sinusoid. The extent of dispersion is denoted by the dispersion number (D_N). Dispersion model incorporates the features of well stirred model and parallel tube model as indicated by the model reducing to well stirred model as the dispersion number approaches infinity and to the parallel tube model as the dispersion number approaches zero. Normal ranges of D_N values reported are 17-0.5. Hepatic clearance is described by the dispersion model expressed as

$$CL_h = Q \left\{ 1 - \frac{4a}{(1+a)^2 \, e^{\left(\frac{(a-1)}{2D_N}\right)} - (1-a)^2 \, e^{\left(\frac{-(a+1)}{2D_N}\right)}} \right\}$$

Where

$$a = (1 + 4R_N D_N)^{\frac{1}{2}}$$

and

$$R_N(efficiency\ number) = \frac{f_u CL_{int}}{Q}$$

Methods of Estimating Human Drug Metabolic Clearance

Conventional methods include the use of animal models to scale up or use an average estimate as predicted human clearance. Allometric scaling is widely used in predicting human data based on information from preclinical species. Since prediction errors are commonly encountered, various correction factors are included to improve the fit and accuracy of predictions. These modifications include *in vitro* metabolic data, correction by maximum life-span potential or brain weight, bile flow and scaling of unbound clearance.

The most recent approaches have been the use of liver microsomes and hepatocytes. There could be two approaches in the prediction of human metabolic clearance. One approach is to use varying amount of substrate and monitor the metabolite formation and to assess the enzyme kinetic parameters of V_{max} (maximum velocity) and substrate concentration at half-maximal velocity (Michaelis Menten constant K_m). Intrinsic clearance can then be assessed as the ratio of V_{max} over K_m. The alternate approach most commonly used in drug discovery is the substrate depletion approach. Basing on the Michaelis Menten equation when the substrate concentration becomes much smaller than the K_m, the rate of reaction approaches the numerical value of intrinsic clearance (V_{max}/K_m). With the advent of sensitive bioanalytical techniques like LC-MS, and the convenience of estimating only the parent compound remaining in reaction, makes this approach widely acceptable in drug discovery screening. Estimated intrinsic clearance values can be normalized for protein and microsomal content and extrapolated to *in vivo* intrinsic clearance. *In vivo* intrinsic clearance therefore can be represented by the following equation [1].

$$CL_{int\ in\ vivo} = \frac{0.693}{invitro\ t1/2} \times \frac{incubation\ volume}{mg\ of\ microsomes} \times \frac{microsomal\ protein}{g\ of\ human\ liver} \times \frac{liver\ weight}{kg\ of\ human\ body}$$

Using the various models (well stirred parallel tube, sinusoidal perfusion model etc.) described above, *In vivo* intrinsic clearance can be extrapolated to *in vivo* hepatic blood clearance with the incorporation of additional parameters like hepatic blood flow, fraction unbound in plasma and fraction unbound in microsomes. The various human scale up parameters used for *in vitro* scaling to *in vivo* clearance are provided in Table 3.

Table 3: *In Vitro* Scale Up Values for Estimating *In Vivo* Intrinsic Clearance in Humans

Parameter	Unit	Value
Microsomal protein per gram of liver	mg	52.5
Liver weight per kg of body weight	g	25.7
Hepatic blood flow	mL/min/kg	20.6
Hepatocellularity	Million cells/g liver	120

1.5.   Partial Least Square Regression and its Role in Current Research

The lead optimization step in drug discovery aims to identify a suitable clinical candidate from a large series of chemical compounds that fits the Target Product Profile (TPP). The initial efforts would be to run various screens and pick and choose a best that fits broadly within a defined individual screening parameter range and further evaluate the selected compounds for *in vivo* properties and a projected human profile in comparison with TPP. However the answer to this quest is not easy due to the multivariate nature of the problem. To illustrate, as well as to correlate with the current research objective; if the screening results of various physicochemical and ADME properties (solubility, permeability, Log P etc, n being the number of estimates) are plotted together to assess the trend in data, this would result in a highly complex n dimensional (n axes, one for each parameter) scatter plot indicating the above mentioned complexity. On the contrary if the compounds are made to rank order based on individual properties, it could provide a different rank order of compounds for each property, making the choice of a lead compound difficult. This multivariate nature of a combination of properties effecting a particular *in vivo* human pharmacokinetic profile makes it difficult to identify trends in the screening data and to further assess the influence of various physicochemical and ADME properties on an outcome or rationally modify the chemical series to develop a lead compound with good chances of clinical success. Additional complexity is added by the nature of the individual data itself. Some of the estimates (Y values) in the data set may be mutually exclusive or independent, whereas some may be interrelated. Multivariate analysis procedures and most importantly principal component analysis (PCA) and partial least square regression (PLS) are of great importance in this area.

Originally developed by the Swedish scientist Wold in 1966, mainly for social sciences, PLS became popular in chemometrics (through his son Svante Wold) and is very popular in areas of anthropology, genomics, digital imaging etc. In handling numerous and collinear X-variables, and response profiles (Y), PLS allows us to investigate more complex problems than before and analyze available data in a more realistic way.

PLS regression [67] is a procedure that relates a set of predictors to multiple response variables (screening data and PK parameters, respectively as applied in the current research). PLS reduces the predictors to a set of uncorrelated components based on the covariance between X and Y and then performs a least square regression on these components. PLS generalizes and combines features for principal component analysis and multiple regression. It is particularly useful to predict a set of dependent variables (response variables) from a very large set of independent variables (predictors). The goal of PLS regression is to predict Y from X and to describe their common structure. When Y is a vector and X is full rank (implying a case where there are few parameters, which are mutually unrelated and explain each property fully), the goal could be accomplished by ordinary multiple regression. When the number of predictors is large compared to number of observations (as in the case of drug discovery where multiple properties of the compound estimated by screening, determines its final developability aspect as a clinical candidate), the regression approach will not be feasible due to collinearity (meaning that within a set of independent variables some are defined by totally different independent variables). PLS regression finds components from X (physicochemical or ADME or biological attributes estimated by screening) that are also relevant for Y (list of desirable pharmacokinetic properties ensuring sufficient biological profile and favorable toxicity profile). PLS searches for a set of components called as latent vectors (underlying trends) that performs a simultaneous decomposition of X and Y with the constraint that these components explain as much possible of the covariance between X and Y. This step generalizes the popular method of principal component analysis (PCA) and this is followed by a regression step where the decomposition of X is used to predict Y. In the current research X variables are more restricted to physicochemical and ADME properties and Y values are key pharmacokinetic parameters that define its *in vivo* PK profile.

Results of PLS depend on the scaling of the data. With appropriate scaling one can focus the model on more important Y variables and use experience to increase the weights of more

informative X variables (this is a high level interpretation of how knowledge of biology process explains an outcome and weights different causative factors in order of relevance for analysis, a process statistical methods might not achieve). In the absence of knowledge about relative importance of variables the standard approach in PLS is to scale and centre data. Scaling implies the reduction of each variable to unit variance by dividing them with their standard deviations (for example as in the current research, divide all solubility data at pH 6.8 by the mean of the entire data set of 13 compounds). The data can be centered by subtracting their averages, and is also called auto scaling. This corresponds to giving each variable the same weight, and the same prior importance to the analysis. This would make the centroid (point of intersection of medians) of the whole data set to zero and would thus provide new standardized axes with data points at the same relative locations in space. To further illustrate, In many cases with lower dimensions (<3) visual analysis of data rotating across the axis, trends (principal components) which may be in various directions can be visually observed. The first Principal component (PC) is chosen as the line that fits a trend in this space that goes through the centroid, but also minimizes the square of the distance of each point to that line, being as close to all the data as possible. Subsequently the second PC axis must also go through the centroid but with a certain constraint that it must be completely uncorrelated or in other words should be orthogonal to the first PCA axis. This rationality would also continue with subsequent components.

Figure 1: Pictorial Depiction of (from Left to Right) 3 Dimensional Scatter Sets of Data, Scaled and Centered Showing the Principal Components 1 and 2
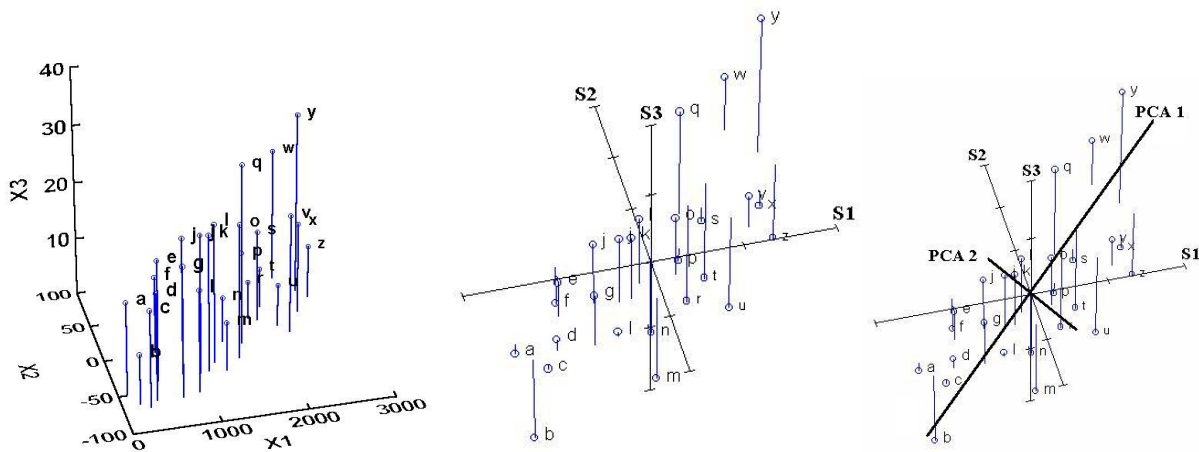
Note: adopted from ordination.okstate.edu/PCA.htm.

As mentioned before, PLS involves a principal component analysis as its first step. PCA works by decomposing the X matrix as the product of two smaller matrices which are the loading and score matrices. The loading matrix is composed of few (lesser than the original number of parameters in x) vectors which are obtained as linear combination of original X variables. These are what can be distinguished as trends in data (visually recognizable in lower dimensions of 3 or 2) or latent vectors or principal components.

The score matrix contains information about the objects (which mean hypothetical replacements of trending data). Each object is described in terms of projection into principal components (instead of original variables).

General Overview of Computational Methodology of PLS [67-69]

PLS regression decompose both X and Y as a product of a common set of orthogonal factors and a set of specific loadings. The main purpose of PLS is to build a linear model

$$Y = XB + E$$

Where Y is an n x m reponse matrix (n indicating the number of observations and m indicating the number of reponses), X is an n x p variable predictor matrix (p indicating the number of parametes eg. PK parameters in the current research), B is a p x m regression coefficient matrix and E is the noise term. As mentioned earlier as part of the latent factor extraction step in PLS the X and Y variables are scaled and centered followed by the computation of factor score matrix T such that

$$T = X W$$

Columns of W are weight vectors for the X matrix (screening data on various properties) which are computed such that each of them maximizes the covariance between responses and the corresponding factor scores. Finally ordinary least square procedures for the regression of Y on T are then performed to produce Q, the loadings for Y (coefficients, that indicate the relative weightage of parameters) such that

$$Y = TQ + E$$

This indicates

$$Y = X WQ + E$$

37

Which gives the linear form $Y=XB + E$ where $B=WQ$

The matrix of coefficients (loadings) is of importance in the current research as it is used to identify the relative contribution of various properties (ADME or physicochemical in case of the current study) to a specific response variable (PK parameter).

In general methods of multivariate analysis the latent vectors could be chosen in a lot of different ways, for PLS regression, this amounts to finding two sets of weights w and c in order to create a linear combination of the columns of X and Y such that these two linear combinations have maximum covariance. The first two vectors are found as follows

$$t=Xw \text{ and } u=Yc$$

With the constraint that $w^T w=I$ (I stands for Identity matrix or unit matrix which returns the same matrix as product on multiplication) and $t^T t=I$ and $t^T u$ is maximal. When the first latent vector is found, it is subtracted from both X and Y and the procedure is reiterated until X becomes a null matrix. In other words the vectors are found in such a way that they explain most of the variance in the data.

The iteration process in PLS is highly intensive and requires automated processing. The most common algorithm for PLS analysis is the NIPALS algorithm. A brief description of the algorithm is given below. The entire analysis in the current research was performed using Minitab software (version 6) which automates the whole procedure.

Brief Description of NIPALS algorithm [67]

The first step in PLS analysis is the creation of two matrices containing the data: $E = X$ variables and $F = Y$ variables. These matrices are then column centered and normalized (i.e., transformed into Z-scores). The sums of squares of these matrices are denoted as SSX and SSY, respectively. Before starting the iteration process, a vector 'u' is initialized with random values. The following steps denote the iteration process with the symbol $\propto$ meaning "to normalize the result of the operation".

Step 1. $w \propto E^T u$ (estimate X weights).

Step 2. $t \propto E w$ (estimate X factor scores).

Step 3. $c \propto F^T t$ (estimate Y weights).

Step 4. $u = Fc$ (estimate Y scores).

If t has not converged, then go to Step 1, if t has converged, then compute the value of b which is used to predict Y from t as $b = t^T u$, and compute the factor loadings for X as $p = E^T t$. Further, subtract (i.e., partial out) the effect of t from both E and F as follows $E = E - tp^T$ and $F = F - btc^T$. The vectors t, u, w, c, and p are then stored in the corresponding matrices, and the scalar b is stored as a diagonal element of B. Compute sum of squares of X and of Y are explained by the latent vector, as $p^T p$ and b^2, respectively. Obtain the proportion of variance by dividing the explained sum of squares by the corresponding total sum of squares (i.e., SS_X and SS_Y). If E is a null matrix, then the whole set of latent vectors has been found, otherwise the procedure can be re-iterated from Step 1 onwards.

Key Output Parameters of PLS Regression Analysis using Minitab*

a) **Analysis of variance tables:** Minitab displays one analysis of variance table per response based on the selected model. The table shows the amount of variance in the response explained by the model and the amount of variation left unexplained.

b) **p-Value:** The p-value can be used to analyze whether the regression coefficients are significantly different from zero. A p-value smaller than a pre-selected α-value (generally 0.05, corresponding to 95% CI), it can be deduced that at least one coefficient is not zero.

c) **Number of components and X-variance**: Minitab displays the models and constituting components identified for each response (Y parameter) in PLS analysis. The first model has one component, the second model has two components, and the third model has three components and so on. Minitab also estimates the X variance indicating the extent of variance in the predictors (X variables) that is explained by the model.

d) **Model selection and validation parameter R-Sq**: The R-Sq value provides the proportion of variation in each response that is explained by the predictors, indicating how well each model fits your data. Minitab displays the R^2 values for all the calculated models. The R^2 for the selected model is based on the sum of squares in the analysis of variance table.

e) **Standardized coefficient plot:** The coefficient plot is a projected scatter plot showing the standardized coefficients for each predictor. This plot can be used along with the

regression coefficients to compare the sign and magnitude of the coefficients for each predictor. The plot makes it easier to quickly identify predictors that are more or less important in the model.
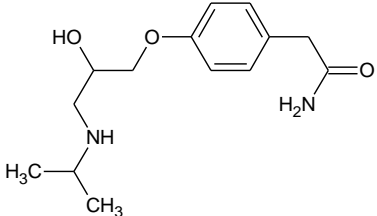
*adopted from Minitab statistical guide.
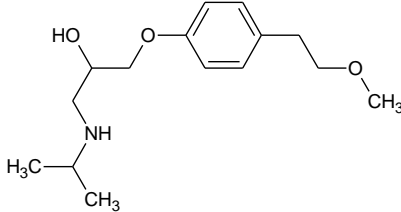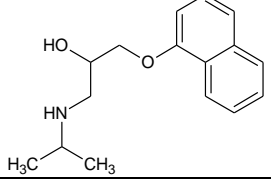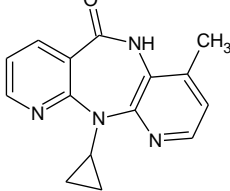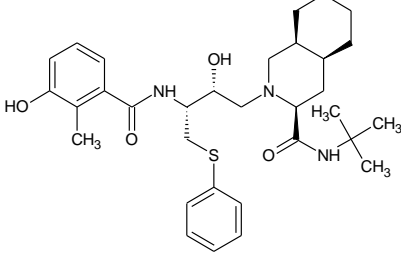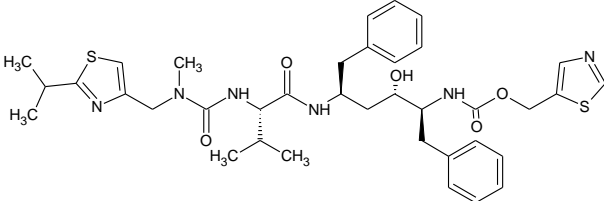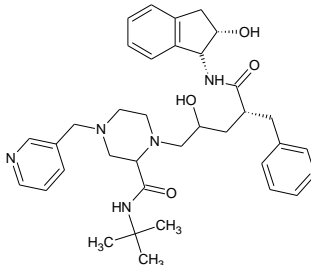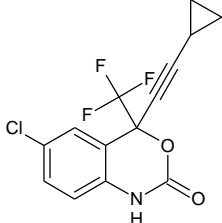
1.6. Compounds Used in Current Research
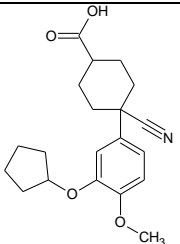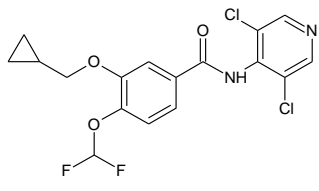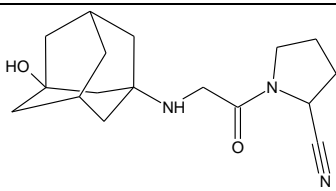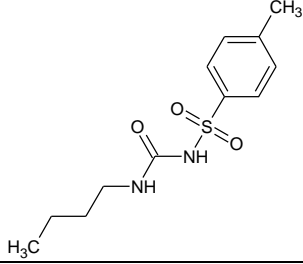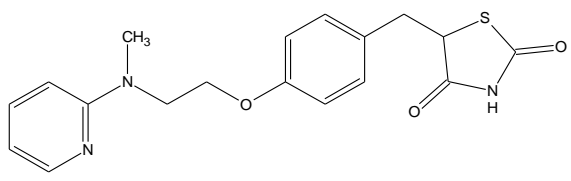
The compounds used in the current research belonged to various therapeutic categories of cardiac beta blockers, anti-retrovirals, chronic obstructive pulmonary disease (COPD) drugs, as well as anti-diabetic compounds. The details of the compounds are listed in Table 4. The compounds are representative in terms of exhibiting wide range of properties of Log P, solubility, protein binding as well as clearance which was the primary requirement for a study set for developing the research hypothesis. Additionally the selection of the compounds were based on the following criteria

- Availability in the laboratory
- Diversity of structure
- Spread across therapeutic area
- Lead compounds that represent a huge volume of optimization effort
- Extensively used with PK-PD information available
- Categorization in terms of renal clearance
- Applicable in Polypharmacy

Table 4: Compounds Used in the Current Research

Compound	Structure	Mol. wt	Category
Atenolol		266.3	Anti-hypertensive

Metoprolol		267.4	Anti-hypertensive
Propranolol		259.3	Anti-hypertensive
Nevirapine		266.3	Anti-retroviral
Nelfinavir		567.8	Anti-retroviral
Ritonavir		720.9	Anti-retroviral
Indinavir		613.8	Anti-retroviral
Efavirenz		315.7	Anti-retroviral

Cilomilast		343.4	COPD
Roflumilast		403.2	COPD
Vildagliptin		303.4	Anti-diabetic
Tolbutamide		270.3	Anti-diabetic
Rosiglitazone		357.4	Anti-diabetic

1.7. Therapeutic Areas of Selected Compounds in the Current Research: Overview

Beta Blockers (β adrenergic receptor blockers)

Beta blockers are an important class of drugs due to their high prevalence of use. Beta blockers are commonly used systemically in the treatment of conditions including hypertension, cardiac arrhythmia, angina pectoris, acute anxiety and topically for open angle glaucoma.

Thus the main pharmacological action of beta blockers is the antagonism of cardiac β-adrenoreceptor responses in the heart (mainly β$_1$ adrenoreceptors) and the main side effect is arising due to the antagonism of β$_2$ receptors in airways, resulting in bronchospasm. Therefore

42

more β_1 selective compounds have been developed [70] to overcome this side effect. Each of these drugs possesses at least one chiral centre and an inherent degree of enantioselectivity in binding to the β adrenergic receptor. Except for timolol, all of these drugs used systemically are administered as racemates (an equal mixture of two isomers). The non-selective beta blockers include propranolol, oxeprenolol, pindolol, nadolol, timolol, carvedilol and labetolol. Selective agonists include metoprolol, atenolol, esmolol and acebutolol. As a class beta blockers are quite diverse in their pharmacokinetic properties as they display varying extent of protein binding, metabolic clearance and urinary excretion [71].

Pharmacokinetic-Pharmacodynamic Correlation of Beta Blockers

The affinities of beta blockers to the β_1 receptor and its relative binding affinity with β_2 receptor provide a basic comparison of the compounds used in the current study. In the current study three beta blockers are compared namely, atenolol, metoprolol and propranolol. Atenolol and metoprolol are selective for β_1, whereas propranolol is non-selective. Smith and Teitler [72] reported the equilibrium dissociation constants of these drugs and other beta blockers based on a radioligand binding assay performed with membrane preparations from recombinant cell lines expressing human beta receptors (Table 5).

Table 5: Affinity of Various Beta Blockers Used in the Research with Beta Adrenergic Receptors

Beta blocker	Equilibrium dissociation constant K_i (nM)	
	β_1	β_2
Atenolol	1520 ± 110	8600 ± 1360
Metoprolol	204 ± 24	1227 ± 270
Propranolol	3.6 ± 0.3	1.1 ± 0.2

Baek et al. [73] reported the PK-PD relation between the cardiovascular effects and plasma concentrations of beta blocker drugs carvedilol and atenolol. Nineteen subjects received 50 mg of atenolol and 32 subjects received 25 mg of carvedilol. The subject data was fitted to a two compartment pharmacokinetic model. A PK-PD model with a hypothetical effector compartment

(biophase) was utilized to describe the relationship between the plasma concentration and cardiovascular effects.

Anti-retroviral

At present six classes of anti-retroviral drugs have received FDA approval. These are nucleoside/nucleotide reverse transcriptase inhibitors, non-nucleoside reverse transcriptase inhibitors, protease inhibitors, fusion inhibitors, entry inhibitors (CCR-5 co-receptor antagonist) as well as human immunodeficiency virus (HIV) integrase strand transfer inhibitors. The current compounds under consideration belong to the class of non-nucleoside reverse transcriptase inhibitor (nevirapine and efavirenz) and protease inhibitors (nelfinavir, ritonavir, indinavir and efavirenz) [74]. Non-nucleoside reverse transcriptase inhibitors bind directly and noncompetitively to the enzyme reverse transcriptase at a site that is distinct from the substrate, blocking DNA polymerase activity [74]. This mechanism inhibits the conversion of viral RNA to DNA. Protease inhibitors [74] inhibit the HIV protease blocking the function of this enzyme in creating functional proteins allowing maturation of HIV virion. Inhibition of HIV protease results in the release of structurally disorganized and noninfectious viral particles.

With the introduction of highly active anti-retroviral therapy (HAART) regimen which uses combination of drugs (for e.g. commonly comprise two nucleoside-analogue RTIs and one non-nucleoside-analogue RTI or protease inhibitor) the AIDS related mortality has declined tremendously. However the most important aspect that affects the effectiveness, improving life expectancy by turning HIV from a terminal infection to a chronic disease is adherence or compliance [75]. As explained below based on PK-PD models, it also has a pharmacokinetic aspect to it which implies the maintenance of sufficient drug level in the blood to ensure reduction in viral replication as indicated by CD4 cell count and copies of viral mRNA in blood stream.

Pharmacokinetic-Pharmacodynamic correlations of anti-retroviral therapy

There are two major categories for PK-PD models for anti-retroviral therapy

    a) Short term dynamics: fit only the early segment of viral load trajectory

    b) Modeling long term treatment: includes the dynamics of viral load trajectory

Legrand et al. [76] reported an *in vivo* PK-PD model for anti-retroviral combination. In the study, patients were given an anti-retroviral combination including two nucleotide reverse transcriptase inhibitors zidovudine (250 mg twice daily) and lamivudine (150 mg twice daily) and one protease inhibitor (indinavir, 800 mg thrice daily) for 28 days. The three drugs were discontinued for 28 days in patients which had reached a plasma viral load of 1000 copies/mL. The same therapy was re-introduced at day 56. For evaluation of PK-PD relationship, only the first phase was studied, with patients being evaluated before and during therapy. Four samples were drawn on first day, three on second day and third day and one sample collected daily during the rest of the first week and on days 8, 10, 12, 14, 21, 25 and 28. Time between drug and sample intake was also recorded. Apart from routine biochemical parameters, HIV-1 viral plasma load and CD4 and CD8 counts in blood were measured at each visit. Compliance was assessed by personal interviews. Isolation of virus from mononuclear cells was performed at days 0, 28, 56 and 112 for complete sequencing of reverse transcriptase and protease. The drug levels were also quantitated by a validated LC-MS method. An indirect response model was utilized to describe the pharmacodynamic property of the drug as represented by the following equation

$$\%E = \frac{E_{max} \times C^{\gamma}}{C^{\gamma} + IC_{50}}$$

Where E is the reduction of viral load, E_{max} is the maximum effect, C is the concentration of the drug and IC_{50} is the drug concentration that reduces viral load by half and γ is the slope factor.

To incorporate the effect of combination the pharmacodynamic model was extended by weighting the concentration of each drug with the *in vitro* IC_{50} to reflect the relative potencies

$$\%E = \frac{E_{max} \times \Sigma C^{\gamma}}{\Sigma C^{\gamma} + EC_{50}}$$

Where $\Sigma C = 0.23\ C_{ZDV} + 0.67\ C_{LMV} + 0.046\ C_{IDV}$

EC_{50} determined by this model therefore represents the weighted concentrations sum of the three agents needed to decrease the viral load by 50%.

Long term–model (mechanistic)

The basic dynamic model describes the population dynamics of HIV and its target cells in plasma. The model considers target uninfected cells (T), infected cells (T*) that produce the

virus and the free virus (V). The model also has a time varying parameter γ(t) which quantifies the antiviral drug efficiency. The differential equations that define the model are

$$\frac{dT}{dt} = \lambda - \rho T - [1 - \gamma(t)]kTV$$

$$\frac{dT^*}{dt} = [1 - \gamma(t)]kTV - \delta T^*$$

$$\frac{dV}{dt} = N\delta T^* - cV$$

Where λ represents the rate at which new T cells are created, ρ is the death rate per T cell, k is the rate at which T cells become infected by the virus, δ is the rate of death for infected T cells, N is the number of virions produced from each of the infected cells and c is the clearance rate of the virions. The time variant parameter γ(t) is the time varying antiviral drug efficacy which is referred to as efficiency index.

In case the drug is not 100% effective the system of ordinary differential equations will have to be solved numerically. If γ(t) >e_c (threshold for drug efficacy) for all 'e' where

$$e_c = 1 - \frac{c\rho}{kN\lambda},$$

This would mean theoretically the entire virus would be eradicated. However if γ(t) <ec (treatment not potent enough), or if the potency falls below the threshold before virus eradication (e.g. due to resistance) , the viral load may rebound. Thus the efficacy threshold may reflect the immune response of the patient and is important parameter to be estimated based on clinical data.

Modified Emax model for drug efficacy of two agents within a class (e.g. protease inhibitors)

$$\gamma^{(t)} = \frac{IQ_1(t)A_1(t) + IQ_2(t)A_2(t)}{\emptyset + IQ_1(t)A_1(t) + IQ_2(t)A_2(t)} = \frac{AIQ_1(t) + AIQ_2(t)}{\emptyset + AIQ_1(t) + AIQ_2(t)}$$

Where

$$IQ_i(t) = \frac{C_{12h}^i}{IC_{50}^i(t)}$$

and

$$AIQ_i(t) = IQ_i(t)A_i(t), (i = 1,2)$$

denote the inhibitory quotient (IQ) and adherence-adjusted inhibitory quotient, respectively. IC_{50} is the drug concentration required to inhibit viral replication by 50%. C_{12h}^i and IC_{50}^i, $(i =$

1,2) are the drug concentrations in plasma measured at 12 hours from doses taken and median inhibitor concentrations for the two agents, respectively. $\emptyset$ is a parameter to be estimated. The concentration parameter C could be replaced with another suitable pharmacokinetic parameter like AUC or Cmax.

Phosphodiesterase 4 (PDE4) inhibitors

The PDE4 inhibitor classes of compounds included in the current research are cilomilast and roflumilast which are used in management of COPD. There are currently 11 recognized families of PDE which have differential regulation and expression. PDE4 is of major interest [77]. PDE4 is predominant in neutrophils, CD4+, CD8+ cells, monocytes and is also present in macrophages. PDE4 is also present in airway smooth muscle and epithelial cells, indicating that PDE4 inhibitors could also have effects on structural cells (Figure 2). Thus there is compelling scientific rationale for the use of PDE4 inhibitors in COPD, although their clinical development has been slow. Major PDE4 inhibitors in clinical trials include rolipram, cilomilast, roflumilast and oglimilast.

Figure 2: Advantages of PDE4 Inhibition
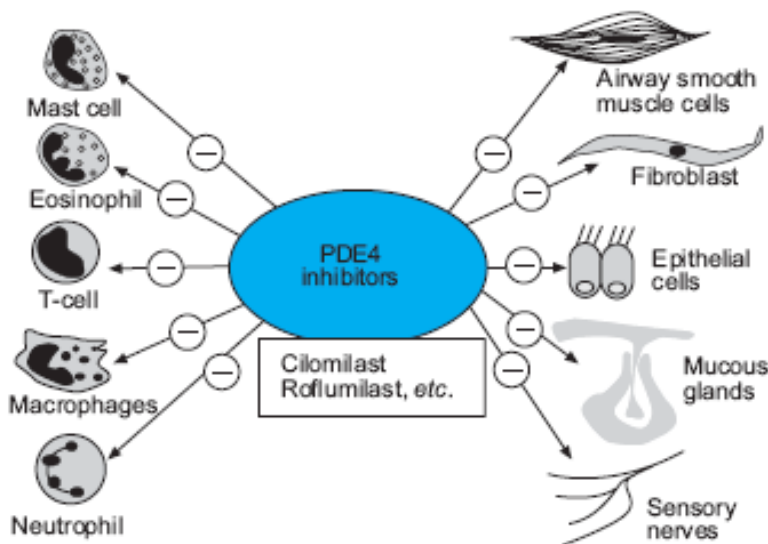
Phosphodiesterase-4 (PDE4) inhibitors have the potential to suppress inflammatory cells and structural cells in chronic obstructive pulmonary disease patients, giving a broad spectrum anti-inflammatory profile. Adopted from P.J Barnes and R.A.Stockley, 2005 [77]

The major adverse effects of PDE4 inhibitors include nausea, diarrhoea and headaches, which have led to the discontinuation of several drugs in early development. The side effects being mechanism related require the development of more subtype selective drugs.

Four human PDE4 isoenzymes have been identified and each has several splice variants. This raises the possibility that subtype-selective inhibitors may be developed that could preserve the anti-inflammatory effect, while having less propensity to side-effects. PDE4D (one of four genes encoding the PDE4 family) appears to be of particular importance in nausea and vomiting and is expressed in the chemo sensitive trigger zone in the brain stem. Targeted gene disruption studies in mice indicate that PDE4B is more important than PDE4D in inflammatory cells. PDE4B-selective inhibitors may, therefore, have a greater therapeutic to side-effect ratio and theoretically might be effective anti-inflammatory drugs. Cilomilast is selective for PDE4D and this would explain its propensity to cause emesis, whereas roflumilast, which is non-selective for PDE4 isoenzymes, has a more favourable therapeutic ratio. Several other potent PDE4 inhibitors with a more favourable therapeutic ratio are now in clinical development for COPD. Other problems with PDE4 inhibitors include ischaemic colitis in animal models, although the mechanism remains unknown, and an increased susceptibility to *Klebsiella pneumoniae* infections, possibly related to decrease TNF-α production.

Due to the side-effects of PDE4 inhibitors, other PDE isoenzymes that are expressed in inflammatory cells have also been investigated. PDE7A, like PDE4, is a cyclic AMP-selective PDE and has a widespread distribution in relevant inflammatory cells, including neutrophils, T-cells, monocytes and macrophages. The PDE7-selective inhibitor BRL 50481 has minimal inhibitory effects on monocytes, macrophages and CD8+ T-cells, but potentiates the anti-inflammatory effects of a PDE4 inhibitor on these cells, suggesting that combinations of PDE inhibitors may prove more effective in targeting causative mechanisms.

Anti-diabetic insulin secretagogues and insulin sensitizers

The anti-diabetic compounds used in the current research are tolbutamide (sulphonyl urea), vildagliptin (DPP IV inhibitor) and rosiglitazone (PPAR ϒ agonist).

The goals of therapy for type 2 diabetes mellitus (DM) are improved glycemic control with near normalization of the HbA1c. While glycemic control tends to dominate the management of type

1 diabetes mellitus, the care of individuals with type 2 DM must also include attention to the treatment of conditions associated with type 2 DM (obesity, hypertension, dyslipidemia, cardiovascular disease) and detection/management of DM-related complications. Diabetes mellitus-specific complications may be present in up to 20 to 50% of individuals with newly diagnosed type 2 DM. Reduction in cardiovascular risk is of paramount importance as this is the leading cause of mortality in these individuals.

Recent advances in the therapy of type 2 DM have generated considerable enthusiasm for oral glucose-lowering agents that target various physiologic processes in type 2 DM. Based on their mechanisms of action, oral glucose-lowering agents are subdivided into agents that increase insulin secretion, reduce glucose production, or increase insulin sensitivity. Oral glucose-lowering agents (with the exception of α-glucosidase inhibitors) are ineffective in type 1 DM and are not be used for glucose management of severely ill individuals with type 2 DM. Insulin is sometimes used as the initial glucose-lowering agent.

Insulin secretagogues stimulate insulin secretion by interacting with the ATP-sensitive potassium channel on the beta cell. These drugs are most effective in individuals with type 2 DM of relatively recent onset (<5 years), who have endogenous insulin production and tend to be obese. At maximum doses, first-generation sulfonylureas are similar in potency to second-generation agents but have a longer half-life, a greater incidence of hypoglycemia, and more frequent drug interactions. Thus, second-generation sulfonylureas are generally preferred.

Thiazolidinediones: Thiazolidinediones (TZD) represent a new class of agents that reduce insulin resistance. These drugs bind to a nuclear receptor (peroxisome proliferator-activated receptor, PPAR-γ) that regulates gene transcription. The PPAR-γ receptor is found at highest levels in adipocytes but is expressed at lower levels in many other insulin-sensitive tissues. Agonists of this receptor promote adipocyte differentiation and may reduce insulin resistance in skeletal muscle indirectly. TZDs reduce the fasting plasma glucose by improving peripheral glucose utilization and insulin sensitivity. Circulating insulin levels decrease with use of the TZDs, indicating a reduction in insulin resistance.

Rosiglitazone is a selective PPAR-γ agonist. Activation of PPAR-γ by TZDs induces the expression of a set of genes involved in adipocyte differentiation and lipogenesis, and these mechanisms are thought to be responsible for the insulin-sensitizing actions of these drugs.

PPAR-γ activation results in increased uptake of free fatty acids (FFAs) into subcutaneous adipose tissue. This, in turn, lowers circulating FFAs, thereby improving insulin resistance in liver and skeletal muscle ('the fatty acid steal hypothesis'). In addition to the direct effects of TZDs on adipose tissue, there are several indirect effects that might contribute to improved insulin resistance. TZDs can decrease tumor necrosis factor (TNF) and 11-β-hydroxysteroid dehydrogenase 1 levels, both of which are known contributors to insulin resistance.

TZD use is accompanied by weight gain and, in approximately 5% of patients, an increase in plasma volume which can lead to peripheral edema. Partial PPAR-γ agonists are being developed in an attempt to combine potent glycemic control with weaker adipogenic potential.

Dipeptidyl peptidase (DPP) IV inhibitors: DPP IV is the founding member of a family of DPP IV activity and structure homologue (DPP IV activity and/or structural homologue (DASH) proteins, enzymes that are unified by their common post proline cleaving serine dipeptidyl peptidase mechanism. DPP IV inhibitors have been prepared since 1977. Their synthesis and the different structural classes have in the meantime been the subject of different reviews. Three substance classes stand out whose representatives are under investigation in man.

a) Reversible product analogue inhibitors (e.g. pyrollidines, thiazolidines)

b) Covalently modifying product analogue inhibitors (e.g. cyanopyrrolidines)

c) Reversible non-peptidic heterocyclic inhibitors (e.g. xanthenes and aminomethylpyrimidines)

DPP IV is a post proline cleaving serine protease, existing as soluble and membrane bound form. It catalyzes the release of N-terminal dipeptides from biologically active peptides with the preference of proline > hydroxyproline > alanine in the penultimate position. DPP IV has high affinity for GLP-1 and thereby inactivates GLP-1 which can be prevented by DPP IV inhibitors leading to potentiating its biological activity on the pancreas augmenting insulin response with food stimulus DPP IV inhibitors have been shown to reduce blood glucose, improve glucose tolerance and improve insulin responsiveness to oral glucose challenges in animal models.

2.0.   RESEARCH GAP

2.1. Parameter Integration in Drug Discovery: Research Gap

In the process of new drug discovery, hundreds of compounds undergo high throughput screening against a specific target which could be a receptor, enzyme, intracellular protein etc. Once random hits are identified, there ensues a rigorous process of identifying the key pharmacophores that can be further optimized with structural modifications to generate compounds with improved potency and drug like attributes. Another approach is the rational design of a chemical series using known attributes already available and use of various molecular modeling tools or evidence based SAR development to design compounds. Regardless of the approach, these intense efforts are aimed to culminate in the optimization process to synthesize the best candidate for the target under consideration. This stage would involve assessment of critical physiochemical and ADME properties which could also become primary screening criteria along with potency. The selected set of compounds after primary screens would then progress into a more detailed evaluation of their activity with secondary pharmacological assays, *in vivo* PK as well as animal pharmacological models. At this level, the interplay of the physicochemical and ADME properties would start influencing the outcome of the efficacy assays. The hurdles thereon could be in terms of identifying the optimum range of characteristic for an ideal clinical candidate or to find the most appropriate properties that can be improved by modification of the series to achieve the clinical candidate. The screening process repeats with newer compounds synthesized with chemical modifications that are anticipated to improve various properties (solubility, lipophilicity, metabolic stability etc), which are evaluated again until a better candidate is identified. Most often, the chemical modification results in a variation of multiple properties and the interplay of them influencing the modulation of biological target makes the lead optimization process complicated. In spite of these efforts, there exists a possibility of the lead compound behaving differently in humans due to interspecies differences.

The development of a target product profile (TPP) becomes important in this context and it would involve a dynamic list of ideal properties that could be aimed to be achieved for a lead compound to be successful in clinic. TPP could also evolve with the understanding about the therapeutic target and competitive landscape which demands making it a best in class with improved properties than existing drugs or a first in class compound with a dosing strategy or regimen that ensures efficacy in clinic etc. The ultimate process in developing a clinical

candidate is to have an integrated comparison of efficacy, ADME and toxicological profiles with the risk factors clearly weighed against the positive attributes to choose a clinical candidate that provides a quantifiable benefit outweighing the known risks for the class. According to Curry and Brown [78] TPP provides a starting point from which the product planning can proceed from integration of planning tools to the development of screening sequence or testing cascade in conjunction with project specific objectives and activities.

The current research, reported in the thesis, limits to the PK aspects of TPP. There is definitely a large role that PK plays in the selection of a drug candidate as both the efficacy as well as safety of any drug depends on the availability and disposition of the drug in the biological system. Many of the areas addressed by TPP invariably have an ADME or PK component. For example the half-life of the drug in humans will govern for a majority of cases, the duration of action of the compound. Penetration rates into site of action are assessed in both qualitative and quantitative terms using PK methods. The dosage forms are assessed by pharmacokinetic methods and the dosing regimen is directly linked to the PK and PD correlation for the drug. Finally adverse reaction, drug-drug interaction and the need for patient therapeutic drug monitoring and/or dosage adjustments in the clinic are all predominantly exposure related and therefore, the role of PK is of paramount importance. Early ADME studies are also often the first "drug-developability" assessments of a compound after initial primary efficacy screens. Positive results allow a fast track entry into further developmental phases earlier without an iterative process of re-defining the clinical candidate. These initial developability studies may also uncover concerns regarding safety or efficacy that must be resolved before beginning the definitive nonclinical studies (e.g. regulatory toxicology evaluation) needed to support an investigational new drug (IND) application filing or before designing the clinical protocols, which will evaluate the candidate's safety and efficacy in humans. The identification and suitable remedial measures of these issues as early as possible allows for a more timely and efficient early development program. This in turn would pave the way for a program with fewer re-confirmatory studies. Hence substantial savings in terms of both time involvement and cost may be achieved with a better chance of successfully completing clinical phases of development.

A successful clinical candidate is thus a result of knowledge and experience accumulated in discovery programs (more precisely at the lead optimization stage). Therefore, being able to simulate human PK early in the discovery process as well as knowing beforehand the key properties that influence it would enable the discovery program to focus on optimizing the series rationally, make early assessment of the success of the particular chemical series, identify obstacles or even make an early decision to discontinue a particular series and eventually make the choice of a better candidate from a set of lead optimized compounds that suits the TPP. This rationale forms the basis of current research. Achieving the above would allow the discovery program to move ahead in a faster pace. The savings could be phenomenal and multidimensional in terms of financial resources, resource allocation, manpower and decision for course correction and/or substitution. A robust process once put in place should also allow the program to realign itself in the wake of newer scientific developments in understanding of the target or disease indication (for example identification of a new downstream pathway, or off target activity or modulation of other targets in a beneficial or detrimental manner, new information from clinical trials etc.)

The above mentioned need for an integrated approach brings certain important research questions that are addressed in the current research work.

a) How to dynamically integrate various screening data to predict human PK and identify key properties that influence a desired *in vivo* profile?

b) Once identified, how can they be put to use to develop or define a clinical candidate that has better chance of success?

c) Of the numerous properties that influence human PK profile, which is/are the most relevant?

d) How can the effect of structural modification be assessed before nomination of a clinical candidate (or initiating an expensive toxicology program)?

e) How to assess and compare the potential clinical efficacy and safety for a set of closely related compounds with subtle differences in various ADME and physicochemical properties?

A literature review on the above aspects revealed the clear inadequacy in addressing many of the research questions. Most of the lead optimization processes in practice today lack an integrated holistic approach, but focus on identifying this research question in a random manner. This observation is based on personal experience as well as lack of available literature reports on efforts in this direction. In other words, the process being followed today appears to be SAR centric from a chemists view point or more of a potency and physicochemical or pharmacokinetic point of view in terms of a biologist as evident from the numerous reports available on developing SAR, improving PK properties by altered solubility, formulation approaches, pro-drug approaches etc.. There have been efforts to develop models to predict various PK parameters prior to any clinical study. Most notable of them are the models to assess the absorption potential of pharmaceutical compounds based on molecular, physicochemical and ADME properties [22, 27, 79], prediction of clinical PK properties based on *in vitro* metabolism studies and *in vivo* animal data [1, 80, 81], extrapolation of animal data to humans using allometry [82, 83] with numerous correction factors that account for species differences in parameters such as clearance, volume of distribution etc. Also important to note are the *in silico* QSAR based models for human bioavailability prediction [84-86].

All these efforts emphasize the need for reliable and quantifiable prediction of human responses from preclinical animal data or *in vitro* data. Obach et al. [1] described a comprehensive retrospective analysis on the reliability of several methods for predicting human PK properties from preclinical data. An important observation in the analysis was the achievement of higher reliability with mixed approaches, where more than a single parameter was considered. For prediction of volume of distribution, the inclusion of plasma protein binding data resulted in a better prediction. Also an allometric (*in vivo*) volume prediction method was combined with *in vitro* clearance prediction method and the combination methods were generally found to be more successful in their ability to predict the human related parameter values. Parameter sensitivity analysis [87] was another technique used to address the outcomes of prediction across a parameter range. This method employs a series of simulations run over a range of different doses to examine how different parameters vs. time curve are affected. In a review by Venkatesh et al. [88] on the role of development scientist in compound lead selection and optimization, the early consideration of development criteria along with receptor potency and specificity has also been highlighted.

55

While these approaches are definitely valuable and necessary, there is a need for development and implementation of a strategy that allows collating and mechanistically integrating inputs from various screening data. The primary focus of the strategy should be the integration of numerous screening data as building blocks to simulate human PK profile for compounds early in the discovery stage with inputs from commonly employed pre-clinical screening data. It is important to have a mechanistic integration incorporating physiological factors as well, which would enable the model to closely resemble a physiological system which can be used as a predictive analysis tool for lead optimization, which will not be feasible with empirical models. Further, to optimize the chemical series, it requires understanding of the key properties that influence a PK parameter. This can be achieved by a multivariate approach utilizing pooled screening data of all the compounds and identifying the trends in data and relatively analyze the contribution of various properties to a PK parameter under consideration for improvement. This approach should bring forth a novel concept of mechanistic integration as well as identification of key properties for rational lead optimization.

2.2. Key Research Gaps Identified

The following key research gaps are identified which form the basis for the current research

a) How to integrate various screening information mechanistically that allows the prediction of human PK parameters in a way that could relate with its biological efficacy as well as physicochemical, chemistry and ADME properties?

b) How can the relative contribution of various screening properties be assessed and how to prioritize them to give a feed back to medicinal chemist?

c) How to assess the influence of changes made in these properties on the three basic PK parameters of absorption distribution and elimination that defines *in vivo* human PK profile?

To summarize, the current research focuses on the research need for a broad methodology to relate various physicochemical and ADME properties to predict human PK parameters and analyze the relative influence of various properties on them allowing their selective optimization and permit rational choice of a candidate with most probable chance of success in the clinic.

3.0.   RESEARCH OBJECTIVES, SCOPE AND LIMITATIONS

3.1.   Objectives of Current Research

The current research utilizes a set of 13 clinically proven compounds belonging to the class of beta blockers, anti-retroviral, PDE4 inhibitors (for COPD) as well as anti-diabetics. The research aims to develop a new methodology to be used in drug discovery research for a rational lead optimization and selection of clinical candidate. Choice of clinically used compounds therefore would allow the verification of many of the outcomes of the new methodology like prediction of human PK parameters and plasma concentration profile in comparison with reported clinical data. Based on the exhaustive literature review, PBPK models have been identified as an ideal method for integrating various screening data in the current research to predict key pharmacokinetic parameters of absorption tissue distribution and clearance. These parameters would then be applied for simulation of human oral concentration-time profile using one compartment kinetic equation, assuming first order absorption. Since there are few reports of PBPK based prediction of human PK profile after oral dose with most of the effort in prediction of absorption or volume of distribution or clearance, the current research would also add value in terms of utilizing them for prediction of oral concentration-time profiles. To analyze the effect of various trends in the data and to assess the contribution of individual properties to the final outcome, a multivariate analysis approach has been adopted using partial least square regression (PLS) analysis.

The following are the broad objectives of the current research

a) To develop a new methodology to assess the influence of various physicochemical and ADME screen data on the human pharmacokinetic profile with a retrospective study of few selected compounds belonging to different therapeutic areas, with known clinical outcome.

b) The research involves experimental generation of various physicochemical and ADME screening data mimicking a discovery process (as well as avoiding variability of any reported data from various sources) followed by the mechanistic modeling (PBPK) to predict key pharmacokinetic parameters and simulate human pharmacokinetics with one compartment PK model equation.

c) Validate the mechanistic predictions with the reported clinical human pharmacokinetic data as the clinical information of the compounds is known. In the current research the predicted human PK parameters and *in vivo* PK profiles have been compared with reported literature values and the reliability of predictions have been assessed with precision and bias estimates.

d) Using a multivariate approach (PLS), analyze the latent trends in screening data and estimate the relative contribution of various properties on the human pharmacokinetic profile. The result is a standardized PLS coefficient plot rank ordering the various properties in their order of relevance which can be taken up for optimization by chemical modification.

e) Demonstrate the utility of above analysis in lead optimization : The utility of focusing on identified parameters and optimizing them in a discovery program has been illustrated with the following two steps considering that current research has not included any experimental chemical synthesis or modification within its scope

   i. Illustrate the effect of chemical modifications on human *in vivo* profile by simulation using the same approach of PBPK modeling with one compartment model simulation, as used in this research. The modifications made are assumed as two fold variation (0.5 x and 2.0 x) of few individual basic ADME or physiochemical properties (microsomal clearance, solubility and Log P). In a discovery program this would reflect chemical modifications made on the pharmacophore resulting in a change of these properties (solubility, permeability, metabolic stability etc.). For ease of illustration only a single parameter is changed at a time though the PBPK methodology and simulation can incorporate multiple variations at a time which is a more practical scenario.

   ii. Correlation of the modified human PK profiles obtained as above with PK-PD information demonstrating effect on efficacy, dosing regimen etc.

To summarize, the current research aims to develop a new methodology for application in drug discovery which integrates various screening data mechanistically and predicts *in vivo* human PK profile using PBPK, analyzes the relationships with PLS to prioritize key properties for optimization allowing efficient integration between medicinal chemistry pharmacokinetics and

biology by giving valuable inputs on optimization, permits evaluation of modified compounds with the same approach and doing so allows a rational selection of lead compound basing on a TPP.

3.2. Steps Involved in the Research

a) Perform individual screens on various physicochemical and ADME properties for the selected 13 compounds: solubility (pH 1.8, 3.0, 4.5, 6.8 and 7.4), Caco-2 permeability liver microsomal clearance, plasma protein binding and blood plasma partitioning and collate all generated data.

b) Incorporate the individual data to PBPK models for prediction of human PK parameters and simulate human PK assuming one compartment kinetics with first order absorption.

c) Compare the simulated PK parameters with reported human values from literature.

d) Assess the influence of various physicochemical and ADME properties on key pharmacokinetic parameters using partial least square (PLS) analysis of pooled data.

e) Illustrate rational lead optimization by predicting the influence of two fold (0.5 x and 2.0 x) change of key properties identified by PLS on the simulated human PK profiles.

f) Using the results discuss on the application of the new methodology for a rational selection of clinical candidate by correlating with efficacy, with representative examples.

3.3. Scope of Current Research

a) The research aims to find a methodology that can be adopted in a research laboratory at the lead optimization stage for generation of a viable clinical candidate for early drug development.

b) The different mathematical models used in the research are a result of extensive literature research with complete understanding of mechanistic models and as such, these models can be used for prediction of various human PK parameters as well as simulation of *in vivo* PK profile

c) The novel utility of the multivariate analysis technique PLS to critically analyze the role of various properties on a response pharmacokinetic parameter using a series of compounds has been demonstrated for implementation in lead optimization stage

d) Application of this methodology would allow a research team to predict human PK profile well in advance. However the industry standard *in vitro* assays need to be employed for incorporation of the physicochemical and ADME properties of the compounds.

e) The methodology would enable the discovery scientist working in pharmacokinetics to interface with chemistry and biology scientists by giving valuable feedback to achieve acceptable chemical and biopharmaceutical properties that can result in clinical efficacy and reduced adverse effects.

f) The predicted human PK profile can then be used to extend the PK-PD correlation developed basing on animal model data with more reliability and would allow to choose clinical candidates that would exhibit a better human profile.

g) The flexibility of mechanistic models would allow incorporating future advances in understanding and mathematical modeling of the processes (inclusion of transporter effects, induction effects, biliary excretion etc.)

h) Overall the methodology would allow the discovery research team to make rational decisions, assess risks earlier in terms of critical properties to be modified and assess the feasibility beforehand and allocate material and human resources effectively, avoid redundancies and save time and cost.

3.4. Limitations of Current Research

a) The current research limits to the PK attributes of the compound in a manner that enables it to interface with other disciplines in drug discovery and for rational decisions in candidate selection. The methodology however can be extended to biological properties as well and many of the biological parameters like receptor affinity, association and dissociation rates, and fold selectivity over undesirable homologous targets (e.g. DASH members for DPP IV inhibition, PPAR α vs. γ selectivity), threshold levels for

exaggerated pharmacological effects (e.g. emesis in PDE4 inhibition) etc. can also be included as part of the optimization. These are not included as part of the current research

b) Effect of transporters, mechanism based inhibition of drug metabolism (reactive species generation), CYP induction, biliary excretion and entero-hepatic recirculation etc. are definitely additional biological phenomenon that influence the final outcome which are not part of the current research methodology. However the methodology (PBPK models) is chosen keeping these parameters in mind, so that they can be incorporated in future. There are research efforts reported in this direction with incorporation of fold change in AUC with induction and inhibition [89], effect of GI metabolism and transporters on absorption [90] etc. are being incorporated into these models and definitely need more computational and mathematical modeling. The ability to incorporate these properties with development of further understanding is an important advantage of using mechanistic models and has been thought about in its conception.

c) The current research methodology is ideally meant for compounds within a series (homologous series) or comparison across sets of diverse chemical scaffolds. Since the current research aims to prove this hypothesis retrospectively with clinically proven compounds, the availability of multiple compounds for a single target is limited to few numbers. Being of different class has a bearing on the PLS analysis using pooled data as the correlations observed with properties and PK parameters are purely a demonstration and does not indicate for a specific chemical series. However this is not considered to have any bearing on the objective of research as the focus is on the methodology rather than any individual chemical series. Inclusion of different chemical series on the other hand enhances the reliability of simulation techniques in the study.

d) An alternate approach to one compartment PK model based simulation could be the application of whole body physiological models incorporating a series of differential equation predicting the various tissue levels as well as the plasma concentration profiles directly. This effort though computational and mathematically intensive and practically impossible without software resources, could have had the advantage of predicting multi-compartment kinetics, not limiting to a one compartment model.

e) There could be some effects that are likely to be masked in the current research as the test compounds used were clinically optimized and must have been devoid of many adverse characters that are not desirable clinically. Few aspects include the presence of impurities in the drug substance that influences its screening results, lack of optimized physical (amorphous crystalline, uniform particle size) and chemical (appropriate salt form or free base) forms of the drug etc. which would be common in the early discovery stages. However it is believed that a systematic assessment of these parameters would alert the scientist and the robust methodology (application of mechanistic models as well as PLS) would enable the scientist to differentiate the outcomes.

f) The methodology applies to all types of small molecule based drug discovery in its principle and application (which is the objective and the expected utility of this research), however the results and observations (for e.g. relative influence of each parameter on the outcome) would definitely vary for each chemical series to which it is applied and also the complexity of overcoming it through efforts in chemistry would also vary. This could also depend on the expectation setting on the compound (TPP). For example, in the design of a better drug in terms of duration of action, clearance may be a major challenge identified and the scaffold due to its chemical characteristics may limit possibilities of overcoming it while simultaneously ensuring target activation.

4.0.   MATERIALS AND METHODS

4.1. Test Compound Properties and Experimental Details

The molecular weight, Log P as well as pKa estimates of the test compounds were taken from literarure . Log P_{vow} was derived from Log P_{ow} using the following empirical relation [51].

$$LogP_{vow} = 1.115 \, LogP_{ow} - 1.35$$

Log D_{vow} as well as the neutral fraction at pH 6.8 and 7.4 was estimated basing on the Handerson-Hasselbalch equation [8, 51] .

1) For monoprotic acids

$$LogD_{vow} = LogP_{vow} - Log\,(1 + 10^{pH-pKa})$$

2) For monoprotic base

$$LogD_{vow} = LogP_{vow} - Log\,(1 + 10^{pKa-pH})$$

3) For diprotic acids

$$LogD_{vow} = LogP_{vow} - Log\,(1 + 10^{pH-pKa1+pH-pKa2})$$

4) For diprotic base

$$LogD_{vow} = LogP_{vow} - Log\,(1 + 10^{pKa1-pH+pKa2-pH})$$

5) For zwitterionic compounds

$$LogD_{vow} = LogP_{vow} - Log\,(1 + 10^{-pKa2+pH+pKa1-pH})$$

Where pKa1 is acidic and pKa2 is basic.

6) For neutral compounds

$$LogD_{vow} = 1.115 \, LogP_{ow} - 1.35$$

The neutral fraction at pH 6.8 and 7.4 were estimated using the following relation

$$f^0(z) = \frac{1}{1 + 10^{\pm(pH(z)-pKa)}}; \; (+for\ acids\,, -for\ bases)$$

4.1.1. Determination of Solubility at Various pH

Equilibrium solubility of the test compounds were measured at various pH (1.8, 3.0 4.5, 6.8 and 7.4). The technique involved the preparation of various buffers.

Buffer pH 1.5: 0.05M sodium chloride, pH adjusted to 1.8 with hydrochloric acid

Buffer pH 3.0: 0.05M sodium chloride pH adjusted to 3.0 with hydrochloric acid

Buffer pH 4.5: 0.05M Sodium dihydrogen orthophosphate, adjusted to pH 4.5 with sodium
hydroxide

Buffer pH 6.8: 0.05M Sodium dihydrogen orthophosphate, adjusted to pH 6.8 with sodium
hydroxide

Buffer pH 7.4: 0.05M Sodium dihydrogen orthophosphate, adjusted to pH4.5 with sodium
hydroxide

Methodology

The assay was performed using a shake flask method. Around 1.5-2.0 mg of test compound was weighed into a flat bottom glass vial for each pH tested and mixed with buffer at the proportion of 500μL per mg. The glass vials were then placed in a shaker and was shaken for 24 hours at room temperature (22-25°C). The samples were the filtered using syringe filters (0.45 micron, Millipore, USA) and were analyzed by high performance liquid chromatography (HPLC) against a known standard.

HPLC Analysis

Two ternary gradient generic methods were developed for the compounds. A short run generic method of 15 minute duration was used for compounds atenolol, metoprolol, propranolol, nelfinavir, indinavir, efavirenz, cilomilast, vildagliptin and rosiglitazone and the extended run (40 minute duration) was used for the remaining compounds (nevirapine, ritonavir, roflumilast and tolbutamide). The standards consisted of DMSO stocks of the compounds (0.5mg/mL) which were correlated with their respective area for various quantities introduced on column (by varying the injection volumes 1.3, 2.5 and 5μL, respectively). The test solution was injected at an appropriate volume of 25, 50 or 100μL and compared with the closest standard or a three point calibration curve. From the back calculated value corrections were made for the injection volumes and the solubility was estimated per unit volume (mg/mL) of the buffer.

HPLC Parameters

Column   : Inertsil ODS 3V (250 x 4.6 mm, 5μm)
Mobile Phase

    Component A (buffer) : Ammonium acetate 10mM, pH 6.8

    Component B   : Methanol: Buffer (95:5, v/v)

    Component C   : Acetonitrile: Buffer (95:5, v/v)

Gradient Program

Time (minutes)	%A	%B	%C
0	100	-	-
1	100	-	-
3	30	30	40
6	5	25	70
11	5	25	70
12	100	-	-
15	100	-	-

Gradient Program (extended run)

Time	%A	%B	%C
0	100	-	-
2	100	-	-
3	90	-	10
9	50	30	20
12	50	25	25
25	30	20	50
28	5	10	85
35	5	10	85
36	100	-	-
40	100	-	-

4.1.2. **Determination of Caco-2 Permeability**

Reagents and Equipment

a) Dulbecco's Modified Eagle Medium: Gibco BRL, Gaithersburg, MD (Catalog No.12430-054)

b) Fetal bovine serum: Gibco BRL, Gaithersburg, MD (Catalog No. 10082-147)

c) L-glutamine: Sigma chemical Co. USA (Catalog No. G7513)

d) Sodium bicarbonate: Sigma chemical Co. USA (Catalog No. S1554)

e) D-glucose: Sigma chemical Co. USA (Catalog No G7528)

f) HEPES: Sigma chemical Co. USA (Catalog No. H3375).

g) Sodium chloride: Sigma chemical Co. USA (Catalog No. S7653)

h) HBSS (Hanks buffered salt saline): Sigma chemical Co. USA (Catalog No. H1387)

i) PBS (Phosphate buffered saline): Gibco BRL, Gaithersburg, MD (Catalog No.10010-049)

j) Caco-2 cells: American Type Culture Collection, Rockville, MD (Catalog No. HTB 37)

k) Tissue Culture plates and flasks: Nalge Nunc International, USA (Catalog Nos. 156472 and 140685)

l) Transwell tissue culture inserts: Nalge Nunc International, USA (Catalog No.137435)

m) Millicell- ERS voltameter and electrode: Millipore India Pvt. Ltd.

n) Hot air incubator maintained at 37°C (New Brunswick Scientific).

o) Refrigerated centrifuge (Eppendorf)

Methodology

Caco-2 cells (HTB 37) were procured from American Type Cell Culture (ATCC). The cells were cultured in T75 flasks using Dulbecco's Modified Eagle Medium (DMEM; supplemented with 10% FBS and 2mM L-glutamine), at 37°C in an atmosphere of 5% carbon dioxide and 95% relative humidity. For experiments, cells within a passage number of 30 to 60 were used. Passage of the cells was done within 70-90% confluence using trypsin EDTA. To prepare the cell monolayer, the cells were seeded in 6 well or 24 well polycarbonate inserts (Nunc, 3μm pore size, placed over plates) at a density of 52000 cells per insert. The media was changed after 3 days of seeding and thereafter every alternate day until day 21. To assess the growth and integrity of cell monolayer the Trans Epithelial Electrical Resistance (TEER) was measured on day 21. The resistance measured is a direct function of intact monolayer formation with TEER values increasing with growth of cells and stabilizing after monolayer formation. Transwells expressing a TEER value of >400 ohms were used for the study. The TEER value of inserts without any monolayer ranged 150 ohms. The permeability experiments were conducted within day 21 to day 23 of seeding. On the day of the experiment the cell monolayer (in inserts) was washed with sterile phosphate buffered saline (PBS) pH 7.4, to remove traces of culture media. The inserts were subsequently added with 0.5mL of HBSS buffer (pH 7.4) to the basolateral compartment and 0.25mL of HBSS buffer (pH 6.5) to the apical compartment and incubated for at least 30 minutes at 37°C in the incubator, before initiating the experiment.

A primary stock solution of the test compound was prepared in DMSO. The working solutions (preparation in buffer, used for the experiment) were prepared in HBSS buffer pH 6.5 (pH of the small intestine). The proportion of organic solvent was limited to 0.5%. An appropriate test

concentration in the range of 10 to 50µM was chosen based on the available solubility information at pH 6.8.

The permeability experiment was performed outside the laminar hood. The buffer solutions added for conditioning the monolayer was removed and the study was initiated by the addition of 250µL drug working stocks prepared in HBSS pH 6.5 to the donor (apical) side and 500µL of HBSS buffer (pH 7.4) containing 0.5% DMSO, to the acceptor (basolateral) side. The plate was placed in a hot air incubator shaker maintained at 37°C. Periodic aliquots of 150µL was withdrawn from the basolateral compartment at 15, 30, 45, 60, 90 and 120 min time intervals and was stored for analysis at -20°C. After sampling an equal volume of media was replenished every time. At 120minutes, samples (150µL) were also withdrawn from apical side for mass balance studies. The concentration of test compound in study solution and samples were estimated by a suitable HPLC or LC-MS based analytical method and using a suitable calibration curve. Using the concentrations estimated the cumulative amount transported (Q) at each time point was estimated as follows.

$$Q_{15} = C_{15} \times V_R$$

$$Q_{30} = C_{30} \times V_R + C_{15} \times V_S$$

$$Q_{45} = C_{45} \times V_R + (C_{15} + C_{30}) \times V_S$$

$$Q_{60} = C_{60} \times V_R + (C_{15} + C_{30} + C_{45}) \times V_S$$

Where

V_R is the volume in the receiver compartment (0.5mL for a 24 well plate).

V_S is the sampling volume from basolateral side (150uL).

C is concentration in micromoles

The cumulative amount (Q in µM) transported was plotted as a function of time and the slope of the linear segment, which is the linear appearance rate of the test compound into the basolateral compartment (dQ/dt), was calculated.

The apparent permeability was calculated using the equation

$$P_{app} = \frac{dQ}{dt} \times \frac{1}{A \times C_0}$$

Where

dQ/dt is the slope of the best fit line of the function; cumulative rate of appearance vs. time

A is the area of the cell monolayer (4.2 cm^2 for 6 well plate and 0.78 cm^2 for 24 well plate)

C_0 is the concentration of the test compound used (micromoles)

4.1.3. Determination of Plasma Protein Binding

Reagents and Equipments

a) Phosphate buffer saline pH 7.4 (PBS): Gibco BRL, Gaithersburg, MD (Catalog No. 10010-049).

b) Human plasma

c) Protein separation tubes and 96 well plates (Millipore, 10 KD)

d) Test compound stock in DMSO (200 and 2000μg/mL)

e) Refrigerated centrifuge (Eppendorf)

Methodology

An aliquot of 0.5mL human plasma added into test tubes was used in duplicates for each test concentration. After 5 minute incubation in a hot air incubator 2.5μL of the test compound (to provide a final concentration of 1μg/mL and 10μg/mL in plasma) was spiked into plasma and mixed well by vortexing. The plasma was then incubated at 37°C for 30 minutes in a hot air incubator shaker.

After incubation, 300μL of plasma was transferred to 96 well protein separation plates (regenerated cellulose membrane filters with 10000 Daltons cut off, Millipore, USA). The protein filtration assembly consisted of a 96 well filter plate placed over a collection plate and a cover holding the plates together (Millipore, USA). After transferring plasma, the assembly was centrifuged in a swing rotor at 2000 rpm (1800 x g) for 30 min and the ultra-filtrate was collected. The test compound was estimated in both the whole plasma and the ultra-filtrate sample using an appropriate HPLC method and the % bound was calculated as per the following equation.

$$\text{\% Bound to plasma} \quad = \quad 100 \times (1 - C_{uf}/C_p)$$

Where,

C_p = Initial concentration of test compound in plasma

C_{uf} = concentration of test compound in ultra-filtrate.

Warfarin was used as the standard and was tested at a concentration of 0.25 µg/mL with the expected % plasma binding of > 99%. The unbound fraction of the compounds was estimated from % bound as f_u=1-(%bound/100).

4.1.4. Determination of Blood to Plasma Partitioning

Reagents and Equipments

a) Test compounds, accurately weighed and dissolved in DMSO (100 and 1000µg/mL)

b) Human blood and plasma

c) Hot air incubator maintained at 37°C.

d) Centrifuge

Methodology

The blood-plasma ratio of compounds was estimated at 0.5 and 5µg/mL. An aliquot of 0.5 mL blood (heparinized) and plasma were added to plastic centrifuge tubes (Tarson) and were placed in a hot air incubator. After an incubation of 15 minutes, 2.5µL of test compound stock was spiked into blood and plasma for each concentration tested. The samples were then incubated for 30 minutes at 37°C. At the end of incubation the blood samples were centrifuged at 5000 x g (Eppendorff, refrigerated centrifuge) for 5 minutes and the plasma was separated. The concentration of the test compound was estimated in all the plasma samples using a suitable analytical method and was read against a standard curve prepared in plasma. The test compound estimated in whole plasma samples was considered as the standard equivalent to whole blood concentration. The hematocrit of the blood samples was estimated and an average hematocrit of 46.9 was used for human blood. The concentration of the test compound estimated from plasma separated from blood was corrected for the hematocrit and the blood plasma partitioning (R_B) was estimated.

$$C_{PB} = C_P(1 - H_t)$$

$$R_B = \frac{C_{WP}}{C_{PB}}$$

Where,

C_P: concentration of test compound in plasma separated from whole blood

H_t: hematocrit (0.469 for human blood)

C_{PB}: Concentration of test compound in plasma separated from blood corrected to hematocrit

C_{WP}: Concentration of test compound spiked in whole plasma

4.1.5. **Determination of Intrinsic Clearance in Liver Microsomes**

Reagents and Equipments

a) Test compound/NCE, diluted from a suitable stock solution to achieve 100 uM in DMSO

b) Human liver microsomes (20mg/mL, BD Biosciences, USA)

c) Phosphate buffer pH 7.4 (100mM)

d) NADPH regenerating system consisting of 5mg/mL of magnesium chloride, nicotinamide adenine dinucleotide phosphate (sodium salt), glucose 6 phosphate and 40 IU of glucose 6 phosphate dehydrogenase enzyme

e) Quenching solvent [mixture of acetonitrile/methanol: ethanol: acetic acid (79:20:1, v/v)] containing internal standard to arrest the reaction.

f) Hot air incubator maintained at 37°C

g) Tecan automated liquid handling system (automated assay)

h) Refrigerated centrifuge

Intrinsic clearance was determined in human liver microsomes at a test compound concentration of 0.5μM. The metabolic reaction mixture was prepared by addition of 400μL of NADPH regenerating solution, 25μL of liver microsomes (0.5 mg/mL of protein in the final reaction mixture) and made up to volume of 995μL with phosphate buffer (100mM, pH 7.4). The reaction mixture was prepared in glass vials and was placed in orbital shaker (Teshake, Tecan). The mixture was incubated for 10 minutes at 37°C and the metabolic reaction was initiated by

the addition of test compound (5µL of 100µM stock). Periodic aliquots of 70µL were withdrawn at 0, 3, 6, 9, 12, 15, 18, 21, 24 and 30 minutes. The aliquots were immediately transferred to a 1mL deep well plate containing 570µL of quenching solvent [mixture of acetonitrile:ethanol: acetic acid (79:20:1, v/v)] containing internal standard (IS) and was mixed thoroughly using a multichannel pipette. After the last sample was collected the plate was centrifuged at 2500 x g in a swing rotor centrifuge and the supernatant was used for analysis. The parent compound remaining was estimated at each time point from the samples and was expressed as percentage of 0 minute. The data was fit into a one-phase exponential decay function using GraphPad Prism (version 4.02, San Diego, USA) software and the first order degradation rate constant (k) was estimated based on the following relation

$$Y = span \times e^{-kt} + C$$

Where Y is the percent remaining of test compound, span is the value of y-intercept at t=0 (which is kept at value of 100), k is the first-order rate constant, t is the time and C is the constant to account for the plateau, determined by the software. The first order rate constant was normalized to unit protein content and was multiplied by the microsomal protein per gram of liver (52.5mg/g of human liver) to derive the intrinsic clearance. The intrinsic clearance was expressed in units of mL/min/g liver. An internal synthetic compound with high clearance (> 50 mL/min/kg) was used as control to ensure the functionality of microsomes in the reaction.

The analysis of various study samples were performed by LC-MS/MS based method. An API-4000 triple quadrupole system (Applied Biosystems) coupled with a HPLC or UPLC (Shimadzu) was used for analysis. For compounds in positive ion mode, rolipram was used as the internal standard and for cilomilast, which was ionized in negative ion mode, an in-house synthetic compound was used as an internal standard. The mobile phase consisted of a mixture of 10mM ammonium formate buffer and acetonitrile separated using a C18 column (Hypurity Advance, 50 × 4.6 mm, 5µm). The LC-MS parameters used in the detection of various compounds at the multiple reaction monitoring modes (MRM) are summarized in Table 6.

73

Table 6: Summary of LC-MS Method Parameters Used for Various Compounds

Compound	Ion mode	Ion spray voltage	Source temperature (°C)	Parent/ daughter ion	Declustering potential (DP)	Entrance potential (EP)	Collision energy (CE)	Collision cell exit potential (CXP)
Atenolol	+ve	5500	500	267.2/145.1	80	10	25	9
Metoprolol	+ve	5500	500	267.9/116.1	80	10	25	9
Propranolol	+ve	5500	500	260.3/116.2	80	10	35	10
Nevirapine	+ve	5500	500	267.3/226.1	90	10	38	13
Nelfinavir	+ve	5500	500	568.4/330	130	10	46	20
Ritonavir	+ve	5500	500	721.4/296	42	5	11	13
Indinavir	+ve	5000	495	614.3/421.1	40	10	40	10
Efavirenz	+ve	4500	495	316.1/244.1	40	10	19	10
Cilomilast	-ve	5500	600	342.1/213.9	39	10	15	18
Roflumilast	+ve	5500	500	405.2/187	80	10	30	10
Vildagliptin	+ve	5500	500	304.5/154.0	80	10	35	10
Tolbutamide	+ve	5500	500	271.1/91.1	68	10	45	17
Rosiglitazone	+ve	5000	500	358/135	60	10	30	15

4.2.   Prediction of Pharmacokinetic Parameters

4.2.1.   Prediction of Absorption Rate Constant and Fraction Absorbed

Method 1: Usansky et al.

To derive the absorption rate constant (K_a) the experimentally determined Caco-2 permeability and the predicted volume of distribution of highly perfused tissues and reported surface area of intestine were used and was based on the relationship by Usansky et al. [6]

$$K_a = \frac{P_m S}{V_c}$$

Where P_m is the Caco-2 permeability (cm/sec) which was experimentally determined, S is the reported absorptive surface area of the intestine (200m^2) [91] and V_c is the determined volume of distribution of highly perfused tissue (refer methods section on determination of volume of distribution)

Based on the above computed value of absorption rate constant, the fraction absorbed was calculated from the following relation by Usansky et al. [6].

$$F_a = \frac{K_{a,eq}}{K_i + K_{a,eq}}$$

Where $K_{a,eq}$ is the intestinal absorption rate constant at equilibrium, which is same as the K_a estimated using the above equation. K_i is the first order rate constant of intestinal transit (0.005025 /min) [6].

Method 2: Estimation of Fraction Absorbed Using Simplified GI Compartmental Modeling

In the GI compartmental transit model the compartments of stomach, duodenum, jejunum, ileum and colon were considered. At every segment of the intestine (stomach, duodenum, jejunum, ileum and colon), the available drug was estimated based on the product of solubility of the compound at that particular pH (estimated from solubility studies) and the volume of segment. In case it was found that the amount of drug that was estimated to transit from the previous segment after absorption yielded a value lower than intrinsic solubility at that pH, then the soluble amount of the compound at that segment was considered limited by availability of the drug and the exact

value was used (amount of drug transited to the segment multiplied by volume of segment). The absorption rate constant at each segment (ka) was estimated as per the relation provided by Usansky et al. [6]

$$k_a = \frac{P_m s}{V_c}$$

In this case P_m denoted permeability (estimated from Caco-2 assays, no corrections were made for pH), s denotes effective surface area of the segment and V_c, the volume of distribution of the compound in rapidly perfused tissues.

Further the maximum absorbable dose at segment was estimated by the following relation

$$MAD_{seg} = s \times k_a \times v \times t$$

Where s denotes solubility at the compound at the pH of the segment k_a, the absorption rate constant estimated for that segment, v, the luminal volume (assuming no limitation of fluid availability) and t, the transit time of the intestine.

Thus for a fixed dose input in the model the absorption rate constant and the maximum absorbable dose were estimated and the total drug absorbed was estimated as the sum of MAD_{seg} estimates for stomach, duodenum, jejunum, ileum and colon. The fraction absorbed was estimated as the fraction of the MAD to the total dose administered.

For simulation of human PK method 1 (Usansky et al.) which gives an equilibrium estimate of absorption rate constant was used, being representative of the average K_a in the GI tract. For assessing the effect of fold change (0.5 x and 2.0 x) in solubility, Method 2 was applied due to a higher sensitivity of GI compartmental approach in assessing changes in solubility and permeability.

4.2.2. **Prediction of Fraction Bioavailable**

For simulation of human PK, the fraction bioavailability was derived from the fraction absorbed (F_a) using the following relation [3]

$$F = F_a \times \left(1 - \frac{CL_h}{Q_h}\right)$$

4.2.3. **Prediction of Volume of Distribution**

Volume of distribution was estimated as per the following relation [3, 42]

$$V_{ss} = V_p + \sum_{i=1}^{n} P_{t:p}V_t + (V_E \times C_E{:}C_P)$$

Where V_t denotes the volume of tissue, P_{tp} the tissue plasma partitioning ratio, V_E, the volume of erythrocytes. $C_E{:}C_P$ denotes the ratio of concentration of drug in erythrocytes to plasma estimates as

$$C_E{:}C_P = (R_B - (1 - Ht)/Ht)$$

Where R_B stands for blood to plasma partitioning ratio (estimated experimentally) and Ht for hematocrit. The tissue plasma partitioning ratios were estimated based on the Poulin-Theil method [4, 47, 48] and modified further by Berezhkovskiy [52].

$$P_{tp} = \frac{P_{vow}(V_{NLt} + 0.3V_{PHt}) + 0.7V_{PHt} + (V_{Wt}/f_{ut})}{P_{vow}(V_{NLp} + 0.3V_{PHp}) + 0.7V_{PHp} + (V_{Wp}/f_{up})}$$

Where P_{vow} is the vegetable oil-water partitioning coefficient (olive oil) estimated with the empirical relation from the octanol, water partition coefficient [51]

$$logP_{vow} = 1.115\ logP_{ow} - 1.35$$

V is the fractional tissue (t) or plasma (p) volume content of neutral lipids (NL), phospholipids (PH) ad water (W). The various physiological constants of volume of tissue, volume fraction of neutral lipids and phospholipids in tissue and plasma (VNLT, VNLP, VPHT and VPHP) were used from the compilation by Poulin-Theil from literature. The values are presented in Table 2. For estimating the plasma tissue partitioning of adipose tissue using the above equation the vegetable oil-water partition coefficient of the non-ionized compound (D_{vow})was used instead of P_{vow}.

4.2.4. **Prediction of Fraction Unbound in Microsomes**

The unbound fraction in microsomes was estimated from octanol water partitioning data as per the relation reported by Austin et al. [64]

$$f_{u\ microsomes} = \frac{1}{e^{(0.53\ logD\ o/w - 1.42)} + 1}$$

4.2.5. **Prediction of Clearance**

In Vivo **Hepatic Clearance**

For determination of *in vivo* hepatic blood clearance, experimentally determined microsomal intrinsic clearance, fraction unbound in plasma (fu_p), blood to plasma partitioning (R_B) and derived values of fraction unbound in microsomes (fu_{inc}) were used. A well stirred model for predicting *in vivo* hepatic clearance was used as per the following relationship.

$$CL_{H,blood} = \left[\frac{\frac{fu_p}{R_B} \times Q_h \times (\frac{CL_{int\ in\ vivo}}{fu_{inc}})}{Q_h + \left(\frac{CL_{int\ invivo}}{fu_{inc}}\right) \times \frac{fu_p}{R_B}} \right]$$

Physiological constants of hepatic blood flow (Q_h) microsomal protein per gram of liver and liver weight per kg body weight were derived from literature reports [62]. CL_{int} *in vivo* was derived from microsomal intrinsic clearance values (mL/min/g liver) multiplied by the physiological constant of liver weight per kg of body weight. The various physiological constants used are presented in Appendix II.

Renal Clearance

To incorporate for the amount of compound excreted through urine, the renal clearance was predicted assuming insignificant metabolism and tubular secretion or re-absorption based on the following relationship

$$CL_{renal} = GFR \times fu_p$$

Where GFR denotes glomerular filtration rate.

Total Clearance and Elimination Rate Constant

The total clearance (also mentioned as total body clearance) was estimated as the sum of renal and hepatic clearance. For the purpose of simulation of human concentration time profile, the elimination rate constant (K_{el}) was estimated as the ratio of clearance over volume of distribution.

4.3. Validation of Predictions

The following steps were performed to assess the validity and prediction accuracy, prior to applying them in the optimization process.

a) Correlation with literature reported values

b) Precision and bias in predictions estimated as root mean square error (rmse) and average fold error (afe), respectively [1, 92].

Root mean square error was estimated using the following relationship [5]

$$\text{mse (mean square error)} = \frac{1}{N}\sum(\text{predicted} - \text{reported})^2$$

$$\text{rmse (root mean square error)} = \sqrt{\text{mse}}$$

Average fold error (afe) was estimated as [5]

$$\text{afe} = 10^{\frac{\Sigma \log\frac{\text{predicted}}{\text{reported}}}{N}}$$

Where N indicates the number of observations

Qualifying criteria: As a general qualifying criteria all individual predicted parameters a two-fold error is considered acceptable and not less than 80% of compounds remaining within 2 fold root mean square error. For derived pharmacokinetic parameters (AUC, Cmax, half-life), an estimate with 3 fold of reported is considered as an acceptable prediction. For afe, an estimate ≤ 2 is considered for a successful prediction.

4.4. Simulation of Human PK Profile

The pharmacokinetic profiles of the selected compounds anti-retroviral were simulated based on the model estimated parameters of absorption rate constant, volume of distribution of rapidly perfused tissues and predicted human clearance. The simulations were performed using Phoenix WinNonlin (version 6.2, Pharsight Corporation) using the following relation representing a first order absorption and elimination process for the lower clinically approved doses (therefore valid at dose ranges which do not saturate absorption or clearance mechanisms).

$$C_p = \frac{F \times D \times K_a}{V_c(k_a - k_{el})}(e^{-K_{el}t} - e^{-K_a t})$$

The simulation of human PK profile would thus require the prior knowledge of absorption rate constant (K_a), volume of distribution (for rapidly perfused tissues, as per the term V_c), clearance (denoted by the elimination rate constant K_{el}) and fraction bioavailable (F). As described earlier, the absorption rate constant was extrapolated from the Caco-2 permeability, pH dependent solubility and the physiological input data of small intestinal surface area. The volume of distribution was estimated using Berezhkovskiy method, which incorporates lipid partitioning equation with Log P_{vow}, Log D_{vow} pKa, and fraction unbound in plasma as the input data. Considering the observation from Rowland and Tozer [42] that the initial drug distribution (which is also a concentration gradient driving for absorption) is limited by perfusion, the volume of distribution of rapidly perfused tissues was considered for simulation. The total clearance was estimated as sum of renal and *in vivo* hepatic clearance. The elimination rate constant was estimated as the ratio of clearance over volume of distribution.

4.5.   Identification of Key Properties for Optimization Using PLS Analysis

Once the predictions were validated, a multivariate analysis was performed to assess the data relationships and to identify the key properties that could be prioritized for optimization to design a lead compound with optimum pharmacokinetic properties.

The various experimentally determined or derived values of physicochemical and ADME properties as well as the derived PK parameters of all the test compounds were grouped together and summarized. The data was then categorized as predictors and dependent variables. Predictors consisted of the various experimentally determined properties that were used to predict various PK parameters (dependent variables).

List of Predictors
a) Solubility at pH 1.8, 3.0, 4.5, 6.8, 7.4

b) Log P

c) Log $D_{7.4}$

d) pKa

e) Neutral fraction at pH 6.8

f) Neutral fraction at pH 7.4

g) Caco-2 Permeability

h) Fraction unbound in plasma

i) Blood to plasma partitioning

j) Microsomal clearance

List of Dependent Variables (Response Variables)

a) Absorption rate constant (K_a)

b) Steady state volume of distribution (V_{ss})

c) Total clearance (CL)

d) Area under plasma concentration-time curve (AUC)

In case of dependent variables, the predicted values from PBPK models (using experimental data) were used. The trends in the sample data was identified using PLS analysis (latent vectors) with the objective of assessing the most relevant properties that influence the outcome and their relative degree of influence [67, 93]. PLS analysis involved mean centering and normalizing of both X and Y values and identifying latent vectors in X that have maximum covariance with Y values. The influence of each X variable on each Y variable was expressed graphically in terms of standardized coefficients derived by PLS. The PLS analysis was performed using Minitab statistical software (Minitab® version 16, Minitab Inc, 1829 Pine Hall Rd, State College PA 16801-3008, USA).

The coefficient plot was prepared for all the four response variables. The most important properties influencing the outcomes were identified based on the coefficients.

4.6. Illustration of Utility of the New Methodology in Lead Optimization

Subsequent to PLS analysis based identification of key properties influencing a particular pharmacokinetic parameter, the following steps were performed to illustrate the utility of the methodology in lead optimization. Since chemical modification of the test compounds and demonstration of favorable changes were not the intended scope of current research (and

additionally would require a clinical study to prove the advantage of modifications), the following two steps were undertaken to mimick the lead optimization process and to demonstrate the utility of the new methodology.

Step 1: Effect of Variation in Key Properties on *In Vivo* Pharmacokientic Profile

The effect of 2 fold variation (0.5 x and 2.0 x) in key properties of microsomal clearance, solubility and Log P on the human predicted concentration time profile was assessed using PBPK modeling and 1 compartment model simulation. This step mimicks a scenario in lead optimization stage where careful modification of chemical structure, after identification of key properties that influence a vital PK parameter, has resulted in new compounds with altered physicochemical or ADME properties. For the sake of simplicity, only one property was changed at a time. In a real time discovery research, this could also be compared to evaluation of various analogues of a pharmacophore.

Step 2: Utility of the Methodology: Correlation with Efficacy

To demonstrate the utility of the research methodology, selected *in vivo* pharmacokinetic profiles after two fold variation (0.5 x and 2.0 x) in key properties were overlaid over a relevant efficacy parameters like PK-PD correlation estimates, receptor affinity or inhibition estimates. This step demonstrates the utility of the current methodology in selection of lead compound addressing the research gaps as envisaged in the current research.

5.0. RESULTS AND DISCUSSION

5.1. Experimental Results

A compilation of various raw data is presented in Appendix I. Few representative HPLC and LC-MS chromatograms are presented in Appendix II.

5.1.1. Basic Molecular Properties

Basic molecular properties such as molecular weight (Mol. Wt), Log P and pKa were obtained from literature. Log $P_{vo/w}$ and Log $D_{vo/w}$ were derived as explained in the methods section using Log P and pKa as input values. The properties are summarized in Table 7.

Table 7: Basic Physicochemical Properties of Test Compounds*

Category	Compound	Mol. wt	Log $P_{o/w}$	Log $P_{vo/w}$	Log $D_{vo/w}$	$pK_a(1)$	pKa(2)
Beta blocker	Atenolol	266.3	0.34	-0.98	-0.98	9.4	13.9
	Metoprolol	267.4	1.632	0.47	0.47	9.4	13.9
	Propranolol	259.3	2.90	1.88	-6.66	9.5	13.84
Anti-retroviral	Nevirapine	266.3	2.64	1.59	0.07	4.3	12.1
	Nelfinavir	567.8	7.28	6.76	1.22	6.2	14.1[#]
	Ritonavir	720.9	2.33	1.25	1.25	2.5	11.5
	Indinavir	613.8	3.44	2.48	0.27	5.2	14.2[#]
	Efavirenz	315.7	4.38	3.53	3.53	10.2	-
COPD	Cilomilast	343.4	2.11	1.00	-2.05	4.4	-
	Roflumilast	403.2	2.31	1.22	1.22	0.4	9.9
Anti-diabetic	Vildagliptin	303.4	0.17	-1.16	-2.19	8.4	-
	Tolbutamide	270.3	2.36	1.28	-0.87	5.3	-
	Rosiglitazone	357.4	3.02	2.02	1.97	6.5	-

* database C. ChEMBLdb. [Online]. [cited 2011 July 31. Available from: https://www.ebi.ac.uk/chembldb/ **[94]** # taken from drug bank database (www.Drugbankca, accessed last on 7 October 2011). Estimated values of other properties including neutral fraction at pH 6.8 and 7.4, fraction unbound in tissue and microsomal unbound fraction are provided in appendix I.

5.1.2. **pH Dependent Solubility**

Equilibrium solubility was determined for the compounds at various pH buffers using shake flask method (Table 8) at room temperature.

Table 8: pH Dependent Solubility of Test Compounds

Category	Compound	Solubility (mg/mL)				
		pH 1.5	**pH 3.0**	**pH 4.5**	**pH 6.8**	**pH 7.4**
Beta blocker	Atenolol	1.32	1.26	1.26	1.37	1.33
	Metoprolol	5.01	4.91	5.65	4.99	5.44
	Propranolol	3.10	3.12	2.90	3.20	3.06
Anti-retroviral	Nevirapine	0.765	0.140	0.104	0.102	0.098
	Nelfinavir	0.201	0.241	0.713	0.008	0.008
	Ritonavir	0.008	0.001	0.001	0.001	0.001
	Indinavir	0.998	1.314	1.643	0.045	0.039
	Efavirenz	0.007	0.007	0.007	0.008	0.022
COPD	Cilomilast	0.012	0.392	0.014	0.593	1.348
	Roflumilast	0.005	0.005	0.005	0.005	0.005
Anti-diabetic	Vildagliptin	1.839	1.912	1.879	1.908	2.019
	Tolbutamide	0.094	0.096	0.111	2.497	1.467
	Rosiglitazone	1.246	1.314	1.084	0.047	0.048

5.1.3. **Caco-2 Permeability**

Permeability of the various compounds were assessed using 21 day Caco-2 culture method at a pH of 6.8 (donor side-apical) and 7.4 (acceptor side-basolateral) and are presented in Table 9. The apparent permeability rate was derived from the cumulative rate of appearance of drug to the receiver compartment (Figure 3) normalized to the surface area of the cell layer and the test concentration.

Figure 3: Cumulative Rate of Appearance of Test Compounds in Caco-2 Permeability Assay
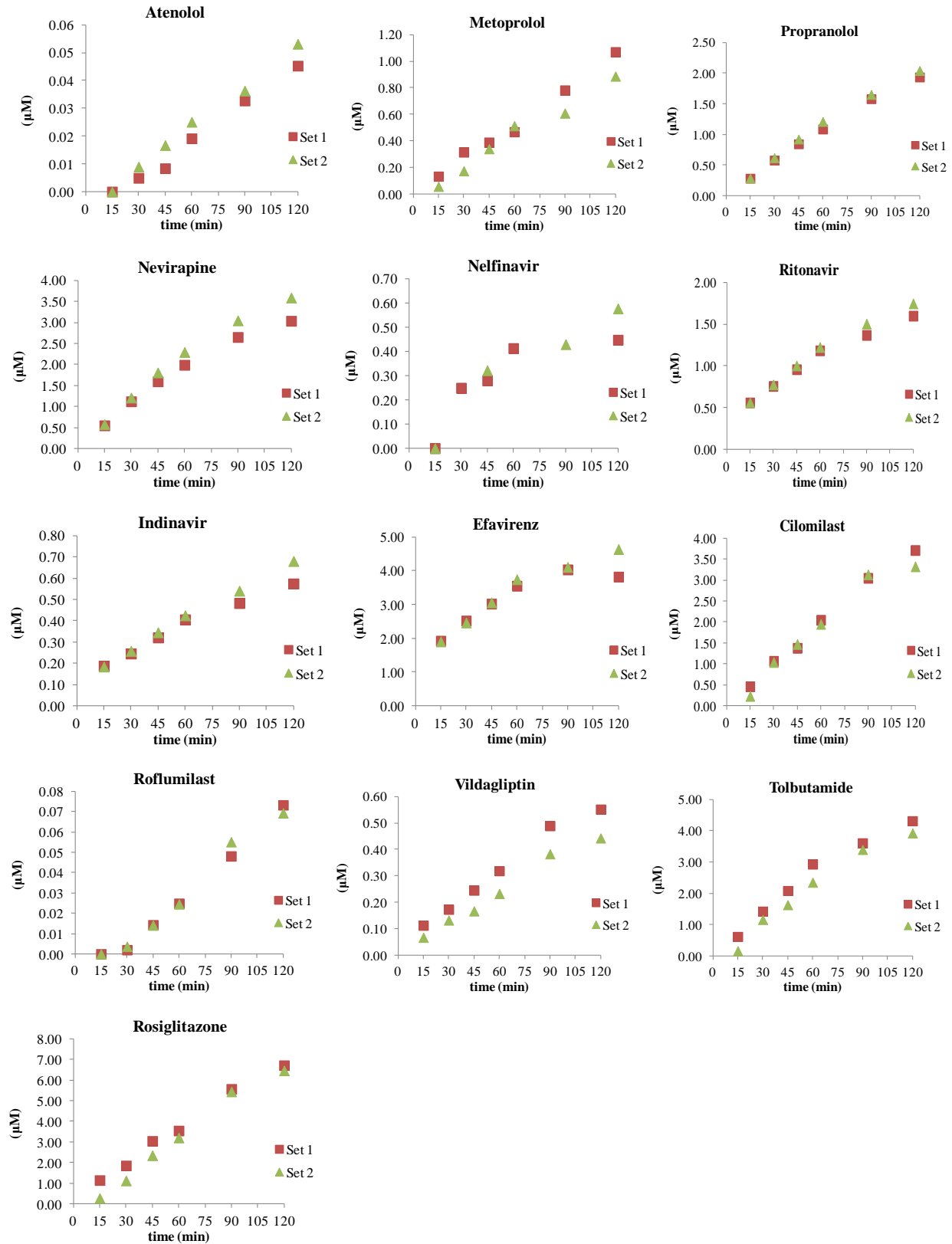
Table 9: Permeability of Test Compounds Across Caco-2 Monolayer

Category	Compound	Apparent permeability, Papp (nm/sec)
Beta blocker	Atenolol	3
	Metoprolol	89
	Propranolol	60
Anti-retroviral	Nevirapine	246
	Nelfinavir	14
	Ritonavir	98
	Indinavir	31
	Efavirenz	84
COPD	Cilomilast	301
	Roflumilast	232
Anti-diabetic	Vildagliptin	16
	Tolbutamide	304
	Rosiglitazone	154

The acceptance criteria for Caco-2 permeability assay were based on permeability of propranolol and was observed in the expected range of 50-75 nm/sec.

5.1.4. **Fraction Unbound in Plasma**

The plasma protein binding of various compounds (Table 10) were estimated using ultra filtration method and the unbound fraction was estimated as '1-fraction bound.'

Table 10: Plasma Unbound Fractions of Various Test Compounds

Category	Compound	Unbound fraction in plasma(f_u)
Beta blocker	Atenolol	0.854
	Metoprolol	0.254
	Propranolol	0.780
Anti-retroviral	Nevirapine	0.421
	Nelfinavir	0.117
	Ritonavir	0.020
	Indinavir	0.400
	Efavirenz	0.001
COPD	Cilomilast	0.006
	Roflumilast	0.004
Anti-diabetic	Vildagliptin	0.794
	Tolbutamide	0.022
	Rosiglitazone	0.002

As an acceptance criteria for the assay warfarin was used as the positive control and was tested at 0.25µg/mL and qualified the acceptance criteria of >99 % binding in human plasma. The protein binding observed for warfarin was 99.5%.

5.1.5. **Blood to Plasma Partitioning Ratio**

The blood to plasma ratio of various test compounds (Table 11) were estimated as the ratio of concentrations in whole plasma to the concentrations estimated in plasma separated from spiked blood.

Table 11: Blood to Plasma Partitioning Ratio of Test Compounds

Category	Compound	Blood-plasma partitioning ratio (R_B)
Beta blocker	Atenolol	3.5
	Metoprolol	2.4
	Propranolol	2.0
Anti-retroviral	Nevirapine	2.2
	Nelfinavir	1.0
	Ritonavir	0.6
	Indinavir	1.7
	Efavirenz	1.2
COPD	Cilomilast	0.8
	Roflumilast	1.4
Anti-diabetic	Vildagliptin	2.1
	Tolbutamide	0.7
	Rosiglitazone	1.4

5.1.6. Intrinsic Clearance in Liver Microsomes

The metabolic stability of various compounds was estimated as intrinsic clearance in liver microsomes. The rate of disappearance was estimated using single phase exponential decay model with GraphPad Prism software (Figure 4).

Figure 4: Metabolism of Test Compounds in Human Liver Microsomes
(% Remaining vs. Time)
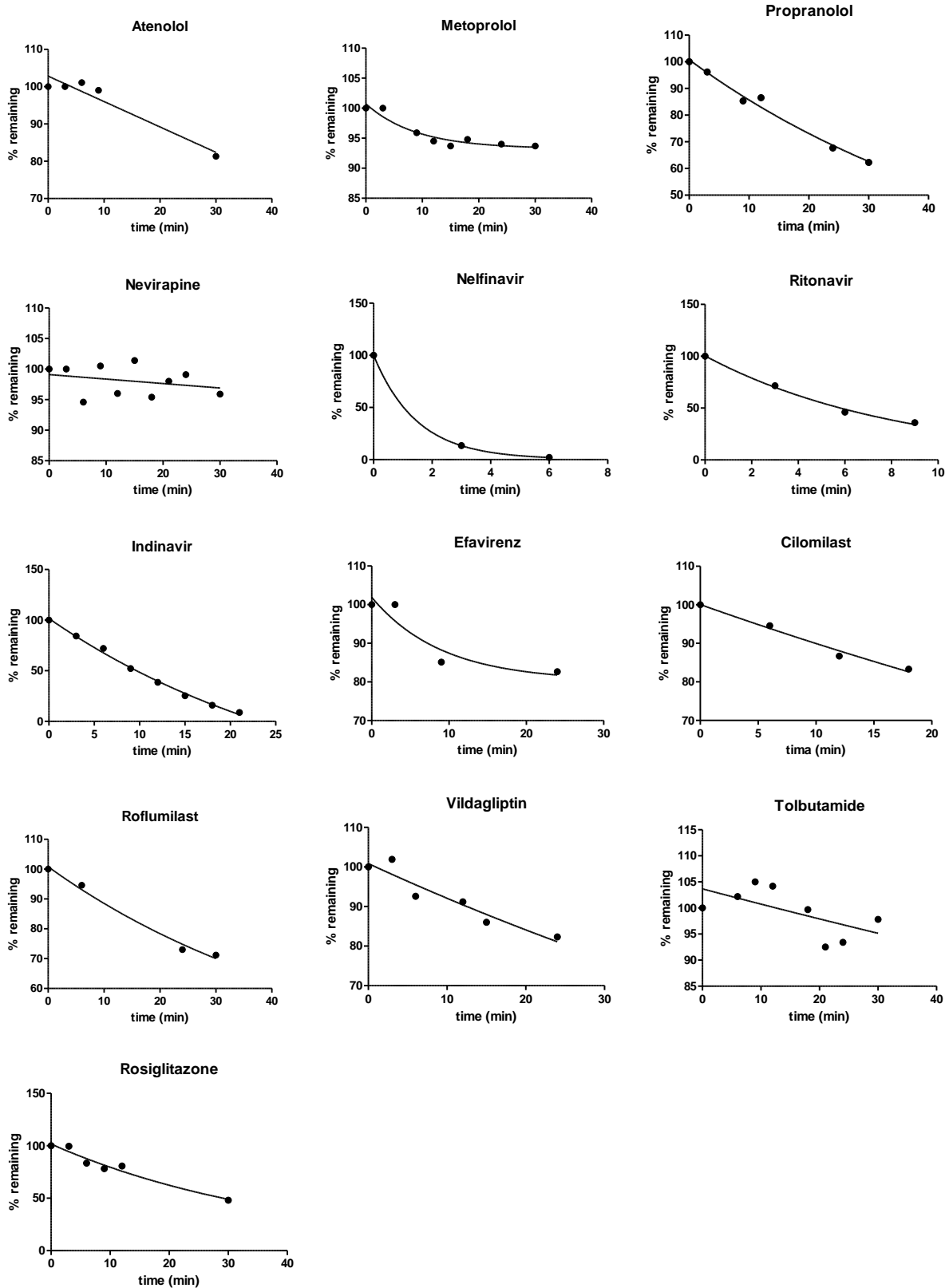
The rate constants were further normalized to unit protein content and scaled to microsomal protein per gram of liver to derive the intrinsic clearance (Table 12). Intrinsic clearance values were further used for prediction of *in vivo* clearance.

Table 12: Intrinsic Clearance (CL$_{int}$) of Test Compounds in Human Liver Microsomes

Category	Compound	Intrinsic clearance CL$_{int}$ (mL/min/g liver)
Beta blocker	Atenolol	0.002
	Metoprolol	11.8
	Propranolol	1.91
Anti-retroviral	Nevirapine	0.08
	Nelfinavir	71.16
	Ritonavir	12.64
	Indinavir	3.37
	Efavirenz	11.58
COPD	Cilomilast	1.12
	Roflumilast	2.03
Anti-diabetic	Vildagliptin	0.96
	Tolbutamide	0.31
	Rosiglitazone	2.62

Using an internal compound with a high intrinsic clearance of > 50 mL/min/kg, the functionality of microsomes was ensured in the assay.

5.2. Prediction of Pharmacokinetic Parameters with Physiological Pharmacokinetic Models

5.2.1. Absorption Rate Constant

The absorption rate constant was derived as per the method described by Usansky et al. [6] assuming steady state and are presented in Table 13. The estimates were derived using the Caco-2 permeability, effective surface area of intestine and predicted volume of distribution of rapidly perfused tissues.

Table 13: Absorption Rate Constants (min^{-1}) of Compounds in Humans: Predicted vs. Reported Values

Category	Compound name	Predicted	Reported
Beta blocker	Atenolol	0.001	0.002 [95]
	Metoprolol	0.037	0.020 [95]
	Propranolol	0.010	0.025 [96]
Anti-retroviral	Nevirapine	0.070	0.060 [97]
	Nelfinavir	0.001	0.002 [98]
	Ritonavir	0.071	0.015 [99]
	Indinavir	0.005	0.043 [100]
	Efavirenz	0.044	0.005 [101]
COPD	Cilomilast	0.214	NA
	Roflumilast	0.138	NA
Anti-diabetic	Vildagliptin	0.006	0.007 [102]
	Tolbutamide	0.212	0.010 [103]
	Rosiglitazone	0.092	0.083 [104]

NA: Not available from literature

To assess the reliability of predictions the precision and bias estimates were made with reported data by estimating the root mean square error and average fold error (Table 14).

Table 14: Precision and Bias Estimates for Prediction of Absorption Rate Constant

Compound	Precision		Bias	
	Predicted-Observed	Square	Predicted/Observed	Log Predicted/Observed
Atenolol	-0.001192	0.000001	0.403756	-0.393881
Metoprolol	0.016695	0.000279	1.834767	0.263581
Propranolol	-0.014554	0.000212	0.417837	-0.378993
Nevirapine	0.010922	0.000119	1.183560	0.073190
Nelfinavir	-0.001197	0.000001	0.401493	-0.396322
Ritonavir	0.056166	0.003155	4.870834	0.687603
Indinavir	-0.038318	0.001468	0.108892	-0.963005
Efavirenz	0.038868	0.001511	9.131339	0.960534
Vildagliptin	-0.001734	0.000003	0.760787	-0.118737
Tolbutamide	0.202264	0.040911	21.226411	1.326877
Rosiglitazone	0.008163	0.000067	1.097956	0.040585
	Sum	0.0477	sum	1.1014
mean square error		0.0043	sum/n (11)	0.1001
root mean square error (rmse)		0.0659	**average fold error (afe)**	1.2593
two fold error		0.1317	afe $\leq$ 2 indicates reliable parameter prediction	
% within 2 fold rmse		**91%**		

The comparison of the *in vitro* estimated absorption rate constant with the reported values indicate an average fold error of only 1.0068 indicating reliable predictions (less than 2 fold). Estimates for all the compounds were within two fold of root mean square error. Predictions for 10 out of a total of 11 compounds (91%) were within 2 fold root mean square error.

5.2.2. Volume of Distribution

The partitioning of compounds to various tissue (Figure 5) were estimated with tissue partitioning equation using Log P and ionization as well as protein binding data as input values.. These were further utilized to predict volume of distribution incorporating tissue volume data (Table 15) as explained in the methods section [47, 52].

Figure 5: Predicted Tissue Plasma Partitioning Ratios of Various Test Compounds
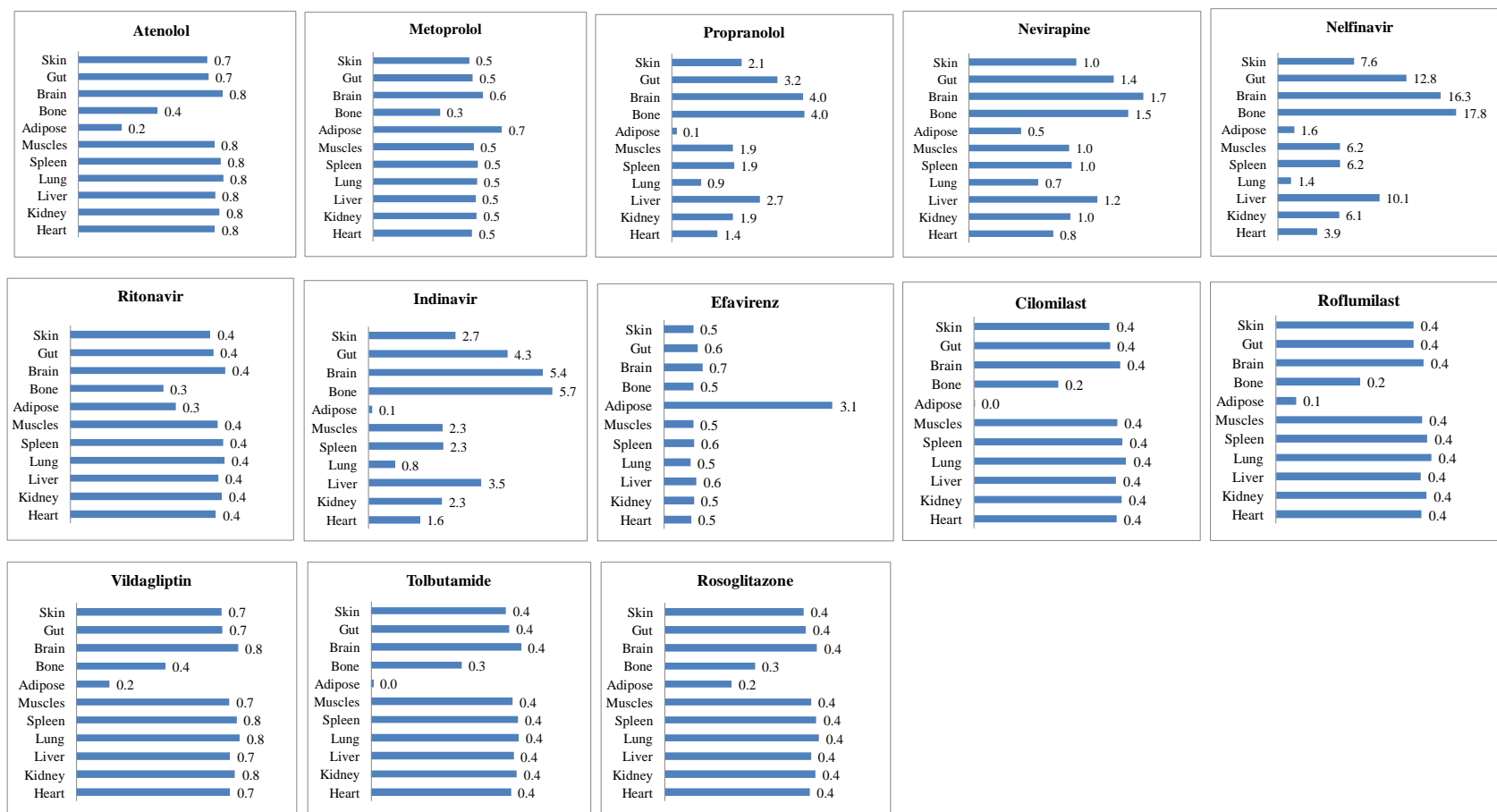
Table 15: Predicted Volume of Distribution (L/kg) of Rapidly Perfused Tissue (V_c) and Comparison of Steady State Volume of Distribution (V_{ss}) with Reported Values

Category	Compound name	V_c Predicted	V_{ss} Predicted	V_{ss} Reported
Beta blocker	Atenolol	0.60	0.72	0.95 [105]
	Metoprolol	0.41	0.56	4.20 [105]
	Propranolol	0.99	1.57	4.30 [105]
Anti-retroviral	Nevirapine	0.60	0.88	2.15 [97]
	Nelfinavir	2.90	5.45	4.50 [98]
	Ritonavir	0.24	0.33	1.38 [99]
	Indinavir	1.13	1.91	1.18 [100]
	Efavirenz	0.33	0.79	3.60 [101]
COPD	Cilomilast	0.24	0.29	0.15 [106]
	Roflumilast	0.29	0.34	2.9 [107]
Anti-diabetic	Vildagliptin	0.48	0.59	1.01 [108]
	Tolbutamide	0.25	0.30	0.10 [105]
	Rosiglitazone	0.29	0.36	0.22 [109]

Table 16 lists the precision and bias estimates for the predicted V_{ss} parameters in comparison with reported data.

Table 16: Precision and Bias Estimates for Prediction of Human Volume of Distribution

Compound	Precision		Bias	
	Predicted-Observed	**Square**	**Predicted/Observed**	**Log Predicted/Observed**
Atenolol	-0.23	0.05	0.76	-0.12
Metoprolol	-3.64	13.22	0.13	-0.87
Propranolol	-2.73	7.45	0.37	-0.44
Nevirapine	-1.27	1.61	0.41	-0.39
Nelfinavir	0.95	0.90	1.21	0.08
Ritonavir	-1.06	1.11	0.24	-0.63
Indinavir	0.73	0.54	1.62	0.21
Efavirenz	-2.81	7.88	0.22	-0.66
Cilomilast	0.14	0.02	1.93	0.29
Roflumilast	-2.56	6.53	0.12	-0.93
Vildagliptin	-0.42	0.18	0.58	-0.23
Tolbutamide	0.20	0.04	3.00	0.48
Rosiglitazone	0.15	0.02	1.68	0.22
	sum	39.56	sum	-2.98
mean square error		3.04	sum/n (13)	-0.23
root mean square error (rmse)		1.74	**Average fold error (afe)**	0.59
two fold rmse		3.49	afe ≤ 2 indicates reliable parameter prediction	
% within 2 fold rmse		92.3		

The predicted values correlated well with reported values with 92.3% of predicted values lying within 2 fold of root mean square error. The average fold error was also observed to be less than 2.

5.2.3. Clearance

The experimental values of intrinsic clearance in liver microsomes, blood plasma partitioning, fraction unbound in plasma and Log P based values of unbound fraction in microsomes were

applied to a well stirred model for hepatic clearance. For renal clearance, a product of glomerular filtration rate and fraction unbound in plasma was used assuming zero renal re-absorption. The total body clearance (total clearance) was derived as the sum of hepatic and renal clearances (Table 17). The precision and bias estimates for the predicted total clearance with reported values are listed in Table 18.

Table 17: Total Body Clearance of Compounds in Humans (mL/min/kg): Predicted vs. Reported Values

Category	Compound name	Predicted	Reported
Beta blocker	Atenolol	1.5	2.0 [105]
	Metoprolol	15.2	15.0 [105]
	Propranolol	14.9	16.0 [105]
Anti-retroviral	Nevirapine	1.4	0.3 [97]
	Nelfinavir	20.6	4.8 [110]
	Ritonavir	9.8	2.5 [99]
	Indinavir	14.2	11.1 [100]
	Efavirenz	0.8	2.2 [101]
COPD	Cilomilast	0.4	0.3 [106]
	Roflumilast	0.3	2.5 [111]
Anti-diabetic	Vildagliptin	9.0	9.8 [102]
	Tolbutamide	0.5	0.2 [105]
	Rosiglitazone	0.2	0.7 [109]

The clearance of nelfinavir and ritonavir were notably higher than the reported values. The reason for the above variation has been found to be the over prediction of clearance for these compounds in liver microsomes. Nelfinavir and ritonavir are actively taken up into hepatocytes (based on rat hepatocyte data) and due to much higher levels inside the hepatocytes they saturate the metabolic clearance *in vivo* [112].

In contrast to nelfinavir or ritonavir, the predicted clearance of roflumilast appeared nearly 9 fold lower in comparison to reported values. Roflumilast undergoes extensive phase I (with involvement of CYP 1A1/2, 2C19 and 3A4) and phase II glucuronide conjugation [113]. The predictions of intrinsic clearance based on liver microsomal assays did not involve the contribution of phase II glucuronidation and this could be the major reason for the lower prediction of roflumilast clearance.

Table 18: Precision and Bias Estimates for Prediction of Human Clearance

Compound	Precision		Bias	
	Predicted-Observed	**Square**	**Predicted/Observed**	**Log Predicted/Observed**
Atenolol	-0.53	0.28	0.74	-0.13
Metoprolol	0.20	0.04	1.01	0.01
Propranolol	-1.06	1.13	0.93	-0.03
Nevirapine	1.10	1.22	4.31	0.63
Nelfinavir	15.80	249.60	4.29	0.63
Ritonavir	7.96	63.42	4.19	0.62
Indinavir	3.07	9.42	1.28	0.11
Efavirenz	-1.62	2.62	0.26	-0.58
Cilomilast	0.06	0.00	1.17	0.07
Roflumilast	-2.22	4.94	0.11	-0.96
Vildagliptin	-0.75	0.56	0.92	-0.03
Tolbutamide	0.24	0.06	1.99	0.30
Rosiglitazone	-0.42	0.17	0.37	-0.43
	sum	333.5	sum	0.20
	mean square error	25.65	sum/n (13)	0.02
root mean square error (rmse)		5.1	**average fold error (afe)**	1.04
two fold rmse		10.1	afe ≤ 2 indicates reliable parameter prediction	
% within 2 fold rmse		92.3		

Note: For nelfinavir there are multiple reported values in literature, mean estimate was used as observed (range from 2.6-7.1)

The predicted values correlated well with reported values with 92.3% of predicted values lying within 2 fold of root mean square error. The average fold error was also observed to be less than 2.

5.2.4. **Fraction Bioavailable**

Based on the estimated fraction absorbed values the fraction of drug orally bioavailable was estimated (Table 19) as described in methods sections, considering the effect of first pass metabolism [3]. The precision and bias estimates of the predictions are listed in Table 20.

Table 19: Predicted Fraction Absorbed and Comparison of Fraction Bioavailable with Reported Values

S.No	Compound	Predicted fraction absorbed (F_a)	Predicted fraction bioavailable (F)	Reported fraction bioavailable
1	Atenolol	0.14	0.14	0.56 [114] [105]
2	Metoprolol	0.88	0.25	0.38 [105]
3	Propranolol	0.68	0.23	0.26 [105]
4	Nevirapine	0.93	0.90	0.91 [115]
5	Nelfinavir	0.14	0.001	0.0088-0.0047 [116]
6	Ritonavir	0.93	0.46	0.59 [99]
7	Indinavir	0.48	0.16	0.23 [100]
8	Efavirenz	0.90	0.86	0.45 [117]
9	Cilomilast	0.98	0.96	1.0 [106]
10	Roflumilast	0.96	0.95	0.79 [111]
11	Vildagliptin	0.52	0.33	0.85 [108]
12	Tolbutamide	0.98	0.96	0.93 [105]
13	Rosiglitazone	0.95	0.94	0.99 [109]

Significant differences are observed in the prediction of bioavailability of few compounds. Vildagliptin is taken up by organic cation transporter and therefore might undergo active uptake from the proximal renal tubules increasing its bioavailability. Additionally, about one quarter of vildagliptin is excreted unchanged through the urine and most of the drug is metabolized by hydrolysis by the kidneys [118], mechanisms which are yet to be incorporated in the PBPK

models and could not be included in the current research. Nelfinavir is a potent CYP inhibitor and undergoes active uptake into hepatocytes increasing the intracellular levels much higher than the plasma and thereby reducing its own clearance [112] due to saturation of clearance mechanism occurs at a lower threshold that the saturation of uptake to hepatocytes. As mentioned earlier the clearance of nelfinavir was over predicted in liver microsomes and with the inclusion of first pass metabolism in the estimation of fraction bio-available, it appears that it has a more pronounced effect on estimation of nelfinavir bioavailability.

Table 20: Precision and Bias Estimates for Prediction of Fraction Bioavailable

Compound	Precision		Bias	
	Predicted-Observed	Square	Predicted/Observed	Log Predicted/Observed
Atenolol	-0.421684	0.177818	0.246992	-0.607317
Metoprolol	-0.131077	0.017181	0.655060	-0.183719
Propranolol	-0.030892	0.000954	0.881185	-0.054933
Nevirapine	-0.009227	0.000085	0.989861	-0.004426
Nelfinavir	-0.007462	0.000056	0.152009	-0.818130
Ritonavir	0.455018	0.207042	78.121754	1.892772
Indinavir	0.160435	0.025739	70.754290	1.849753
Efavirenz	0.450000	0.202500	2.000000	0.301030
Cilomilast	-0.041465	0.001719	0.958535	-0.018392
Roflumilast	0.162171	0.026299	1.205280	0.081088
Vildagliptin	-0.521301	0.271755	0.386705	-0.412620
Tolbutamide	0.026009	0.000676	1.027967	0.011979
Rosiglitazone	-0.053107	0.002820	0.946357	-0.023945
	sum	0.9346	sum	2.0131
	mean square error	0.0719	sum/n (13)	0.1549
root mean square error (rmse)		0.2681	average fold error (afe)	1.4284
two fold rmse		0.5363	afe ≤ 2 indicates reliable parameter prediction	
% within 2 fold rmse		100%		

The precision and bias estimates indicate a reliable prediction of fraction bioavailability with prediction for all the compounds in the series within two fold error and the average fold error lesser than 2.

5.3. Simulation of Human Pharmacokinetics Using Model Predicted Parameters

The derived values of absorption rate constant (K_a), volume of distribution of rapidly perfused tissues (V_c) and *in vivo* clearance ($CL_{in\ vivo\ pred}$) were used for simulation of concentration-time profile after oral administration. The time to maximum concentration (Tmax), maximum concentration in plasma (Cmax) and area under the concentration-time graph (AUC) were estimated for the first dose and were compared with literature values.

The compounds were simulated mostly for their human PK profile (Figures 6-9) at the respective clinically optimized lower doses as mentioned in Table 21. Tables 22 to 25 list the PK parameters of area under curve (AUC), Cmax and half-life in comparison with reported values.

Table 21: Clinically Optimized Doses of Test Compounds Used for Simulation in the Current Study

S. No	Compound name	Clinically optimized dose (mg)
1	Atenolol	50 [119]
2	Metoprolol	50 [120]
3	Propranolol	80 [120]
4	Nevirapine	200 [121]
5	Nelfinavir	750 [121]
6	Ritonavir	600 [121]
7	Indinvair	800 [121]
8	Efavirenz	600 [121]
9	Cilomilast*	15 BID [122]
10	Roflumilast*	0.25 [123]
11	LAF (vildagliptin)*	100 [124]
12	Tolbutamide	500 [105]
13	Rosiglitazone	8 [125]

*Phase III trials.

101

Figure 6: Simulated Steady State Pharmacokinetic Profiles of Beta Blockers after Repeated Oral Dose
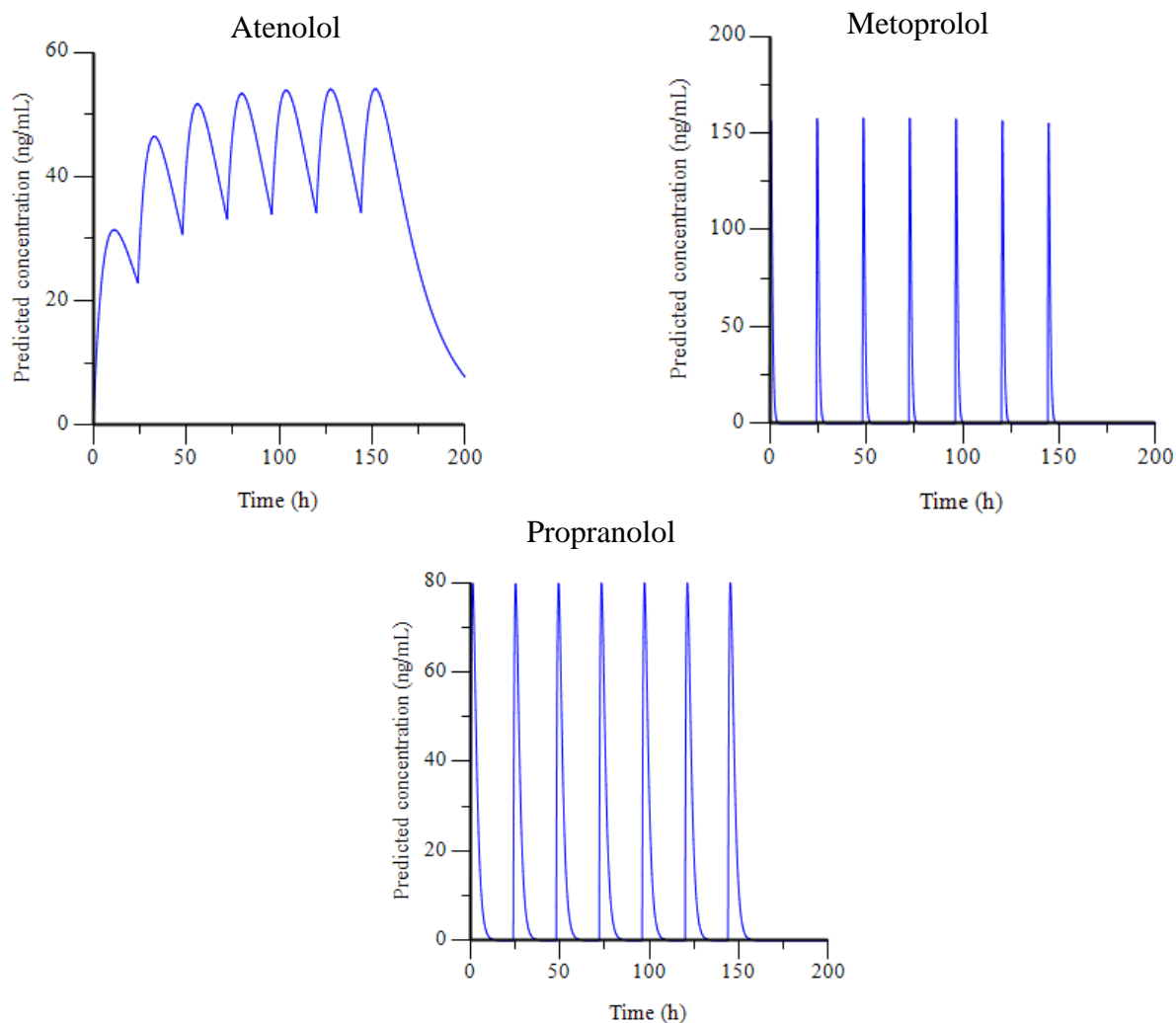
Table 22: Comparison of Simulated vs. Reported PK Parameters of Beta Blockers at Steady State

S. No	Compound	Dose (mg)	AUC (ng.h/mL)		Cmax (ng/mL)		Half-life (h)	
			simulated	reported	simulated	reported	simulated	reported
1	Atenolol [120]	50	1118	2556	31.43	290	4.7	4.8
2	Metoprolol [120]	50	195	557	158	83	0.3	3.7
3	Propranolol [120]	80	292	376	80	77	0.9	3.0

The simulations show a good correlation with reported values in literature with regards to AUC, but with notable differences in Cmax for atenolol as well as differences observed with the half-life estimates, however it should be noted that the predictions are based on properties estimated for the powder form of drug with an assumption of immediate dissolution and does not take into consideration the significant difference that could be brought about by formulation approaches as well as with increased understanding of the chemistry manufacturing and control aspects during the clinical development.

Figure 7: Simulated Steady State Pharmacokinetic Profiles of Anti-Retroviral Drugs after Repeated Oral Dose

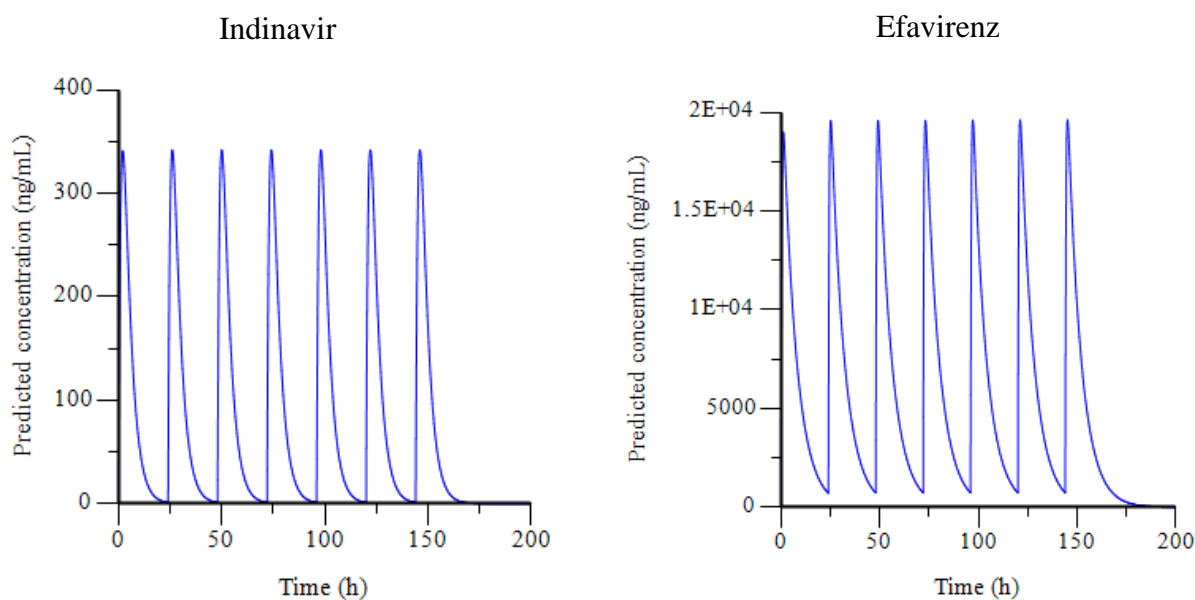|	Indinavir		Efavirenz
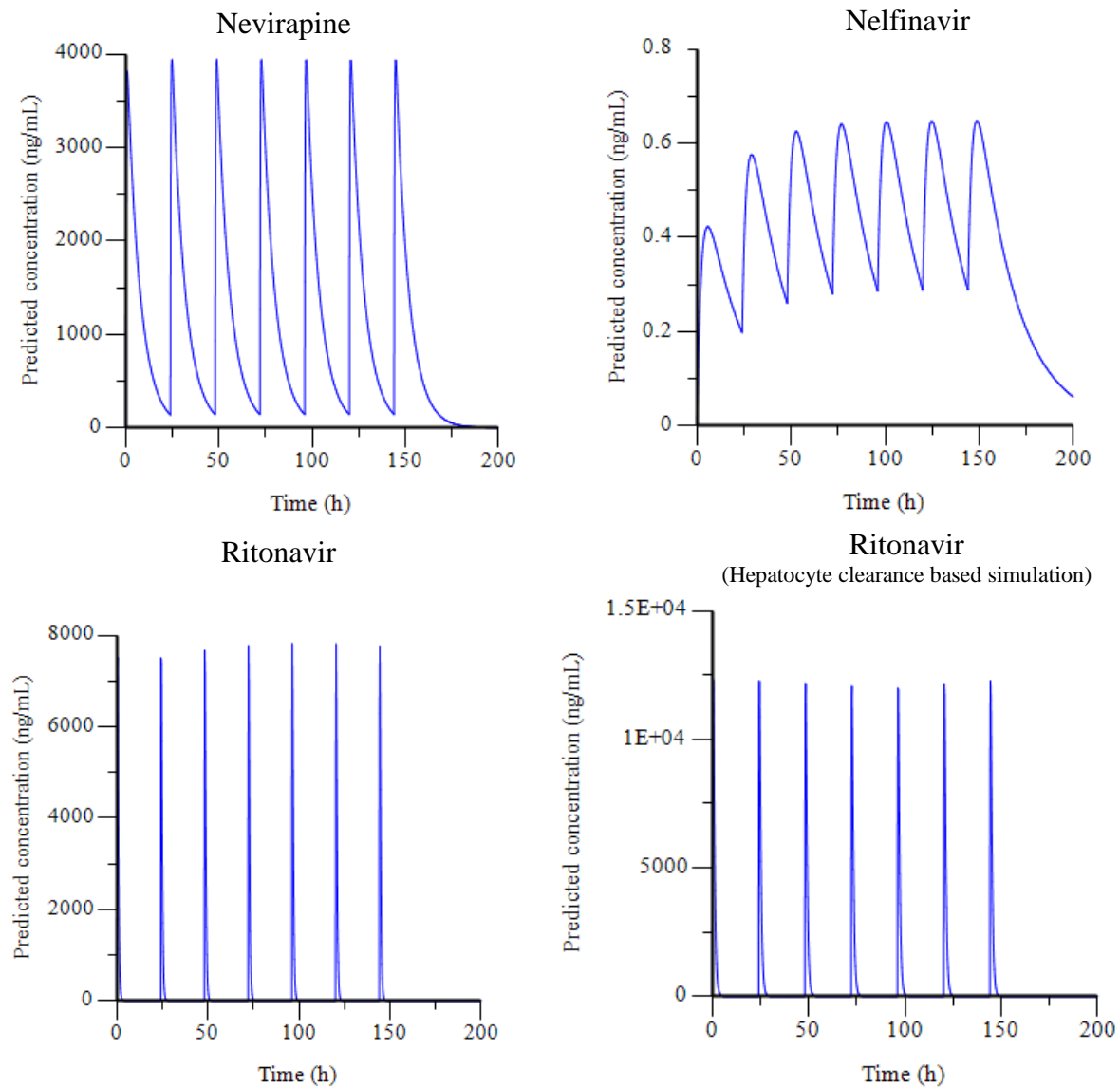
Table 23: Comparison of Simulated vs. Reported PK Parameters of Anti-Retroviral Drugs at Steady State

S. No	Compound	Dose (mg)	AUC (ng.h/mL)		Cmax (ng/mL)		Half-life (h)	
			simulated	reported	simulated	reported	simulated	reported
1	Nevirapine [121]	200	29851	86000	3817	5000	4.8	25-30
2	Nelfinavir [121]	750	11.59	18000	0.4	4000	1.62	3.5-5
3	Ritonavir [121]	600	6719	61000	7828	11200	0.3	3-5
4	Ritonavir [80] (hepatocyte CL)	600	14705	61000	12338	11200	0.5	3-5
5	Indinavir [121]	800	2182	17000	341	7000	0.9	1.5
6	Efavirenz [121]	600	153846	58000	19011	4100	4.7	40-55

The predicted AUC of nelfinavir and ritonavir were much lower than reported due to the influence of high clearance estimates based on liver microsomal assays which are an over prediction due to factors as explained under section 5.2.3. Therefore substitution with human hepatocyte based clearance estimates [80] from literature showed a marked improvement in the prediction of ritonavir AUC and Cmax. This indicates the relative advantage of hepatocyte based estimations of clearance that takes into account the interplay of compound permeability and metabolic process including the complex interplay of transporters and saturation mechanisms.

However literature report on nelfinavir hepatocyte clearance could not be obtained after an exhaustive search.

The overall predictions for indinavir (Table 23) were also different as compared to the literature values. Indinavir was predicted an 8 fold lower absorption rate constant as well as a 27% higher clearance than the reported clearance. A closer examination of the simulation parameters (absorption rate constant, volume of distribution and clearance) indicates the requirement of a near 6 fold difference in clearance to match the reported mean exposure estimate for indinavir. Although no direct evidence could be found from literature search, this again points to the over prediction of clearance using liver microsomes. Additionally there could also be the effect of polymorphism of metabolic pathways that could result in increased first pass clearance [126].

Figure 8: Simulated Steady State Pharmacokinetic Profiles of PDE4 Inhibitors after Repeated Oral Dose
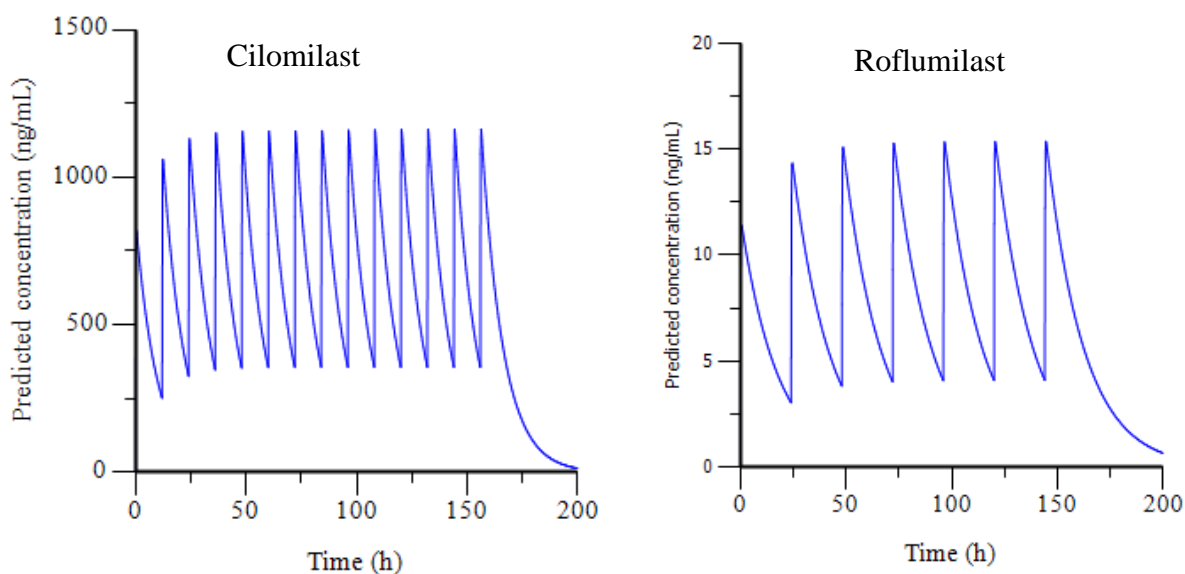
Table 24: Comparison of Simulated vs. Reported PK Parameters of COPD Drugs at Steady State

S. No	Compound	Dose (mg)	AUC (ng.h/mL)		Cmax (ng/mL)		Half-life (h)	
			simulated	reported	simulated	reported	simulated	reported
1	Cilomilast [127]*	15**	8333	8470	819	1160	6.7	6.93
2	Roflumilast [128]	0.250	208	17	11	3	12.2	15.99

*single dose study, **BID

105

The predicted parameters for cilomilast match the reported values, but in case of roflumilast the predicted AUC is much higher than the reported. One major reason for higher prediction is the 10 fold low estimates of predicted clearance of roflumilast obtained from liver microsomal assays which were used for simulation. As explained under the section on prediction of clearance (section 5.2.3), the liver microsomal assays did not include the contribution from phase II glucuronidation and therefore could have under predicted clearance.

Figure 9: Simulated Steady State Pharmacokinetic Profiles of Anti-Diabetic Drugs after Repeated Oral Dose
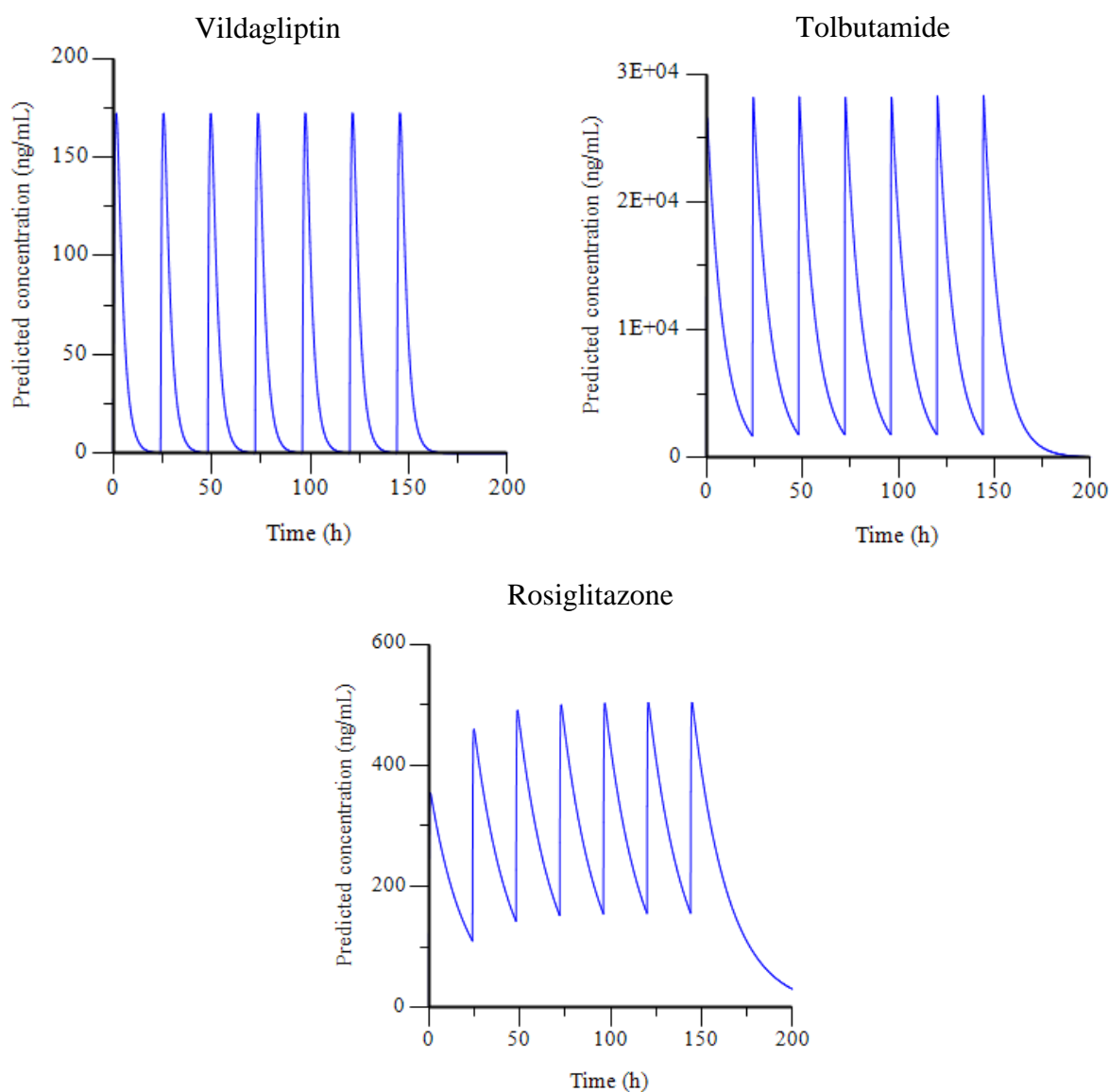
Table 25: Comparison of Simulated vs. Reported PK Parameters of Anti-Diabetic Drugs at Steady State

S. No	Compound	Dose (mg)	AUC (ng.h/mL)		Cmax (ng/mL)		Half-life (h)	
			simulated	reported	simulated	reported	simulated	reported
1	Vildagliptin [129]	100	868	2362	172	445	0.6	2.3
2	Tolbutamide [130]	500	238095	721000	26598	63000	5.9	9.1
3	Rosiglitazone [131]*	8	7272	2971	354	598	13.6	3.37

To assess the reliability of predictions in drug discovery set up the ratio of simulated to reported values were estimated and are presented in Table 26.

Table 26: Comparison of PK Estimates: Ratio of Simulated to Reported Values

Compound	AUC fold	Cmax fold	Half-life fold
Atenolol	0.44	0.1	0.98
Metoprolol	0.35	1.9	0.08
Propranolol	0.78	1.0	0.30
Nevirapine	0.35	0.8	0.16 - 0.19
Nelfinavir	6.4 E^{-4}	1.0 E^{-4}	0.32 - 0.46
Ritonavir	0.11	0.70	0.06 - 0.10
Ritonavir (hepatocyte data)	0.24	1.10	0.10 - 0.17
Indinavir	0.13	0.05	0.60
Efavirenz	2.65	4.6	0.09 - 0.12
Cilomilast	0.98	0.7	0.97
Roflumilast	12.24	3.5	0.76
Vildagliptin	0.37	0.4	0.26
Tolbutamide	0.33	0.4	0.65
Rosiglitazone	0.26	0.6	4.04

The fold estimates (within 3 fold of reported in most cases) indicate that the simulations can predict the AUC estimates with significant reliability in comparison to other parameters of Cmax and half-life. This also indicate that the utility of AUC or a derived parameter from AUC like the average plasma concentration (AUC/dosing interval) to be used as a reliable optimization parameter for the rank ordering of compound and for correlation with efficacy parameters.

For compounds nelfinavir, ritonavir and roflumilast whose prediction has deviated from reported estimates, the major underlying reasons have been discussed under section 5.2.3 and majorly involve variation in prediction of clearance due to influences of active uptake to hepatocytes, saturation of clearance mechanisms as well as involvement of phase II glucuronidation. Few additional *in vivo* biological processes that could alter the clearance from the predicted values include the following

a) Significant biliary excretion and entero-hepatic re-circulation.

b) Active uptake of efflux of the compound in the intestine and kidneys.

c) Significant metabolism or degradation of the drug in the intestine before getting completely absorbed.

d) General bioanalytical variability in various estimations.

e) Polymorphism of metabolizing enzymes and/or excretory process.

f) CYP induction and mechanism based inhibition (time dependent inhibition, effect of reactive metabolite species).

g) Prominent renal metabolism and active re-absorption/secretion.

Incorporation of measures to minimize variability in individual assessment of properties can be an appropriate step in enhancing the reliability of predictions. For example, liver microsomes from pooled subjects can minimize the variability of predictions since individual donors can sometimes produce misleading data. Utilization of better clearance estimation techniques like hepatocyte based intrinsic clearance assays can incorporate effects of active uptake mediated saturation of clearance, membrane permeability, phase II conjugations etc. and improve the prediction reliability.

Additionally, by incorporating experimental variability estimates (error estimates) as well as provision for pharmacogenetic variabilities (e.g. polymorphism), appropriate window of fold variability and confidence interval can be assessed for predictions and by doing so there could be a prior expectation set on the range of variability for predictions.

5.4. Multivariate Analysis and Identification of Key Properties that Influence Pharmacokinetic Parameters

After prediction of human PK using appropriate PBPK models, the assessment of relative influence of the various physicochemical and ADME properties on the predicted human PK parameters has been performed using partial least square regression (PLS regression).

PLS analysis was performed for four pharmacokinetic parameters (termed as response variables in PLS analysis) namely absorption rate constant (K_a), steady state volume of distribution (V_{ss}), total clearance (CL) and area under curve after oral dosing (AUC) using Minitab software (version 16, Minitab Inc., USA). Various screening data comprising of physicochemical and ADME properties (termed as predictors in PLS analysis), were thus related with the PBPK model derived parameters (termed as dependent variables in PLS analysis) of absorption rate constant (K_a), steady state volume of distribution (V_{ss}) and total clearance (CL) as well as area under curve after oral dosing (AUC). Various iterations were performed in PLS to finally arrive at a model consisting of the appropriate set of predictors (compound properties) that best explain the covariance between the properties and PK parameters, basing on the statistical criteria of the p value, x variance and regression coefficient R square. While a few predictors apparently do not exhibit a direct logical relation with the response variables (for eg. pH dependent solubility and volume of distribution), however they were included as part of the model set after iteration because their inclusion improved the co-variance between predictors and response variables allowing a reliable PLS analysis. This could be due to common underlying factors (latent vectors) that determine both properties though apparently they do not relate to each other. The list of response variables and corresponding predictors are presented in Table 27.

Table 27: List of Response Variables and Corresponding Predictors

Response variable (Y)	Correlating properties (predictors X)	
Absorption rate constant (K_a)	solubility pH 1.8 solubility pH 3.0 solubility pH 4.5 solubility pH 6.8 solubility pH 7.4	pKa Log P Log $D_{7.4}$ Caco-2 permeability
Steady state volume of distribution (V_{ss})	solubility pH 1.8 solubility pH 3.0 solubility pH 4.5 solubility pH 6.8 solubility pH 7.4 pKa	Log P Log $D_{7.4}$ Caco-2 permeability neutral fraction at pH 7.4 fraction unbound in plasma blood plasma partitioning
Total clearance (CL)	solubility pH 1.8 solubility pH 3.0 solubility pH 4.5 solubility pH 6.8 solubility pH 7.4 pKa	Log P Caco-2 permeability neutral fraction at pH 7.4 microsomal clearance fraction unbound in plasma blood plasma partitioning
Area under curve after oral dosing (AUC)	solubility pH 1.8 solubility pH 3.0 solubility pH 4.5 solubility pH 6.8 solubility pH 7.4 pKa Log P	Log $D_{7.4}$ Caco-2 permeability neutral fraction at pH 6.8 neutral fraction at pH 7.4 fraction unbound in plasma blood plasma partitioning microsomal clearance

The reliability of the PLS model was estimated with the following statistical estimates performed as part of PLS analysis. Analysis of variance (ANOVA) was performed using Minitab software on each response variable showed a statistical significance ($p<0.05$) in all the analysis indicating that the regression coefficients are significantly different from zero and therefore the PLS estimates are meaningful. Secondly, the estimated values for X variance are closer to 1 indicating that the variance in the predictors is well explained by the PLS. Also a higher R square value indicated a good fit. The PLS model parameters are summarized in Table 28.

Table 28: PLS Model Statistical Parameters

Parameter	Analysis	Estimate	Significance
p (ANOVA)	PLS K_a	0.000*	Regression coefficients are significantly different from zero. The model estimates are meaningful
	PLS V_{ss}	0.011	
	PLS CL	0.000*	
	PLS AUC	0.006	
X variance	PLS K_a	0.9788	Fraction of variance in the predictors explained by the model (maximum of 1)
	PLS V_{ss}	0.9996	
	PLS CL	0.9020	
	PLS AUC	0.9994	
R sq (coefficient)	PLS K_a	0.9845	Proportion variation in each response explained by the predictors indicating how well each model fits the data (maximum of 1)
	PLS V_{ss}	0.9980	
	PLS CL	0.9901	
	PLS AUC	0.9988	

- Indicates high significance ($p <<< 0.5$) and limited by the Minitab software output of 4 significant digits

PLS analysis effectively reduced the predictors to a set of uncorrelated components (orthogonal latent vectors) which indicate the trends in data. This is followed by a least square regression on these components. The number of components (orthogonal trends) observed in the correlation are presented in Table 29.

Table 29: Number of Principal Components Identified in the PLS Regression Model

Analysis	Number of principal components
PLS K_a	4
PLS V_{ss}	10
PLS CL	5
PLS AUC	10

A standardized PLS coefficient plot of various 'X' parameters that influence a desired 'Y' parameter was plotted using Minitab. The unit of coefficient denotes the change in the response

Y when the variable (X) changes from 0 to 1. The values could exceed 1 only in case of extreme covariance of various properties. Using these coefficients, the relative influence of various properties on the predicted parameters (Y) was assessed. The relative influences of these properties are denoted by the coefficient values with +ve or −ve sign indicating direct or indirect correlation.

5.4.1. Partial Least Square Regression Analysis of Absorption Rate Constant (K_a)

Objective

a) To develop a PLS model relating the selected set of physicochemical and ADME properties (screening data as shown in Table 27) with PBPK based estimates of absorption rate constant (K_a) for the test compounds.

b) Interpret the PLS analysis data and identify the relative influence of various properties on absorption rate constant based on standardized coefficients.

c) Prioritize the various properties for lead optimization based on the interpreted results.

PLS regression analysis identified a 4 component model (latent vectors) that best described the combined effect of nine ADME and physicochemical properties (Table 29). The relative contributions of all nine predictors are graphically presented in Figure 10 and the numerical values of standardized coefficients are presented in Table 30.

Figure 10: Relative Influence of Various Properties on Absorption Rate Constant (K_a)
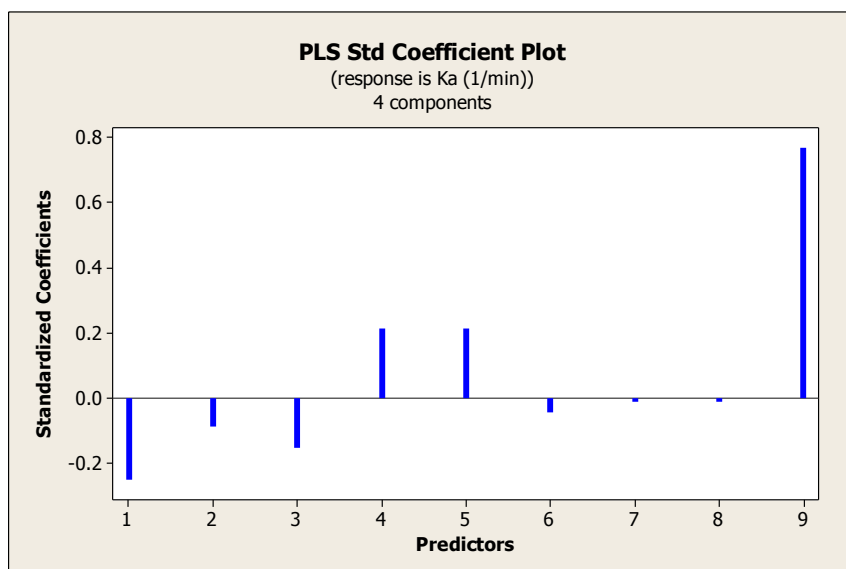
The predictors (properties) in numerical order (1- 9) are solubility pH1.8, solubility pH 3.0, solubility pH 4.5, solubility pH 6.8, solubility pH 7.4, pKa acidic, Log P, Log $D_{7.4}$ and Caco-2 permeability.

The standardized PLS coefficients expresses the change in the response (K_a) when the variable (X) changes from 0 to 1 indicates the relative importance of each property with a positive or negative sign indicating a direct or inverse relationship.

Table 30: Standardized PLS Coefficients of Various Properties with Absorption Rate Constant (K_a)

Predictor no.	Predictor name	Coefficient magnitude
1	solubility pH1.8	-0.25
2	solubility pH 3.0	-0.09
3	solubility pH4.5	-0.15
4	solubility pH 6.8	0.21
5	solubility pH 7.4	0.21
6	pKa	-0.05
7	Log P	-0.01
8	Log D7.4	-0.01
9	Caco-2 permeability	0.77

Interpretation of PLS analysis

PLS analysis indicates permeability of the compounds had a predominant influence in the current dataset, as indicated by a coefficient value of 0.77. The solubility of the compounds also influences especially at pH 6.8 and 7.4 for a higher absorption rate, whereas solubility at relatively acidic pH (1.8-4.5) seems to have an inverse relationship. Both lipid solubility and ionization data played a lesser role.

Using above analysis, further optimization of lead could be rendered using permeability as a key driver with improving solubility at 6.8 and 7.4 while retaining the other attributes. As a future scope of this research, addition of more molecular descriptors (polar surface area, hydrogen

donors or acceptors etc.) to the above kinds of analysis can provide more meaningful interpretations to the chemist. Another important application could be the inclusion of dissolution rate in case of formulation development or optimization.

5.4.2. **Partial Least Square Regression Analysis of Volume Of Distribution at Steady State (V_{ss})**

Objective

a) To develop a PLS model relating the selected set of physicochemical and ADME properties (screening data, as shown in Table 27) with PBPK based estimates of steady state volume of distribution of the test compounds.

b) Interpret the PLS analysis data and identify the relative influence of various properties on volume of distribution based on standardized coefficients.

c) Prioritize the various properties for lead optimization based on the interpreted results.

PLS regression analysis identified a 10 component model (latent vectors) that best describes the combined effect of 12 ADME and physicochemical properties (Table 29). Based on the model the relative contributions of all 12 properties are graphically presented in Figure 11 and the numerical values of standardized coefficients are presented in Table 31.

Figure 11: Relative Influence of Various Properties on Steady State Volume of Distribution (V_{ss})
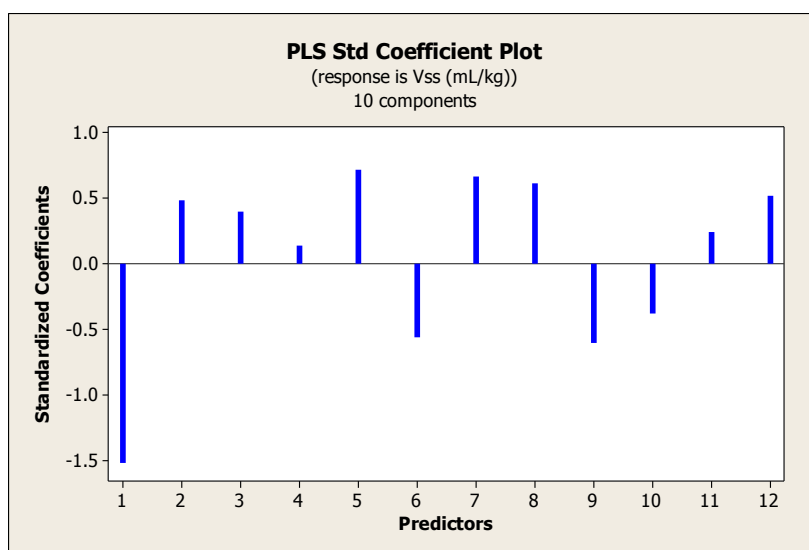
114

The predictors in numerical order (1 to 12) are solubility pH 1.8, solubility pH 3.0, solubility pH 4.5, solubility pH 6.8, solubility pH 7.4, pKa acidic, Log P, Log $D_{7.4}$, neutral fraction pH 7.4, fraction unbound in plasma, microsomal clearance and blood plasma partitioning. The standardized PLS coefficients presented in Table 31, expresses the change in the response (V_{ss}) when the variable (X) changes from 0 to 1 indicates the relative importance of each property with a positive or negative sign indicating a direct or inverse relationship.

Table 31: Standardized PLS Coefficients of Various Properties with Steady State Volume of Distribution (V_{ss})

Predictor no.	Predictor name	Coefficient magnitude
1	solubility pH 1.8	-1.52
2	solubility pH 3.0	0.49
3	solubility pH 4.5	0.40
4	solubility pH 6.8	0.14
5	solubility pH 7.4	0.72
6	pKa	-0.56
7	Log P	0.67
8	Log $D_{7.4}$	0.61
9	Caco-2 permeability	-0.60
10	neutral fraction pH 7.4	-0.38
11	fraction unbound in plasma	0.24
12	blood plasma partitioning	0.51

Interpretation of PLS analysis

The above analysis indicate the direct influence of partitioning coefficients (Log P and Log $D_{7.4}$), plasma protein binding and blood plasma partitioning on volume of distribution. Additionally there is considerable reverse trend observed between the increased membrane

permeability and ionization profiles (pKa). Although solubility may not have a direct influence on volume of distribution but, the inclusion of solubility data significantly improved the model fit for the compounds in the current set with a direct correlation for solubility at pH 3.0-7.4 and an inverse correlation for solubility at pH 1.8, indicating common underlying molecular properties. A more direct relationship with pKa could be interpreted as an increase in acidic pKa of compounds resulting in higher ionization at physiological pH, resulting in lower tissue partitioning and hence reducing volume of distribution.

Based on the above analysis the medicinal chemist can focus on Log P and pKa as major properties that can be optimized with the additional knowledge that, substitutions that alter ionization or solubility might also influence the apparent volume of distribution.

5.4.3. Partial Least Square Regression Analysis of Total Clearance (CL)

Objective

a) To develop a PLS model relating the selected set of physicochemical and ADME properties (screening data as shown in Table 27) with PBPK based estimates of total clearance of the test compounds.

b) Interpret the PLS analysis data and identify the relative influence of various properties on total clearance based on standardized coefficients.

c) Prioritize the various properties for lead optimization based on the interpreted results.

PLS regression analysis identified a 5 component model (latent vectors) that best describes the combined effect of 12 ADME and physicochemical properties (Table 29) on total clearance. Based on the model, the relative contributions of all 12 properties are graphically presented in Figure 12 and the standardized coefficients are presented in Table 32.

Figure 12: Relative Influence of Various Properties on Total Clearance (CL)
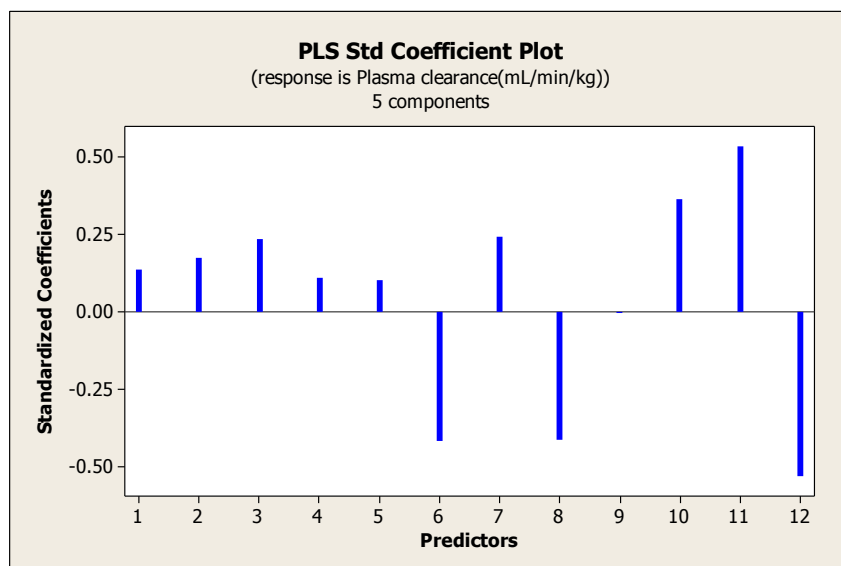
The predictors in numerical order (1 to 12) are solubility pH1.8, solubility pH 3.0, solubility pH 4.5, solubility pH 6.8, solubility pH 7.4, pKa acidic, Log P, Caco-2 permeability, neutral fraction at pH 7.4, microsomal clearance, fraction unbound in plasma and blood plasma partitioning. The standardized PLS coefficients presented in Table 32, expresses the change in the response (CL) when the variable (X) changes from 0 to 1, indicates the relative importance of each property with a positive or negative sign indicating a direct or inverse relationship.

Table 32: Standardized PLS Coefficients of Various Properties with Total Clearance (CL)

Predictor no.	Predictor name	Coefficient magnitude
1	solubility pH 1.8	0.14
2	solubility pH 3.0	0.17
3	solubility pH 4.5	0.23
4	solubility pH 6.8	0.11
5	solubility pH 7.4	0.10
6	pKa	-0.42
7	Log P	0.24
8	Caco-2 permeability	-0.41
9	neutral fraction pH 7.4	-0.01
10	microsomal clearance	0.37
11	fraction unbound in plasma	0.54
12	Blood plasma partitioning	-0.53

117

Interpretation of PLS analysis

For the current data set, there is evidently a prominent influence of microsomal metabolism (metabolic clearance) on the total clearance of the drug. Apart from this, clearance was largely influenced by fraction unbound in plasma and inversely by blood to plasma partitioning. Contribution from permeability could be related to the intracellular permeation to access drug metabolism sites. Ionization (pKa) could be correlated with basicity and the proportion of ionized or unionized species exists in solution and their binding to macromolecules. Influence of Log P can be interpreted with the association to lipid partitioning and ability to partition through lipid bilayers to reach drug metabolizing enzymes. Based on the magnitude of coefficients the relative influence of each contributing factor can be assessed.

Based on the above analysis, the medicinal chemist can plan further optimization by reducing or eliminating metabolic soft spots which reduces microsomal clearance (metabolic clearance). The interplay between the plasma binding and red blood cell (RBC) partitioning appear to be prominent, however the underlying property could be the charged state of the molecules at physiological pH or lipophilicity that might improve its protein binding.

In a review on enhancing metabolic stability as a step to improving decision making process in structural modification of drug candidates, Nassar et al. [132] has reviewed the general strategies to improve metabolic stability. Major initiatives could include addition of stable functional groups (blocking groups) at the metabolically vulnerable sites or by decreasing the lipophilicity reducing its affinity to lipophilic drug metabolizing enzymes. Few specific structural modification strategies described include deactivation of aromatic rings through substitution with electron withdrawing groups (CF_3, SO_2NH_2, SO_3^-), introduction of N-butyl group to prevent N-dealkylation, replacement of labile ester linkage with amide group, stearic shielding of labile groups, avoidance of phenolic group preventing glucuronidation etc.

The current analysis does not include the structure based descriptors for assessing consequences of metabolic soft spots in the chemical structure or factors that improve protein binding. However in the future scope to expand this methodology, there is the flexibility to integrate them as well.

Partial Least Square Regression Analysis of Area Under Curve (AUC) After Oral Dosing

Objective

a) To develop a PLS model relating the selected set of physicochemical and ADME properties (screening data as shown in Table 27) with predicted plasma AUC of the test compounds.

b) Interpret the PLS analysis data and identify the relative influence of various properties on plasma AUC based on standardized coefficients.

c) Prioritize the various properties for lead optimization based on the interpreted results.

PLS regression analysis identified a 10 component model (latent vectors) that best describes the combined effect of 14 ADME and physicochemical properties (Table 29). Based on the model the relative contributions of all 14 properties are graphically presented in Figure 13 and the numerical values of standardized coefficients are presented in Table 33.

Figure 13: Relative Influence of Various Properties on Area Under Curve (AUC)
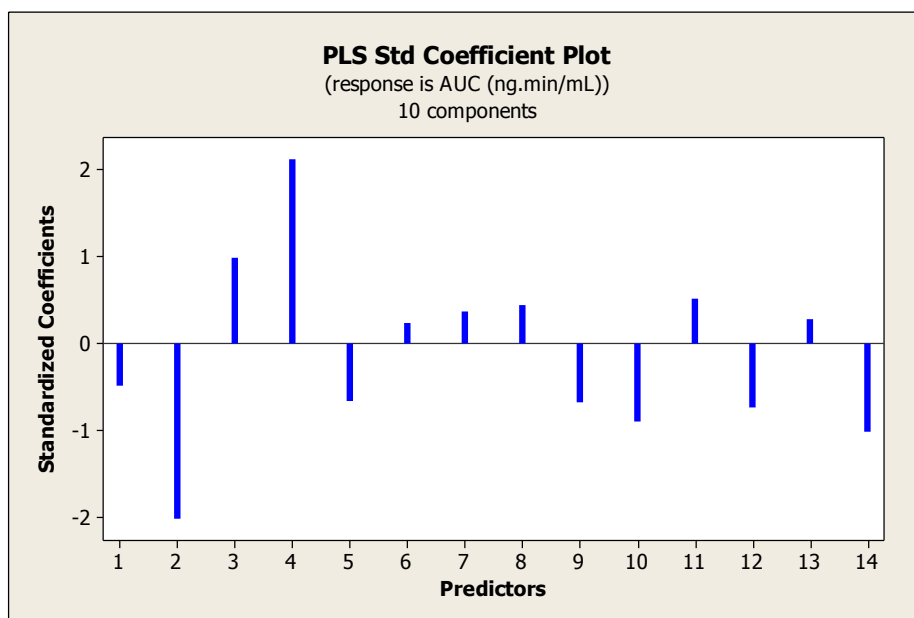
The predictors in numerical order (1 to 14) are solubility pH 1.8, solubility pH 3.0, solubility pH 4.5, solubility pH 6.8, solubility pH 7.4, pKa acidic, Log P, Log $D_{7.4}$, Caco-2 permeability,

neutral fraction at pH 6.8, neutral fraction at pH 7.4, fraction unbound in plasma, blood plasma partitioning and microsomal clearance. The standardized PLS coefficients presented in Table 33, expresses the change in the response (CL) when the variable (X) changes from 0 to 1, indicates the relative importance of each property with a positive or negative sign indicating a direct or inverse relationship.

Table 33: Standardized PLS Coefficients of Various Properties with Area Under Curve (AUC)

Predictor no.	Predictor name	Coefficient magnitude
1	solubility pH 1.8	-0.49
2	solubility pH 3.0	-2.02
3	solubility pH 4.5	0.98
4	solubility pH 6.8	2.12
5	solubility pH 7.4	-0.66
6	pKa	0.24
7	Log P	0.37
8	Log $D_{7.4}$	0.43
9	Caco-2 permeability	-0.68
10	neutral fraction pH 6.8	-0.90
11	neutral fraction pH 7.4	0.52
12	fraction unbound in plasma	-0.74
13	blood plasma partitioning	0.28
14	microsomal clearance	-1.02

Interpretation of PLS analysis

The PLS analysis of AUC could provide a very useful assessment of relative contribution by various properties to *in vivo* exposure especially after oral dosing, however there is an inherent complexity in this analysis with AUC being a composite parameter influenced by various

independent factors like absorption, tissue distribution, clearance, transporter effects, disease state etc. In the current analysis, pH dependent solubility seems to have the greatest influence followed by ionization potential and clearance. These observations provide options for chemical scaffold modification to achieve better *in vivo* profile also considering synthetic feasibility, cost and time.

The above analysis is a good example indicating the multivariate nature of lead optimization efforts with numerous parameters contributing to human pharmacokinetics (parameter AUC, in this case). The complexity of the interplay between numerous properties that influence the AUC cannot be merely explained by simple visual observation of data or rank ordering of compounds. For example Caco-2 permeability in the current AUC analysis seems to influence exposure negatively whereas the expectation is that it should have contributed directly by its direct influence on absorption rate constant. This observation therefore needs a careful understanding in the context of the current data set that an increased permeability for many compounds has been associated with decreased exposure due to the extra dimension of metabolic liability or fraction bioavailability or solubility limiting absorption. For example metoprolol with a near 30 fold higher Caco-2 permeability than atenolol (89 nm/sec vs. 3 nm/sec) had an exposure which is 5 fold lower (195 ng.h/mL vs. 1118 ng.h/mL). In general it appears that for correlation with various properties for lead optimization, specific analysis of individual parameters of absorption rate, volume of distribution, and/or clearance may be better suited than using AUC due to reduced complexity.

5.5. Optimization of Identified Properties: Illustration with Examples Mimicking Lead Optimization

To demonstrate lead optimization exercise that can be undertaken based on the above PLS analysis, scenarios of changes in physicochemical or ADME properties and their impact on pharmacokinetic parameters as well as simulated human *in vivo* PK are investigated. Since a chemical modification of the test compounds was beyond the scope of current research, an illustration of the lead optimization by chemical modification has been made with a hypothetical scenario of changing a single property at a time by two fold, below and above its original value (0.5 x and 2.0 x), mimicking a scenario where the chemical modification has resulted in a two-fold higher solubility or decreased it by half and so on. The properties chosen are liver

microsomal clearance, solubility and Log P. To generate the modified human oral concentration-time profile, the modified screening data (corresponding to 0.5 x and 2.0 x) were incorporated into PBPK models and the modified parameters of K_a, V_{ss} and CL are derived which were used for simulating the human PK profile using the one compartment equation. Even though the current illustration changes only one parameter at a time, in reality the chemical modifications could result in the change of more than one property, and can be easily implemented using the current methodology. Additionally, altering a single property could change multiple ADME parameters as well. Illustrations of varying a single property therefore have been undertaken for simplicity.

In practice, this step could allow the discovery chemist to assess the result of various chemical modifications resulting in change of properties; for example, what if the chemical modifications result in increase of microsomal clearance by two fold or V_{ss} is decreased, would the PK profile change favorably. Subjecting the modified compounds to physicochemical and ADME screening would provide assessment of the changed values for properties. These estimates can then be incorporated into the mechanistic PBPK models for final derivation of human PK parameters of absorption, volume of distribution and clearance which can be used to simulate human plasma concentration-time profile. These PK profiles of modified compounds can be compared with earlier set of compounds to understand the effect that these changes might have on the *in vivo* profile, as well as compared with efficacy parameters to evaluate the impact on efficacy and duration of action. For example, in case of beta blockers the reported beta 1 blocking efficiency (Ki estimates [72]) after correction of protein binding or EC_{50} from PK-PD model can be used. The alteration in Cmax and Caverage can be used as a guide to assess the relative beta 1 and beta 2 (undesirable) blocking when compared with the Ki estimates for beta 2 inhibition. This would allow choice of the right compound with the right set of pharmacokinetic properties (not crossing peak plasma threshold levels for beta 2 inhibition, while ensuring sufficient levels and duration for beta 1 inhibition) as well as efficacy (relative fold selectivity for receptor binding that ensures good margin of safety avoiding adverse effects).

5.5.1. Effect of Variation in Key Properties on *In Vivo* Pharmacokinetic Profile

After assessing the key parameters that contribute to various PK parameters the effect of a two-fold change in certain key properties namely microsomal clearance, solubility and Log P on *in*

vivo PK profile were assessed using simulation after incorporating the influence of changes in these properties on the various PK parameters using PBPK models.

Influence of Liver Microsomal Clearance on *In Vivo* Pharmacokinetic profile

Microsomal clearance is a direct indication of the metabolic phase I clearance of the molecule. This has two major consequences on the *in vivo* pharmacokinetic profile. Change in the microsomal clearance has the first effect on bioavailability where metabolism in the liver clears a portion of drug absorbed from the GI tract by first pass, reducing the fraction bioavailable. The second consequence is on the elimination of drug from the system where compounds with significant phase I clearance get reduced half-life due to increase in metabolic clearance and vice versa. Depending on the rate of absorption, volume of distribution and plasma binding, the Cmax and half-life would also get affected. From the perspective of a medicinal chemist the current exercise could mean the following

a) Assessing the changes made in the metabolic soft spots in the chemical scaffold

b) Consequence of masking the functional groups

c) Effect of favorable substitutions for efficacy that might influence the metabolic clearance

The effect of 2 fold variation in microsomal clearance was incorporated into the PBPK models as follows**:**

a) The lower (0.5 x) and higher (2.0 x) microsomal clearance values were extrapolated to intrinsic clearance using the microsomal scaling factors and subsequently to *in vivo* hepatic clearance using well stirred model

b) The hepatic clearance was used to assess the corresponding change in fraction bioavailable using the relation

$$F \ (fraction \ bioavailable) = F_a \left(1 - \frac{CL_h}{Q_h}\right)$$

c) The modified values (lower and upper) of clearance as well as fraction bioavailable were used to simulate the *in vivo* concentration-time profile and compute AUC using the one compartment model equation (described in methods section) keeping all other parameters

(absorption rate constant and volume of distribution of rapidly perfused tissues) to their original value.

A detailed explanation of each methodology has been provided in literature review as well as methods section. The change in simulated AUC due to two fold variation in microsomal clearance (0.5 x and 2.0 x) is presented in Table 34.

Table 34: Effect of 2 Fold Variation in Microsomal Clearance (CL_{int}) on AUC

Compound	CL_{int} (mL/min/g liver)	Lower fold (0.5 x)	Higher fold (2.0 x)	Simulated AUC * (ng.h/mL)	Simulated AUC after modification (ng.h/mL)	
					Lower	Upper
Atenolol	0.002	0.001	0.004	965	971	953
Metoprolol	11.792	5.896	23.583	197	390	44
Propranolol	1.907	0.953	3.814	293	574	75
Nevirapine	0.077	0.039	0.155	30589	39861	19996
Nelfinavir	71.159	35.579	142.317	13	25	0.1
Ritonavir	5.500	2.750	11.000	16221	32671	6752
Indinvair	3.368	1.684	6.737	2198	4337	559
Efavirenz	11.582	5.791	23.163	115354	155832	70681
Cilomilast	1.118	0.559	2.237	8347	16903	4017
Roflumilast	2.027	1.013	4.053	124	151	87
Vildagliptin	0.963	0.482	1.926	873	1593	354
Tolbutamide	0.311	0.156	0.623	230792	444296	114587
Rosiglitazone	2.617	1.309	5.234	8868	16216	4352

*Estimated in Microsoft EXCEL therefore values would differ slightly with WinNonlin estimates

Figure 14: Plasma Concentration vs. Time Plot of Representative Compounds Indicating Effect of 2 Fold Variation (0.5 x and 2.0 x) of Microsomal Clearance
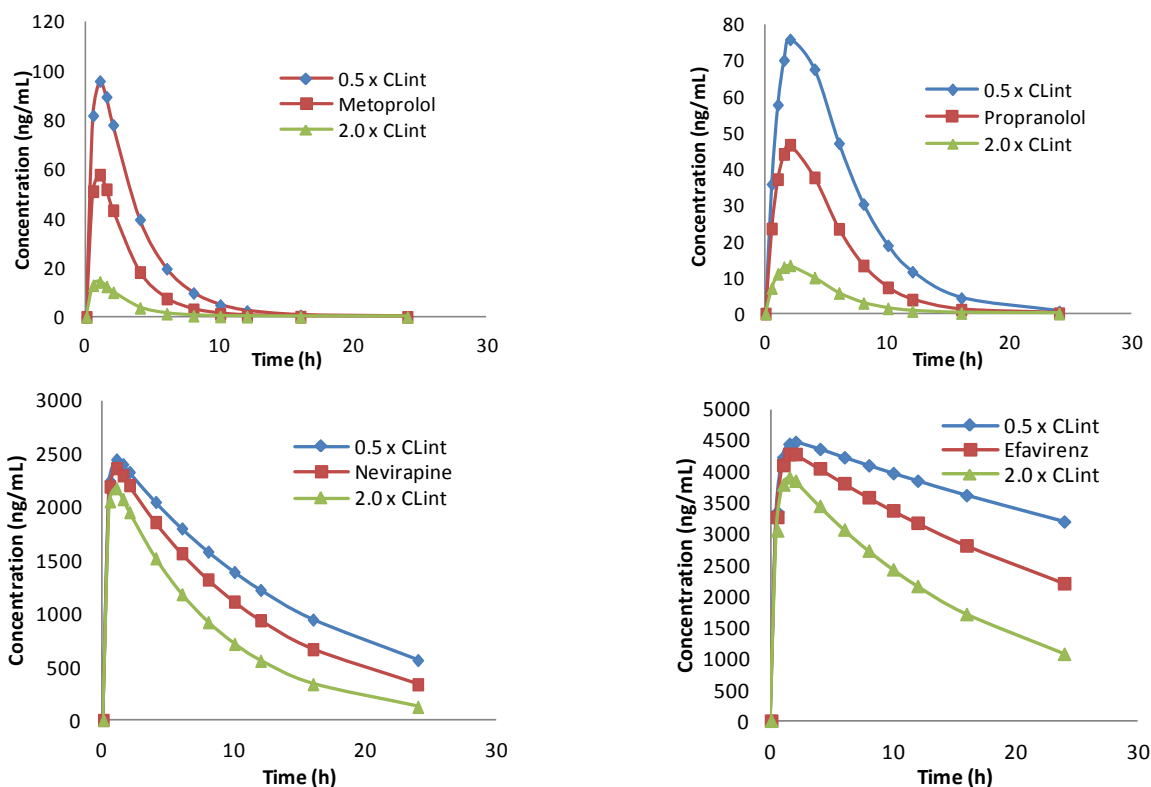
The above simulations demonstrate a hypothetical scenario of the impact of chemical modifications aimed to alter microsomal clearance, on the plasma concentration profile. First two sets of compounds demonstrate marked increase in Cmax as well as AUC with a low clearance (0.5 x), and the reverse trend for 2 fold increase in microsomal clearance. This could be observed largely as a consequence of higher impact of clearance rates than absorption in influencing the plasma concentration-time profile (K_{el} of 0.45 and 0.33 per hour and K_a of 2.2 and 0.66 per hour for metoprolol and propranolol, respectively). Plasma levels approach to near zero at nearly 10 hours post dose in case of a higher clearance whereas it gets extended well beyond 20 hours in case of a 2 fold reduction in clearance. The second set of compounds (corresponding to nevirapine and efavirenz and their modified clearance simulations) has markedly changed terminal levels with relatively lesser impact on Cmax. These compounds had higher predicted absorption rates (K_a of 3.6 and 2.7 per hour) and lower elimination rate constants (K_{el} of 0.09 and 0.03 per hour) in comparison to the first set.

The increased Cmax can have major impact on efficacy if the mechanism depends on a threshold level and toxicity as well, whereas elongated half-lives could impact the duration of action as

125

well as accumulation on repeated dosing. These correlations allow decision making on the modified compounds and selection of ideal candidate.

Influence of Solubility on *In Vivo* Pharmacokinetic profile

Changes in solubility affects the availability of soluble drug at various segments of the GI tract influencing the net available drug for absorption. In case of solubility limiting the absorption, the improvement of solubility has greater impact on the fraction absorbed. From the perspective of a medicinal chemist or formulation scientist this could mean the following

a) Designing new compounds within the chemical series with improved/optimized solubility

b) Improving compounds by introduction of polar functional groups

c) Increasing surface area by micronization

d) Formulation approaches to improve solubility (solid dispersion, solubility enhancers etc.)

The lower (0.5 x) and higher (2.0 x) limits of solubility across pH that were used for simulation are presented in Table 35 and 36. To reduce the solubility subsets the highest acidic solubility below pH 3.0 was used.

Table 35: Lower Solubility Limit for Assessment of Influence On AUC: 0.5 x of Observed

Compounds	Highest acidic solubility (µg/mL)	Solubility at pH 4.5 (µg/mL)	Solubility at pH 6.8 (µg/mL)	Solubility at pH 7.4 (µg/mL)
Atenolol	650	630	685	665
Metoprolol	2454	2825	2493	2718
Propranolol	1560	1450	1600	1531
Nevirapine	383	52	51	49
Nelfinavir	1207	356	4	4
Ritonavir	4	1	1	1
Indinvair	657	822	22	20
Efavirenz	4	4	4	11
Cilomilast	196	7	296	674
Roflumilast	3	3	3	3
Vildagliptin	955	940	954	1009
Tolbutamide	48	56	1248	734
Rosiglitazone	657	542	24	24

Table 36: Higher Solubility Limit for Assessment of Influence on AUC: 2.0 x of Observed

Compounds	Highest acidic solubility (µg/mL)	Solubility at pH 4.5 (µg /mL)	Solubility at pH 6.8 (µg /mL)	Solubility at pH 7.4 (µg /mL)
Atenolol	1950	1889	2054	1996
Metoprolol	7361	8476	7478	8155
Propranolol	4680	4349	4800	4592
Nevirapine	1148	156	152	147
Nelfinavir	3620	1069	12	12
Ritonavir	12	2	2	2
Indinvair	1971	2465	67	59
Efavirenz	11	11	12	32
Cilomilast	588	21	889	2021
Roflumilast	8	8	8	8
Vildagliptin	2865	2819	2862	3028
Tolbutamide	144	167	3745	2201
Rosiglitazone	1971	1626	71	72

The effect of 2 fold variation in solubility across pH was incorporated into the PBPK models as follows**.**

Assessment

a) Using the compartmental absorption model (described in literature review) the fraction absorbed from the GI tract and the fraction bioavailable were estimated corresponding to the lower and upper limits of solubility with the assumption of no change in the intrinsic permeability of the compounds.

b) The plasma concentration-time profile was simulated using a one compartment PK equation keeping all other parameters to their original value.

The simulated AUC corresponding to two fold variation in solubility (0.5 x and 2.0 x across pH) is presented in Table 37. Few representative compounds with significant variation in AUC are presented in Figure 15.

Table 37: Effect of 2 Fold Variation in Solubility (0.5 x and 2.0 x) on Predicted AUC

Parameter	Predicted exposure Method 2; compartmental transit model	AUC (lower) 0.5 x low solubility across pH	AUC (upper) 2.0 x higher solubility across pH
Atenolol	8081	8081	8081
Metoprolol	222	222	222
Propranolol	433	433	433
Nevirapine	32009	32009	32009
Nelfinavir	1	1	2
Ritonavir	3907	1953	5860
Indinvair	1951	976	2927
Efavirenz	238601	238601	238601
Cilomilast	8755	8755	8755
Roflumilast	212	212	212
Vildagliptin	1660	1660	1660
Tolbutamide	244040	244040	244040
Rosiglitazone	7713	7713	7713

The predicted AUC estimates vary from the WinNonlin estimates presented elsewhere since the compartmental absorption model was used here to incorporate changes in pH dependent solubility (method 2 under materials and methods) against the equilibrium model from Usansky et al. [6] applied in the all other assessments. Both the estimates are very comparable however with few notable differences in estimates for atenolol, nelfinavir and ritonavir.

Figure 15: Plasma Concentration vs. Time Plot of Representative Compounds Indicating effect of 2 Fold Variation (0.5 x and 2.0 x) of Solubility
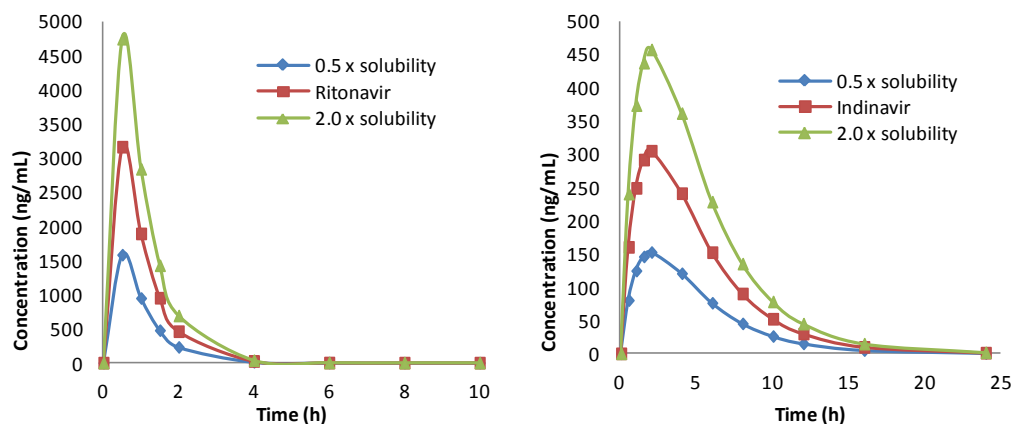
The enhancement of solubility has greater influence on compounds with absorption limited by solubility as influenced by a higher intrinsic permeability. Therefore during lead optimization, solid state characters as well as chemical modifications than enhance solubility but not altering the compound permeability would allow higher absorption and unless influenced by first pass clearance would enhance the Cmax as well as AUC. The careful chemical modifications coupled with above simulations using ADME and physicochemical data of modified compounds would enable a comparison of plasma concentration profiles to understand the effect of modifications and a possible correlation with efficacy and toxicity.

Influence of Log P on *In Vivo* Pharmacokinetic profile

Changes in Log P indicate alteration in lipid partitioning and therefore influence the volume of distribution of the compound in the system. Additionally Log P also affects clearance due to the influence of nonspecific binding (microsomal binding to *in vitro* assays). Log P indirectly influences the absorption rate constant as well as the fraction absorbed due to the effect on distribution to rapidly perfused tissues. From the perspective of a medicinal chemist or formulation scientist this could mean some of the following scenarios

a) Introduction of more lipophilic groups as part of modification of series where increased lipophilicity of the compounds seems to favor receptor binding or approach to target site, improving efficacy

129

b) Deliberate efforts to improve tissue penetrability or

c) Efforts to reduce tissue distribution to avoid possible accumulation and toxicity by using Log P as a parameter.

The effect of 2 fold variation in Log P across pH was incorporated into the PBPK models as follows.

a) Corresponding changes in volume of distribution of rapidly perfused tissues were assessed using tissue partitioning equations.

b) Clearance estimates were corrected corresponding to the variation in unbound microsomal fraction brought about by the changes in Log P (as per the well stirred equation) as per the following relation

$$CL_{H,blood} = \frac{\left[\dfrac{fu_p}{R_B} \times Q_h \times \left(\dfrac{CL_{int\ invivo}}{fu_{inc}}\right)\right]}{\left[Q_h + \left(\dfrac{CL_{int\ invivo}}{fu_{inc}}\right) \times \dfrac{fu_p}{R_B}\right]}$$

c) Absorption rate constants were changed as per the changes in volume of distribution of rapidly perfused tissues

$$k_a = \frac{P_m S}{V_c}$$

d) Corresponding changes in fraction bioavailable were made using the following relation

$$F\ (fraction\ bioavailable) = F_a \left(1 - \frac{CL_h}{Q_h}\right)$$

e) The plasma concentration profiles were simulated using the modified estimates keeping all other parameters to their original value using the one compartment PK model.

The simulated AUC corresponding to 2 fold variation in Log P (0.5 x and 2.0 x across pH) is presented in Table 38. Few representative compounds with significant variation in AUC are presented in Figure 16.

Table 38: Effect of 2 Fold Variation in Log P (0.5 x and 2.0 x) on AUC

Compounds	Measured value	Lower fold (0.5 x)	Higher fold (2.0 x)	AUC Predicted* (ng.h/mL)	Simulated AUC (ng.h/mL)	
					lower	higher
Atenolol	0.335	0.168	0.670	919	934	930
Metoprolol	1.632	0.816	3.264	195	206	127
Propranolol	2.900	1.450	5.800	301	459	113
Nevirapine	2.639	1.320	5.278	30665	35285	12417
Nelfinavir	7.278	3.639	14.556	12	18	12
Ritonavir	2.333	1.167	4.666	11449	13496	4175
Indinvair	3.435	1.718	6.870	2201	3789	1007
Efavirenz	4.380	2.190	8.760	118843	287153	7844
Cilomilast	2.108	1.054	4.216	8185	10318	5351
Roflumilast	2.305	1.153	4.610	123	230	101
Vildagliptin	0.169	0.085	0.338	876	879	866
Tolbutamide	2.362	1.181	4.724	227352	291208	107761
Rosiglitazone	3.023	1.512	6.046	8776	9139	1487

*Estimated with Microsoft EXCEL therefore differ slightly with WinNonlin estimates

Figure 16: Plasma Concentration vs. Time Plot of Representative Compounds Indicating Effect of 2 Fold Variation (0.5 x and 2.0 x) of Log P
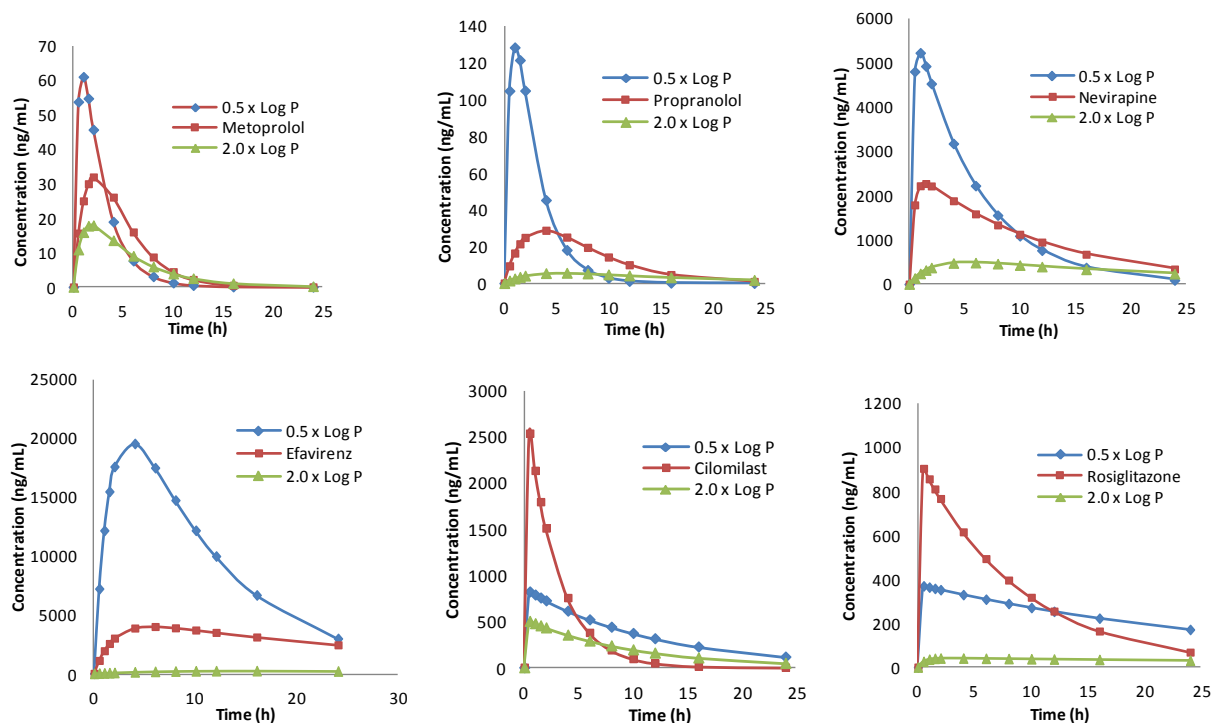
Considerable differences can be observed in Cmax, duration of exposure as well the area under curve for the above given plasma concentration profiles as a result of change in Log P. The primary influence of Log P is on the volume of distribution which indirectly affects the equilibrium rate of absorption due to reduced tissue perfusion. Additionally reduced lipophilicity could result in reduced binding to macromolecules affecting the distribution and clearance due to changes in non specific binding to microsomes. Change in lipophilicity could also influence the metabolism profile due to altered affinity and approachability to drug metabolizing enzymes. Careful evaluation (ADME and physicochemical) and simulation of profiles using the above technique would allow the medicinal chemist to analyze the impact of modifications resulting in changes in Log P.

5.5.2. **Correlation with Efficacy**

As demonstrated above, the mechanistic equations provide flexibility to assess the relative influence of various properties on the pharmacokinetic profile. This opens up the possibility for further extending the methodology to correlate with efficacy. In a preclinical setting an understanding on human efficacy can be obtained in most cases with the extrapolation of PK-PD correlation made in animal models. PK-PD estimates could include receptor binding or inhibition kinetics, modeled efficacy parameters based on a functional response etc correlated with plasma or tissue concentrations to give threshold efficacy levels. These estimates, after correction of receptor affinities or protein binding across preclinical species to human, can be used as target efficacy levels which in comparison with simulated human concentration-time profiles of lead compounds and can be used as a criterion for selection of lead candidate. A demonstration of this correlation is presented in Figure 17, which shows the overlay of various scenarios described with metoprolol and propranolol along with the IC_{50} values estimated from a simple Imax PK-PD model for antihypertensive effect observed (50.6 and 18.1 ng/mL, respectively) in spontaneously hypertensive (SH) rats [133]. For the current illustration no interspecies correction for receptor affinity was made.

Figure 17: Plasma Concentration vs. Time Plot of Two Representative Compounds Along With Various Scenarios, Overlaid Over IC$_{50}$ Estimates from Preclinical PK-PD Model
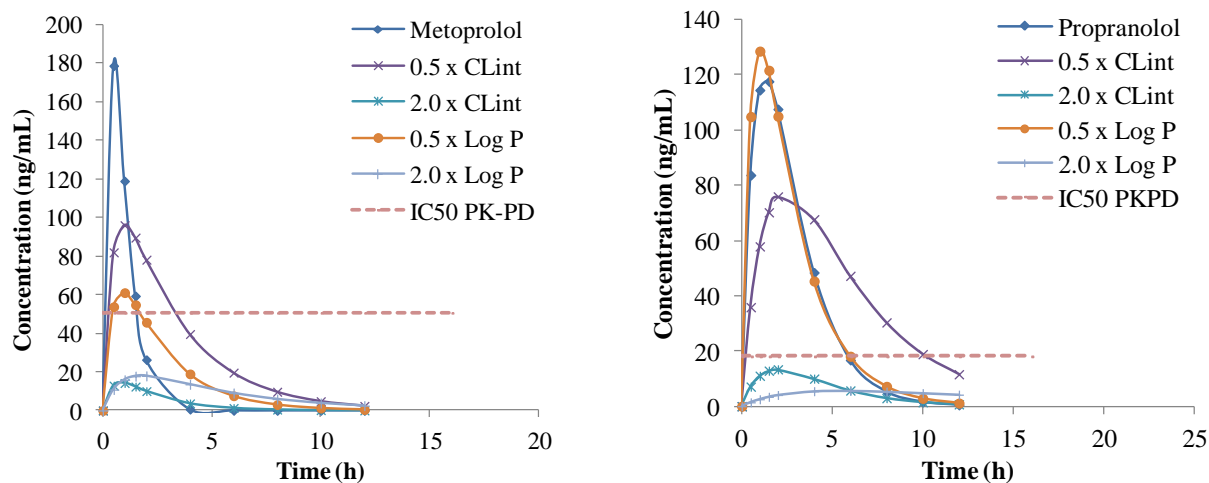
The correlations clearly demonstrate the effect of altering the various properties on human *in vivo* plasma levels in relation with predicted efficacy concentration. A desirable property for a beta blocker could be to have sustained levels above efficacy threshold (beta1 blockade) for a longer duration without exceeding peak threshold levels of known toxicity (eg. beta 2 blockade resulting in bronchospasm). It can be observed in the above illustration that higher clearance does not allow achieving the therapeutic levels, whereas reducing the lipophilicity seems to have a beneficial effect on duration of plasma levels above effective concentrations. Additional evaluations feasible with this approach include the simulation of repeat dose administration and the effect of the peak and trough concentrations on efficacy parameters, correlation with threshold levels for beta 2 inhibition (Ki estimates with human β_2 receptor inhibition) etc. More elaborate evaluations are also feasible with PBPK based simulated cardiac tissue levels which can provide better correlations with efficacy.

In the case of anti-retroviral drugs, there is more reliance on cell based assays (T cells, monocyte cell lines, human primary cells) and also the reliance on using various strains considering the rapid mutation of the human immunodeficiency (HIV) virus. Factors like increased intra cellular levels, efflux transport and protein binding has been considered as major factors determining the drug efficacy apart from compliance to drug regimen to maintain the plasma levels above the effective concentrations. Most of the modeling parameters include CD4

cell count, HIV ribonucleic acid (RNA) levels (Log copies/mL) etc [134] and these can be correlated with simulated profiles generated based on the current methodology.

For PDE4 inhibitors PD markers like cytokines or PBMC (peripheral blood mononucleated cells) based measurements (etc. TNF α release) can form excellent correlation markers [135, 136].

With regard to anti-diabetic compounds, there could be correlation of the simulated plasma levels with inhibition of plasma DPP IV enzyme (in case of DPP IV target), glucose excursion or glycosylated hemoglobin etc in case of other anti-diabetic targets [137, 138].

The above methodology thus allows correlation with efficacy parameters or extrapolated human PK-PD prediction estimates from animal models early in the discovery program allowing the scientist to rationally choose the compound with a better probability to demonstrate efficacy and reduced toxicity in clinical trials.

The various steps on TPP based optimization has been illustrated based on variation of one parameter at a time for the sake of simplicity. In reality, the modification of one parameter eventually influences few others which will be reflected as changes in various physicochemical and ADME parameters. These scenarios can be well assessed due to the application of mechanistic PBPK models in the current methodology bringing in adequate flexibility for simulating various scenarios. This flexibility can also be used as a tool to identify optimum ranges for each parameter that could be aimed to achieve by various chemical modifications of the pharmacophore. Further the modifications in chemical scaffold can be prioritized to improve properties that require more optimization with others maintained within the identified acceptable limits.

While not undermining the various limitations described and possible variability in human prediction with the methodology, the current research demonstrates the utility of the new derived methodology to be employed in a drug discovery effort to mechanistically predict human pharmacokinetic profile, identify key parameters that influence the *in vivo* profile as well as simulate the changes in PK profile on modifying them and correlate with various efficacy parameters to enable rational lead optimization and selection of an ideal clinical candidate.

6.0.   CONCLUSIONS

6.1. General Conclusions

The primary goal of current research was to develop a new methodology for application in lead optimization for rational selection of a clinical candidate. The research involved mechanistic integration of various experimental physicochemical and ADME data using physiological pharmacokinetic models as well as simulation of human concentration-time profile as the initial objective. This was followed by a multivariate analysis of the predictors and response variables to assess the relative contribution of various screened data to enable prioritizing them for lead optimization. As the final step, the utility in lead optimization was demonstrated with few hypothetical examples of assessing the effect of two fold variation (0.5 x and 2.0 x) in some key properties on the concentration-time profile as well as its possible effect on efficacy.

Prediction of human PK profile has been attempted with mechanistic human modeling (physiological based pharmacokinetic modeling). Reliable predictions of human pharmacokinetic parameters were obtained with >90% of compounds within 2 fold error. In the simulation of human concentration-time profiles, 8 compounds out of 13 remained within 3 fold of AUC and for compounds that deviated, critical causes of variability (active uptake, inhibition of metabolism, over prediction of clearance with microsomes) could be identified.

The results presented in the current work represent one of the few works available in this area. The publication from Pfizer in May 2011 (Jones et al.) [3] utilized 21 in-house compounds with relevant preclinical and clinical data for which the intravenous and oral human PK simulations were performed. The simulation results indicated that the predictions using PBPK were superior to those obtained via traditional methods. The other major development has been the Pharmaceutical Research and Manufacturers Association of America (PhRMA) initiative (May 2011) on predictive models of human pharmacokinetics [139], which assessed the effectiveness of PBPK models for simulating human plasma concentration profiles. Many of the discussion points in the current study including the effect of formulations, transporter effects etc. has been acknowledged in the PhRMA study.

The prediction of human pharmacokinetic parameters and *in vivo* PK profile would add value to lead optimization efforts or would accelerate drug development only if it is presented with a systematic and reliable methodology, enabling the scientist to integrate with compound chemistry, biopharmaceutical properties as well as its pharmacology and safety profile. This

approach would enable the scientists to take informed decisions on clinical development of the molecule keeping in mind the resources, time and effort. The current research adds value in this aspect.

To understand the various underlying properties that would influence a favorable PK profile, the application of partial least square regression in this research is the first such attempt in drug discovery to the best of our knowledge, even though it has been widely used in other areas like chemometrics [68, 140, 141]. The results and interpretation of PLS analysis would vary with respect to the chemical series under optimization in relation to the target profile, and the demonstration through the current work reveals the utility of this methodology in lead optimization. Also as demonstrated with simulation of concentration-time profile with two fold variation of properties (0.5 x and 2.0 x), the PBPK based approach would enable to assess the results of chemical modifications as well making it a useful approach in lead optimization for choice of a lead candidate.

To summarize, the methodology developed comprise of carefully executed physicochemical and ADME screens, with careful collation of data and fitting them to mechanistic PBPK models for prediction of human PK parameters and simulate human PK profile. Further, with application of PLS regression, the relative importance of various properties on the *in vivo* PK profile can be assessed for optimization by chemical modification or formulation approaches. The modified compounds can be screened for their physicochemical and ADME properties again and their human *in vivo* profiles simulated to see the impact of chemical modifications on efficacy parameters (PK-PD correlations) allowing a rational approach to identify a lead candidate that fits a target product profile. The research thus provides a novel methodology enabling a faster selection of best candidate for clinical development.

A general schematic of the developed research methodology is given in Figure 18.

137

Figure 18: Summary of Methodology Developed in the Current Research
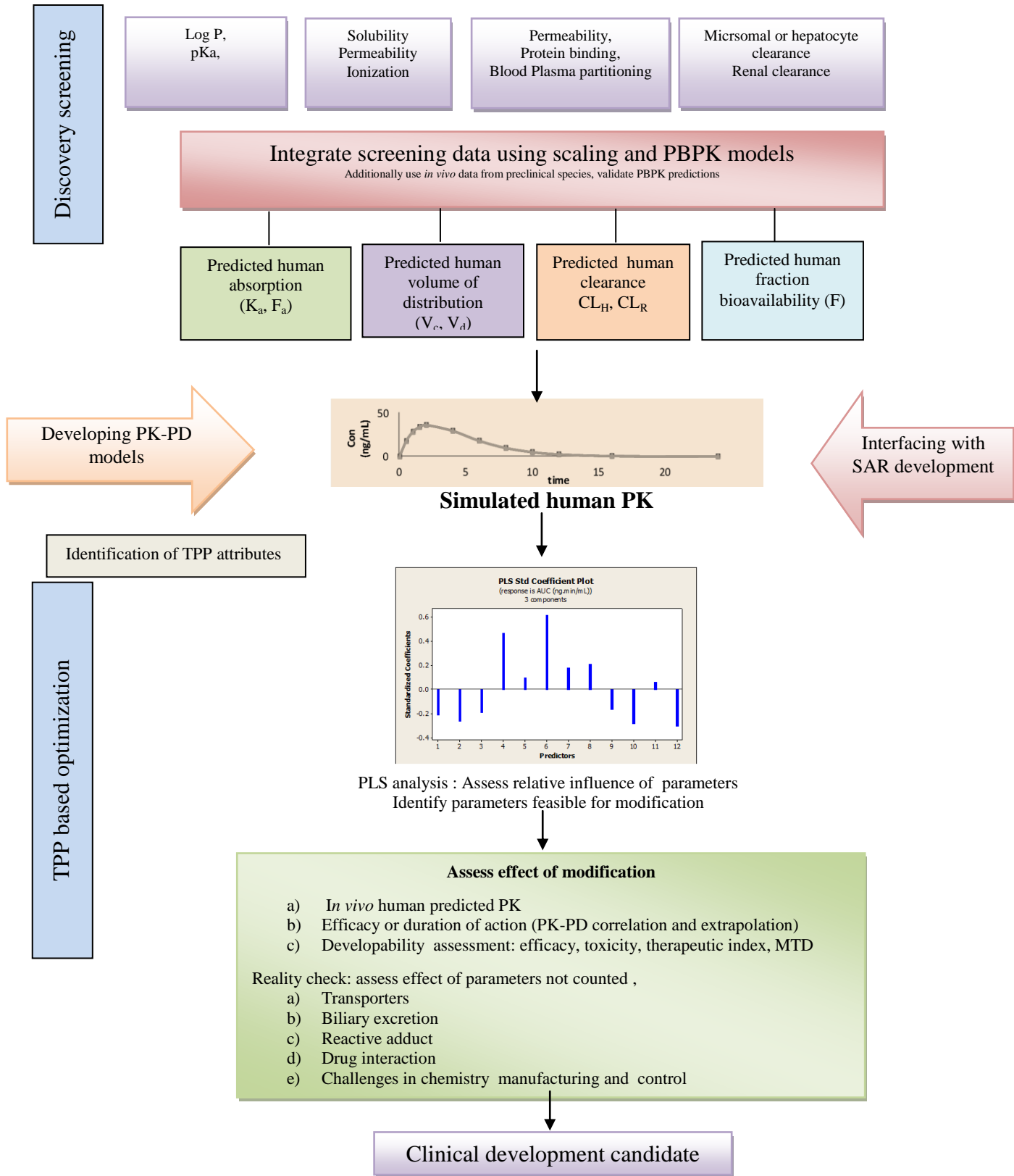
6.2. Specific Contribution from Research

a) The current research provides a new methodology for application in drug discovery and lead optimization using PBPK models and PLS regression.

b) The current research demonstrates the utility of PBPK models to predict human PK early in discovery process with good degree of reliability. The current research is one of the few reports available on PBPK based prediction human oral PK profiles.

c) The application of PLS regression analysis has been a novel approach to rationally choose the compound properties for optimization which has been applied for the first time to the best of knowledge.

d) The current research also represents the best compilation of latest developments in PBPK modeling as well as a novel multivariate approach that could be applied for various TPP based discovery efforts. The various techniques elaborated in the current research inclusive of the *in vitro* assays and modeling techniques can be utilized for various research work in the area of

     i. Optimization of a newly identified chemical series

     ii. Correlation of efficacy with appropriate PK surrogates

     iii. Formulation optimization and clinical strategy

     iv. Choice of better clinical candidate

e) By virtue of its prediction ability of human PK much earlier than other techniques like allometry, the current research opens up the possibility to start assessing human PK-PD relationship. The tissue partitioning equations used which can also provide individual tissue partitioning of drugs at steady state can be used to develop mechanistic PBPK-PD relationships which might provide a better correlation than any empirical model.

f) Incorporation of all major ADME and physiochemical properties in this methodology would enhance the ability to differentiate and choose an ideal candidate from a list of closely related compounds in comparison with other assessments based on individual ADME or PK properties. The prediction model could be further improved with the inclusion of diverse and larger number of compounds.

g) Over all the current research provides an overarching strategy that effectively incorporates the techniques of screening and novel optimization approach for faster selection of ideal clinical candidate based on a Target Product Profile (TPP).

6.3. Future Scope of Work

The current methodology developed as part of the research forms a platform which can be further utilized at various aspects of research.

a) Enhance the scope of structure activity relationships (SAR) by including other molecular descriptors with PLS analysis and identify key properties more specifically

b) Development of PBPK-PD models where use of mechanistic models instead of compartmental models can give better prediction of target tissue concentrations and correlate with efficacy. Successful predictions in this effort could then directly correlate modifications in chemical structure to efficacy for many pharmacological interventions.

c) Further improvements in PBPK models can improve the predictability and application of the current methodology. Incorporation of transporter effects, biliary excretion and entero-hepatic recirculation, effect of inactivation of drug metabolizing enzymes, effect of co-administration of drugs with competing metabolic pathways etc. are some areas where considerable research is underway and would need further advancement.

d) More elaborate work on the current methodology if undertaken with large number of compounds within a series and involving multiple pharmacophores would further validate this approach and enable its effective utilization to accelerate the drug discovery process. The effort would definitely require considerable resources in terms of availability of large chemical series, infrastructure and technical expertise. A significant achievement of reduction in time with faster lead optimization and evolution of a rational decision making process incorporating the current methodology would be a significant contribution to research community.

7.0.   BIBLIOGRAPHY

1. Obach RS, Baxter JG, Liston TE, Silber BN, Jones BC, Macintyre F, et al. The prediction of human pharmacokinetic parameters from preclinical and *in vitro* metabolism data. The Journal of Pharmacology and Experimental Therapeutics. 1997; 283(1): p. 46-58.

2. Teorell T. Kinetics of distribution of substances administered to the body. Archives Internationales de Pharmacodynamie et de Therapie. 1937; 57: p. 205-240.

3. Jones HM, Gardner IB, Collard WT, Stanley PJ, Oxley P, Hosea NA, et al. Simulation of human intravenous and oral pharmacokinetics of 21 diverse compounds using physiologically based pharmacokinetic modelling. Journal of Clinical Pharmacokinetics. 2011; 50(5): p. 331-347.

4. Pouline P, Theil FP. A priori prediction of tissue:plasma partition coefficients of drugs to facilitate the use of physiologically-based pharamcokinetic models in drug discovery. Journal of Pharmaceutical Sciences. 2000; 89(1): p. 16-35.

5. De Buck SS, Sinha VK, Fenu LA, Nijsen MJ, Mackie CE, Gilissen RAHJ. Prediction of human pharmacokinetics using physiologically based modeling: A retrospective analysis of 26 clinically tested drugs. Drug Metabolism and Disposition. 2007; 35(10): p. 1766-1780.

6. Usansky HH, Sinko PJ. Estimating human drug oral absorption kinetics from Caco-2 permeability using an absorption-disposition model: Model development and evaluation and derivation of analytical solutions for Ka and Fa. The Journal of Pharmacology and Experimental Therapeutics. 2005; 314(1): p. 391-399.

7. Magee DF, Dalley AFI. Digestion and the structure and function of gut. Continuing Eduction Series ed.: Karger; 1986.

8. Willman S, Schmitt W, Keldenich J, Lippet J, Dressman JB. A physiological model for the estimation of fraction dose absorbed in humans. Journal of Medicinal Chemistry. 2004; 47(16): p. 4022-4031.

9. Hall JE, Guyton AC. Text Book Of Medical Physiology. 9th ed. Philadelphia: W.B.Saunders; 1996.

10. Kararali TT. Gastrointestinal Absorption of Drugs. Critical Reviews in Therapeutic Drug Carrier Systems. 1989; 6: p. 39-86.

11. Pearsons RL. Drug Absorption in gastrointestinal disease with particular reference to malabsorption syndromes. Clinical Pharmacokinetics. 1977; 2: p. 45-60.

12. International commission on radiological protection task group on reference man: Report of the task group on reference man. New York:; 1992.

13. Hebel R, Stromberg MW. Anatomy and Embryology of Laboratory Rats Worthsee: Biomed; 1986.

14. Malagelada JR, Robertson JS, Brown ML, Remington M, Duenes JA, Thomforde GN, et al. Intestinal transit of Solid and Liquid Components of a Meal in Health. Gastroenterology. 1984; 87: p. 1255-1263.

15. Granger DN, Barrowman JA, Kvietys PR. Clinical Gastrointestinal Physiology Philadelphia: W B Saunders; 1985.

16. davis SS, Hardy JG, Fara JW. Transit of pharmaceutical dosage forms through the small intestine. Gut. 1986; 27: p. 886-892.

17. Avdeef A. Physicochemical profiling (Solubility, Permeability and Charged State). Current Topics in Medicinal Chemistry. 2001; 1: p. 277-351.

18. Kalantzi L, Goumas K, Kalioras V, Abbrahamsson B, Dressman JB, Reppas C. Characterisation of the human upper gastrointestinal contents under conditions simulating bioavailability/bioequivalece studies. Pharmaceutical Research. 2006; 23: p. 165-176.

19. Lindahl A, Ungell AL, Knutson L, Lennernaes H. Charecterisation of fluids from stomach and proximal jejunum in men and women. Pharmaceutical Research. 1997; 14: p. 497-502.

20. Moreno MPC, Oth M, Deferme S, Lammert F, Track J, Dressman J, et al. Charecterization of fasted-state human intestinal fluids collected from duodenum and jejunum. Journal of Pharmacy and Pharmacology. 2006; 58: p. 1079-1089.

21. Lipinski CA, Lobardo F, Dominy BW, Feeney PJ. Experimental and computational approaches to estimate solubility and permeability in drug discovery and development settings. Advances Drug Delivery Reviews. 1997; 23(3): p. 3-25.

22. Veber DF, Johnson SR, Cheng HY, Smith BR, Ward KW, Kopple KD. Molecular properties that influence the oral bioavailability of drug candidates. Journal of Medicinal Chemistry. 2002; 45: p. 2615-2623.

23. Sugano K, Okazaki A, Sugimoto S, Tavornvipas S, Omura A, Mano T. Solubility and dissolution profile assessment in drug discovery. Drug Metabolism and Pharmacokinetics. 2007; 22(4): p. 225-254.

24. Noyes AA, Whitney WR. The rate of solution of solid substances in their own solutions. Journal of the American Chemical Society. 1897; 19: p. 930-934.

25. Nernst W. Theory of reaction velocity in heterogenous systems. Zeitschrift für Physikalische Chemie. 1904; 47: p. 52-55.

26. Brunner E. Velocity of reaction in non-homogeneous systems. International Journal of Research in Physical Chemistry and Chemical Physics (Zeitschrift Physikalische Chemie). 1904; 47: p. 56-102.

27. Thomas S, Brightman F, Gill H, Lee S, Pufong B. Simulation modelling of human intestinal absorption using Caco-2 permeability and kinetic solubility data for early drug discovery. Journal of Pharmaceutical Sciences. 2008; 97: p. 4557-4574.

28. Bohets H, Annaert P, Mannens G, van beijsterveldt L, Anciaux K, Verboven P, et al. Strategies for absorption screening in drug discovery and development. Current Topics in Medicinal Chemistry. 2001; 5(1): p. 367-383.

29. Amidon GL, Sinko PJ, Fliesher D. Estimating human oral fraction dose absorbed: A correlation using rat intestinal membrane permeability for passive and carrier mediated compounds. Pharmaceutical Research. 1988; 10(5): p. 651-654.

30. Perrin DD, Dempsey B, Serjeant EP. pKa prediction for organic acids and bases London: Chapman and Hall; 1981.

31. Albert A, Serjeant EP. The determination of ionisation constants. 3rd ed. London: Chapman and Hall; 1984.

32. Amidon GL, Lennernas H, Shah VP, Crison JR. A theoretical basis for a biopharmaceutic drug classification: The correlation of in-vitro drug product dissolution and in-vivo bioavailability. Pharmaceutical Research. 1995; 12(3): p. 413-420.

33. Pang SK. Modeling of intestinal drug absorption: Roles of transporters and metabolic enzymes (for the Gillette review series). Drug Metabolism and Disposition. 2003; 31: p. 1507-1519.

34. Prueksaritanont T, Gorham LM, Hochman JH, Tran LO, Vyas KP. Comparative studies of drug-metabolizing enzymes in dog, monkey and human small intestines, and in Caco-2 cells. Drug Metabolism and Disposition. 1996; 24(6): p. 634-642.

35. Hilgendorf C, Ahlin G, Seithal A, Artursson P, Ungell AL, Karlsson J. Expression of thirty six drug transporter genes in human intestine, liver, kidney and organotypic cell lines. Drug Metabolism and Disposition. 2007; 35: p. 1333-13340.

36. Johnson KC, Swindell AC. Guidance in the setting of drug particle size specifications to minimize variability in absorption. Pharmaceutical Research. 1996; 13(12): p. 1795-1798.

37. Hilgers AR, Smith DP, Biermacher JJ, Day JS, Jensen JL, Sims SM, et al. Predicting oral absorption of drugs; A case study with a novel class of antimicrobial agents. Pharmaceutical Research. 2003; 20(8): p. 1149-1155.

38. Yuasa H. Science for evaluation and improvement of drug bioavailability Sugiyama Y, Gendaiiryosha , editors. Tokyo; 1998.

39. Willman S, Schmitt W, Keldenich J, Dressman JB. A physiological model for simulating gastrointestinal flow and drug absorption in rats. Pharmaceutical Research. 2003; 20(11): p. 1766-1771.

40. Benjamin B, Barman TK, Chaira T, Paliwal JK. Integration of physicochemical and pharmacokinetic parameters in lead optimisation; A physiological pharmacokinetic model based approach. Current Drug Discovery Technologies. 2010; 7: p. 143-153.

41. Kimura T, Higaki K. Gastrointestinal transit and drug absorption. Biological Pharmaceutical Bulletin. 2002; 2(25): p. 149-164.

42. Rowland M, Tozer TN. Clinical Pharmacokientics. Concepts and applications. 3rd ed. Manchester: B.I.Waverly; 1995.

43. Kansy M, Senner F, Gubernator K. Physicochemical high throughput screening: Parallel artificial membrane permeation assay in the description of passive absorption processes. Journal of Medicinal Chemistry. 1998; 41: p. 1007-1010.

44. Cho MJ, Thompson DP, Cramer CT, Vidmar TJ, Scieszka JF. The Madin Darby Canine Kidney (MDCK) epithelial cell monolayer as a model cellular transport barrier. Pharmaceutical Research. 1989; 6: p. 71-77.

45. Artursson P. Epithelial transport of drugs in cell culture. I : A model for studying the passive diffusion of drugs over intestinal absorbtive (Caco-2) cells. Journal of Pharmaceutical Sciences. 1990; 79: p. 476-482.

46. Oie S, Tozer TN. Effect of altered plasma protein binding on apparent volume of distribution. Journal of Pharmaceutical Sciences. 1979; 68: p. 1203-1205.

47. Poulin P, Theil FP. Prediction of pharmacokinetics prior to *in vivo* studies. I. Mechanism-based prediction of volume of distribution. Journal of Pharmaceutical Sciences. 2002; 91(1): p. 129-156.

48. Poulin P, Theil FP. Prediction of pharmacokinetics prior to *in vivo* studies. II. Generic physiologically based pharmacokinetic models of drug disposition. Journal of Pharmaceutical sciences. 2002; 91(5): p. 1358-1370.

49. Poulin P, Krishnan K. A biological based algorithm for predicting human tissue:blood partitioning coefficients of organic chemicals. Human and Experimental Toxicology. 1995; 14: p. 273-280.

50. Poulin P, Krishnan K. Molecular structure-based prediction of the partition coefficient of organic chemicals for physiological pharmacokinetic models. Toxicology Methods. 1996; 6: p. 117-137.

51. Leo A, Hansch C, Elkins D. Partition coefficients and their uses. 1971; 71: p. 525-615.

52. Berezhkovskiy LM. Volume of distribution at steady state for linear pharmacokinetic system with peripheral elimination. Journal of Pharmaceutical Sciences. 2004; 93(6): p. 1628-1640.

53. Rodgers T, Leahy D, Roland M. Physiologically based pharmacokinetic modeling 1: Predicting the tissue distribution of moderate to strong bases. Journal of Pharmaceutical Sciences. 2005; 94: p. 1259-1276.

54. Berezhkovskiy LM. Determination of volume of distribution at steady state with complete comsideration of the kinetics of protein and tissue binding in linear pharmacokinetics. Journal of Pharmaceutical Sciences. 2004; 93(2): p. 364-374.

55. Larsson B, Ullberg S. Whole -body autoradiography. Journal of Histochemistry and Cytochemistry. 1981; 29(1A): p. 216-225.

56. Brunner M, Langer O. Microdialysis versus other techniques for the clinical assessment of *in vivo* tissue drug distribution. The AAPS Journal. 2006; 8(2): p. E263-E271.

57. Nelson D. University of Tennessee Health Science Centre. [Online]. [cited 2012 June 09. Available from: http://drnelson.uthsc.edu/human.P450.table.html.

58. FDA. Guidance for industry: Drug interaction studies-study design, data analysis, and implications for dosing and labeling. Food and Drug Administration, USA, Centre for Drug Evaluation and Research; 2006.

59. Tompkins LM, Wallace AD. Mechanisms of cytochrome P450 induction. Journal of Biochemical Molecular Toxicology. 2007; 21(4): p. 176-181.

60. Janku I. Physiological modelling of renal clearance. European Journal of Clinical Pharmacology. 1993; 44: p. 513-519.

61. Ghibellini G, Leslie EM, Brower KL. Methods to evaluate biliary excretion of drugs in humans: an updated review. Moleclar Pharmacology. 2006; 3: p. 198-211.

62. Iwatsubo T, Hirota N, Ooie T, Suzuki H, Sugiyama Y. Prediction of *in vivo* drug disposition from *in vitro* data based on physiological pharmacokinetics. Biopharmaceutics and Drug Disposition. 1996; 17: p. 273-310.

63. Pang SK, Weiss M, Macheras P. Advanced pharmacokinetic models based on organ clearance, circulatory and fractal concepts. The AAPS Journal. 2007; 9(2): p. E268-E283.

64. Austin RP, Barton P, Cockroft SL, Wenlock MC, Riley RJ. The influence of nonspecific microsomal binding on apparent intrinsic clearance and its prediction from physicochemical properties. Drug Metabolism and Disposition. 2002; 30: p. 1497-1503.

65. Taylor PJ. Hydrophobic properties of drugs in comprehensive medicinal chemistry Hansch C, Sammes PG, Taylor JB, editors. Oxford: Pergamon Press; 1990.

66. Roberts MS, Rowland M. A dispersion model of hepatic elimination: 1. Formulation of the model and bolus considerations. Journal of Pharmacokinetics and Biopharmaceutics. 1986; 14: p. 227-260.

67. Abdi H. Partial least squares regression and projection on latent structure regression (PLS Regression). WIREs Computational Satistics. 2010; 2: p. 97-106.

68. Wold S, Eriksson L, Trygg J, Kettaneh N. The PLS method - Partial least squares projections to latent structures and its application in industrial RDP (research, development and production). Umea University; 2004.

69. Cliffnotes. [Online]. [cited 2011 October 10. Available from: http://www.cliffsnotes.com /study_guide/Operations-with-Matrices.topicArticleId-20807, article Id-20779.html.

70. Baker JG. The selectivity of β-adrenoreceptor antagonists at the human β1, β2 and β3 adrenoreceptors. British Journal of Pharmacology. 2005; 144: p. 317-322.

71. Mehvar R. Stereospecific pharmacokinetics and pharmacodynamics of beta adrenergic blockers in humans. Journal of Pharmacy and Pharmaceutical Sciences. 2001; 4(2): p. 185-200.

72. Smith C, Teitler M. Beta-blocker selectivity at cloned human beta1 and beta2 adrenergic receptors. Cardiovascular Drugs and Therapy. 1999; 13: p. 123-126.

73. Baek Ih, Yun Mh, Yun Hy, Kwon Ki. Pharmacokinetic/pharmacodynamic modeling of cardiovascular effects of beta blockers in humans. Archives of Pharmacal Research. 2008; 31(6): p. 814-821.

74. Warnke D, Barreto J, Temesgen Z. Antiretroviral drugs. Journal of Clinical Pharmacology. 2007; 47: p. 1570-1579.

75. Vervoort SCJM, Borleffs JCC, Hoepelman AIM, Grypdonck MHF. Adherence in antiretroviral therapy: a review of qualitative studies. AIDS. 2007; 21: p. 271-281.

76. Legrand M, Comets E, Aymard G, Tubiana R, Katlama C, Diquet B. An *in vivo* pharmacokinetic/pharmacodynamic model for antiretroviral combination. HIV Clinical Trials. 2003; 4: p. 170-183.

77. Barnes PJ, Stockley RA. COPD: Current therapautic interventions and future approaches. European Respiratory Journal. 2005; 25: p. 1084-1106.

78. Stephen C, David B. The target product profile as a planning tool in drug discovery research. In: PHARMATECH; 2003. p. 67-71.

79. Reed K, Mereish K, Jensen B. Quantitative relationships between structure and pharmacokinetic parameters using molecular connectivity Chi indices 1: Substituted 2-sulphapyridines. Journal of Pharmaceutical Sciences. 1984; 73(2): p. 237-240.

80. McGinnity DF, Soers MG, Urbanowicz RA, Riley RJ. Evaluation of fresh and cryopreserved hepaticytes as invitro drug metabolism tools for the prediction of metabolic clearance. Drug Metabolism and Disposition. 2004; 32(11): p. 1247-1253.

81. Curry S, McCarthy D, DeCory HH, Marler M, Gabrielsson J. Phase I: The first opportunity for extrapolation from animal data to human exposure. In: Fletcher AJ, Edwards LD, Fox AW, Stonier P, editors. Principles and Practices of Pharmaceutical Medicine.: John Wiley and Sons; 2002. p. 95-114.

82. Feng MR, Lou X, Brown RR, Hutchaleelaha A. Allometric pharmacokinetic scaling: towards the prediction of human oral pharmacokinetics. Pharmaceutical Research. 2000; 17(4): p. 410-418.

83. Tang H, Mayerson M. A novel model for prediction of human drug clearance by allometric scaling. Drug Metabolism and Disposition. 2005; 33: p. 1297-1303.

84. Podlogar BL, Muegge I, Brice LJ. Computational methods to estimate drug development parameters. Current Opinion in Drug Discovery and Development. 2001; 4: p. 102-109.

85. Andrej B, Tatiana N, Yuri N. Early prediction of drug metabolism and toxicity: Systems biology approach and modeling. Drug Discovery Today. 2004; 9: p. 127-135.

86. Darko B, Matthew DS, Katrina F. Predicting ADME properties In Silico: Methods and models. Drug Discovery Today. 2002; 7: p. 83-88.

87. Parrott N, Lave T. Applications of physiologically based absorption models in drug discovery and development. Molecular Pharmaceutics. 2008; 5(5): p. 760-775.

88. Venkatesh S, Lipper RA. Role of the development scientist in compound lead selection and optimization. Journal of Pharmaceutical Sciences. 2000; 89(2): p. 145-154.

89. Kirby BJ, Collier AC, Kharaseh ED, Whittington D, Thummel KE, Unadkat JD. Complex drug interactions of HIV-protease inhibitors 1: Inactivation, induction and inhibition of cytocrome P450 3A by ritonavir or nelfinavir. Drug Metabolism and Disposition. 2011; 39(6): p. 1070-1078.

90. Badhan R, Penny J, Galetin A, Houston BJ. Methodology for development of a physiological model incorporating CYP 3A and p-glycoprotein for the prediction of intestinal absorption. Journal of Pharmaceutical Sciences. 2009; 98(6): p. 2180-2197.

91. Snyder Ws, Cook MJ, Nasser ES, Karhausen LR, Howells GP, Tipton IH, editors. Report of the task group in reference on man New York: Pergamon; 1975.

92. Parrott N, Paquereau N, Coassolo P, Thierry L. An evaluation of the utility of physiologically based models of pharmacokinetics in early drug discovery. Journal of Pharmaceutical Sciences. 2005; 94(10): p. 2327-2343.

93. Yeniay O, Goktas A. A comparison of partial least squares regression with other prediction methods. Hacettepe Journal of Mathematics and Statistics. 2002; 31: p. 99-111.

94. database C. ChEMBLdb. [Online]. [cited 2011 July 31. Available from: https://www.ebi.ac.uk/chembldb/.

95. Lennernas H. Human intestinal permeability. Journal of Pharmaceutical Sciences. 1998; 87(4): p. 403-410.

96. Fujimura A, Kumagai Y, Sugimoto K, Nakashima H, Kajiyama H, Ebihara A, et al. Circadian influence on effect of propranolol on exercise-induced tachycardia in healthy subjects. European Journal of Clinical Pharmacology. 1990; 38: p. 133-137.

97. Elsherbiny D, Cohen K, Jansson B, Smith P, McIlleron H, Simonsson USH. Population pharmacokinetics of nevirapine in combination with rifampicin-based short course chemotherapy in HIV- and tuberculosis infected South African patients. European Journal of Clinical Pharmacology. 2009; 65: p. 71-80.

98. Hirt D, Mentre F, Tran A, Rey E, Auleley S, Salmon D, et al. Effect of CYP2C19 polymorphism on nelfinavir to M8 biotransformation in HIV patients. British Journal of Clinical Pharmacology. 2007; 65(4): p. 548-557.

99. Kappelhoff BS, Huitema ADR, Crommentuyn KML, Mulder JW, Meenhorst PL, Van Gorp ECM, et al. Development and validation of a population pharmacokinetic model for ritonavir used as a booster or as an antiviral agent in HIV-1-infected patients. British Journal of Clinical Pharmacology. 2004; 59(2): p. 174-182.

100. Kappelhoff BS, Huitema ADR, Sankatsing SUC, Meenhorst PL, Van Gorp ECM, Mulder JW, et al. Population pharmacokinetics of indinavir alone and in combination with ritonavir in HIV-1infected patients.British Journal of Clinical Pharmacology. 2005; 60(3): p.276-286.

101. Csajka C, Marzolini C, Fattinger K, Decosterd LA, Fellay J, Telenti A, et al. Population pharmacokientics and effects of Efavirenz in patients with human immunodeficiency virus infection. Clinial Pharmacology and Therapeutics. 2003; 73(1): p. 20-30.

102. Yan-Ling H, Brian M S, Ron S, Sebastien B, Yibin W, Joelle C, et al. The absolute oral bioavailability and population-based pharmacokinetic modelling of a novel dipeptidylpeptidase-IV inhibitor, vildagliptin,in healthy volunteers. Clinical Pharmacokinetics. 2007; 46(9): p. 787-802.

103. Krishnaiah Y, Satyanarayana S, Visweswaram D. Interaction between tolbutamide and ketoconazole in healthy subjects. British Journal of Clinical Pharmacology. 1994; 37: p. 205-207.

104. Kirchheiner J, Thomas S, Bauer S, Tomalik-Scharte D, Hering U, Doroshyenko O, et al. Pharmacokinetics and pharmacodynamics of rosiglitazone in relation to CYP2C8 genotype. Clinical Pharmacology and Therapeutics. 2006; 80: p. 657-667.

105. Harman JG, Limbird LE. The Pharmacological Basis of Therapeutics, Eleventh Edition. 9th ed. Molinoff PB, Ruddon RW, Gilman AG, editors.: Mc-Graw Hill.

106. Zussman BD, Davie CC, Kelly J, Murdoch RD, Clark DJ, Schofield JP, et al. Bioavailability of the oral selective phosphodiesterase 4 inhibitor cilomilast. Pharmacotherapy. 2001; 21(6): p. 653-660.

107. David M, Zech K, Seiberling M, Weimar C, Bethke TD. Roflumilast, a novel, oral, selective PDE4 inhibitor shows high absolute bioavailability. Journal of Allergy and Clinical Immunology. 2004; 113 (suppl 2): p. S220-S221.

108. Gmbh NP. European Medicines Agency. [Online].; 2007 [cited 2011 September 14. Available from: http://www.ema.europa.eu/docs/en_GB/document_library/EPAR_-_product_information/human/000771/WC500020327.PDF.

109. Cox PJ, Ryan DA, Hollis FJ, Harris AM, Miller AK, Vousden M, et al. Absorption, Disposition,and Metabolism of rosiglitazone , a potent thiazolidinedione insulin sensitizer, in humans. Drug Metabolism and Disposition. 2000; 28: p. 772-780.

110. Khaliq Y, Gallicano K, Seguin I, Fyke K, Carignan G, Bulman D, et al. Single and multiple dose pharmacokinetics of nelfinavir and CYP2C19 activity in human immunodeficiency virus-infected patients with chronic liver disease. British Journal of Clinical Pharmacology. 2000; 50: p. 108-115.

111. Hermann R, Nassr N, Lahu G, Peterfai E, Knoerzer D, Herzog R, et al. Steady-state pharmacokinetics of roflumilast and roflumilast N-oxide in patients with mild and moderate liver cirrhosis. Clinical Pharmacokinetics. 2007; 46(5): p. 403-416.

112. Parker AJ, Houston JB. Rate-limiting steps in hepatic drug clearance; comparison of hepaticellular uptake and metabolism with microsomal metabolism of saquinavir, nelfinavir and ritonavir. Drug Metabolism and Disposition. 2008; 36(7): p. 1375-1384.

113. Baye J. Roflumilast (Daliresp), A novel phosphodiesterase-4 inhibitor for the treatment of severe chronic obstructive pulmonary disease. Pharmacy and Therapeutics. 2012; 37(3): p. 157-161.

114. Rubin PC, Scott PJW, McLean K, Pearson A, Ross D, Reid JL. Atenolol disposition in young and elderly subjects. British Journal of Clinical Pharmacology. 1982; 13: p. 235-237.

115. Lamson MJ, Sabo JP, MacGregor TR, Pav JW, Rowland L, Hawi A, et al. Single dose pharmacokinetics and bioavailabilty of nevirapine in healthy volunteers. Biopharmaceutics and Drug Disposition. 1999; 20: p. 285-291.

116. Sarapa N, Hsyu PH, Lappin G, Garner RC. The application of accelerator mass spectrometry to absolute bioavailabilty studies in humans: Simultaneous administration of an intravenous microdose of 14C- nelfinavir mesylate solution and oral nelfinavir to healthy volunteers. Journal of Clinical pharmacology. 2005; 45: p. 1198-1205.

117. Gallant JE, Squires KE. Medscape. [Online].; 2003 [cited 2011 September 14]. Available from: http://www.medscape.org/viewarticle/466167.

118. Flatt PR, Bailey CJ, Green BD. Recent advances in antidiabetic drug therapies targeting the enteroinsular axis. Current Drug Metabolism. 2009; 10(2): p. 1-13.

119. Drug bank. [Online]. Available from: http://www.drugbank.ca/drugs/DB00335.

120. Rigby JW, Scott AK, Hawksworth GM, Petrie JC. A comparison of pharmacokinetics of atenolol, metoprolol, oxeprenolol and propranolol in elderly hypertensive and young healthy subjects. British Journal of Clinical Pharmacology. 1985; 20: p. 327-331.

121. Hoetelmans RMW. Clinical Pharmacokinetics of antiretroviral drugs. AIDS Reviews. 1999; 1: p. 167-178.

122. Compton CH, Gubb J, Nieman R, Edelson J, Amit O, Bakst A, et al. Cilomilast, a selective phosphodiesterase-4 inhibitor for treatment of patients with chronic obstructive pulmonary disease: a randomised, dose-ranging study. The Lancet. 2001; 358: p. 265-270.

123. Rabe KF, Bateman ED, O'Donnell D, Witte S, Bredenbröker D, Bethke TD. Roflumilast—an oral anti-inflammatory treatment for chronic obstructive pulmonary disease: a randomised controlled trial. The Lancet. 2005; 366: p. 563-571.

124. Kikuchi M, Abe N, Kato M, Terao S, Mimor N, Tachibama H. Vildagliptin dose-dependently improves glycemic control in Japanese patients with type 2 diabetes mellitus. Diabetes Research and Clinical Practice. 2009; 83: p. 233-240.

125. Phillips LS, Grunberger G, Miller E, Patwardhan R, Rappaport EB, Salzman A. Once and twice daily dosing with rosiglitazone improves glycemic control in patients with Type 2 diabetes. Diabetes Care. 2001; 24: p. 308-315.

126. Bertrand J, Treluyer JM, Panhard X, Tran A, Auleley S, Rey E, et al. Influence of pharmacogenetics on indinavir disposition and short-term response in HIV patients initiating HAART. European Journal of Clinical Pharmacology. 2009; 65(7): p. 667-678.

127. Murdoch RD, Zussman B, Schofield JP, Webber DM. Lack of pharmacokinetic interactions between cilomilast and theophylline or smoking in healthy volunteers. The Journal of Clinical Pharmacology. 2004; 44: p. 1046-1053.

128. Bethke TD, Bohmer GM, Hermann R, Hauns B, Fux R, Morike K, et al. Dose-proportional intraindividual single and repeated-dose pharmacokinetics of roflumilast, an oral, once-daily phosphodiesterase 4 inhibitor. The Journal of Clinical Pharmacology. 2007; 47: p. 26-36.

129. He YL, Ligueros-Saylan M, Sunkara G, Sabo R, Zhao C, Wang Y, et al. Vildagliptin, a

novel dipeptidyl peptidase IV inhibitor, has no pharmacokinetic interactions with the antihypertensive agents amlodipine, valsartan and ramipril in healthy subjects. The Journal of Clinical Pharmacology. 2008; 48: p. 85-95.

130. Gross AS, Bridge S, Shenfield GM. Pharmacokinetics of tolbutamide in ethnic chinese. British Journal of Clinical Pharmacology. 1999; 47: p. 151-156.

131. 003437 Rosiglitazone Maleate (Avandia). [Online]. [cited 2011 July 02. Available from: http://www.orgyn.com/resources/genrx/D003437.asp.

132. Nassar AEF, Kamel AM, Clarimont C. Improving the decision-making process in the structural modification of drug candidates: enhancing metabolic stability. Drug Discovery Today. 2004; 23(9): p. 1020-1028.

133. Brynne L, Karlsson MO, Paalzow LK. Concentration-effect relationship of l-propanolol and metoprolol in spontaneous hypertensive rats after exercise-induced tachycardia. The Journal of Pharmacology and Experimental Therapeutics. 1998; 286: p. 1152-1158.

134. Buss N, Cammack N. Mesauring effectiveness of antiretroviral agents. Antiviral Therapy. 2001; 6: p. 1-7.

135. Hatzelmann A, Schudt C. Anti-inflammatory and immunomodulatory potential of the novel PDE4 inhibitor roflumilast invitro. The Journal of Pharmacology and Experimental Therapeutics. 2001; 297(1): p. 267-279.

136. Tenor H, Hatzelmann A, Beume R, Lahu G, Zech K, Bethke TD. Pharmacology, clinical efficacy and tolerability of phosphodiesterase-4 inhibitors: Impact of human pharmacokinetics. Handbook of Experimental Pharmacology. 2011; 204: p. 85-119.

137. Furuta S, Goto M, Furuta Y, Yasuda Y, Nakaya K, Tamura M, et al. Pharmacokinetics and pharmacodynamics of SK-043, a novel DPP-IV inhibitor in rat. In American Diabetes Association Conference; 2007; Chicago.

138. Sun L, Kwok E, Gopaluni B, Vahidi O. Pharmacokinetic-pharmacodynamic modeling of metformin for the treatment of type II diabetes mellitus. The Open Biomedical Engineering Journal. 2011; 5: p. 1-7.

139. Poulin P, Jones RDO, Jones HM, Gibson CR, Rowland M, Chien JY, et al. PHRMA CPCDC inititative on predictive models of human pharmacokinetics, part 5: Prediction of plasma concentration - time profiles in human by using the physiologically-based pharmacokinetic modeling approach. Journal of Pharmaceutical Sciences. 2011; 100(10): p. 4127-4157.

140. Tenenhaus M, Vinzi VE, Chatelin YM, Lauro C. PLS path modeling. Computational Statistics and Data Analysis. 2005; 48: p. 159-205.

141. Wold S, Sjostrom M, Eriksson L. PLS-regression: A basic tool of chemometrics. Chemometrics and Intelligent Laboratory Systems. 2001; 58: p. 109-130.

142. Quarterman CP, Kendall MJ, Jack DB. The effect of age on the pharmacokinetics of metoprolol and its metabolites. British Journal of Clinical Pharmacology. 1981; 11: p. 287-294.

143. Mollendroff EV, Reiff K, Neugebauer G. Pharmacokinetics and bioavilability of Carvedilol, a vasodilating beta blocker. European journal of Clinical Pharmacology. 1987; 33: p. 511-513.

APPENDIX I: COMPILATION OF DATA

Estimated parameters	Specifications	Atenolol	Metoprolol	Propranolol	Nevirapine	Nelfinavir	Ritonavir	Indinavir
Mol wt		266.33	267.36	259.34	266.29	567.78	720.94	613.78
pKa	acidic pKa	9.43	9.43	9.5	12.054	14.13	11.467	14.21
	basic pKa	13.881	13.891	13.84	4.247	6.213	2.51	5.191
Solubility at pH (mg/mL)	1.8	1.318	5.013	3.104	0.765	0.201	0.0078	0.998
	3	1.257	4.907	3.120	0.140	0.241	0.0015	1.314
	4.5	1.259	5.651	2.899	0.104	0.713	0.0010	1.643
	6.8	1.369	4.986	3.200	0.102	0.008	0.0010	0.045
	7.4	1.331	5.437	3.061	0.098	0.008	0.0010	0.039
Log $P_{o/W}$		0.335	1.632	2.90	2.639	7.278	2.333	3.435
Log $P_{vo/w}$	olive oil: water	-0.98	0.47	1.88	1.59	6.76	1.25	2.48
Log $D_{vo/w}$	olive oil: water	-0.98	0.47	-6.66	0.07	1.22	1.25	0.27
Neutral fraction (pH 6.8)		1.000	1.000	1.000	0.003	0.206	1.000	1.000
Neutral fraction (pH 7.4)		1.000	1.000	1.000	0.001	0.061	1.000	1.000
Caco-2 permeability (cm/sec)	pH6.8-7.4	0.00000028	0.00000888	0.00000605	0.00002459	0.00000136	0.00000978	0.00000308
Fraction unbound in plasma	Human	0.854	0.254	0.7799	0.421	0.1169	0.0198	0.332
Fraction unbound in tissue (f_{ut}) De Buck et.al	Human non adipose	0.921	0.405	0.876	0.593	0.209	0.039	0.498
	Human adipose	1.000	1.000	1.000	1.000	1.000	1.000	1.000
Blood plasma partitioning (ratio)	Human	3.54	2.4	2.0	2.24	1.03	0.64	1.7
Microsomal binding (fraction unbond %)	Human	0.739	0.614	0.476	0.504	0.117	0.538	0.418
Microsomal clearance (mL/min/g liver)	Human	0.002	11.79	1.9068	0.07749	71.2	12.6	3.4

| Estimated parameters	Specifications	Efavirenz	Cilomilast	Roflumilast	Vildagliptin	Tolbutamide	Rosiglitazone
Mol wt		315.67	343.42	403.21	303.4	270.34	357.42
pKa	aAcidic pKa	10.241		9.887	8.391		
	basic pKa		4.349	0.407		5.25	6.503
Solubility at pH (mg/mL)	1.8	0.00730	0.01202	0.005	1.839	0.094	1.246
	3	0.00730	0.39198	0.005	1.912	0.096	1.314
	4.5	0.00730	0.01373	0.005	1.879	0.111	1.084
	6.8	0.00766	0.59295	0.005	1.908	2.497	0.047
	7.4	0.02150	1.34752	0.005	2.019	1.467	0.048
Log $P_{o/w}$		4.38	2.108	2.305	0.169	2.362	3.023
Log $P_{vo/w}$	olive oil: water	3.53	1.00	1.22	-1.16	1.28	2.02
Log $D_{vo/w}$	olive oil: water	3.53	-2.05	1.22	-2.19	-0.87	1.97
Neutral fraction (pH 6.8)		1.000	0.000	0.999	0.000	0.000	0.335
Neutral fraction (pH 7.4)		0.999	0.000	0.997	0.000	0.000	0.113
Caco-2 permeability (cm/sec)	pH6.8-7.4	0.00000844	0.00003010	0.00002320	0.00000156	0.00003039	0.00001540
Fraction unbound in plasma	Human	0.0011	0.006	0.004	0.794	0.022	0.0024
Fraction unbound in tissue (f_{ut}) De buck et al.	Human non adipose	0.002	0.012	0.008	0.885	0.043	0.0048
	Human adipose	1.000	1.000	1.000	1.000	1.000	1.000
Blood plasma partitioning (R_B, ratio)	Human	1.19	0.78	1.42	2.13	0.73	1.4
Microsomal binding (fraction unbond %)	Human	0.320	0.563	0.541	0.756	0.535	0.468
Microsomal clearance (mL/min/g liver)	Human	11.58	1.12	2.03	0.96	0.31	2.6

| Estimated parameters	Specifications	Atenolol	Metoprolol	Propranolol	Nevirapine	Nelfinavir	Ritonavir	Indinavir
Human Volume of distribution of rapidly perfused tissue Vc (L)70kg	heart,kidney, liver, lung, spleen, muscles, RBC	42.0	29.0	69.5	41.9	203.1	16.6	78.9
Human Volume of distribution V_d (L)70 kg	heart,kidney, liver, lung, spleen, muscles, RBC, Adipose, bone , brain, gut, skin	50.5	39.5	110.00	61.8	381.4	22.8	133.5
Absorption rate constant at equilibrium K_{aeq} (Usansky et al., /min)	Human	0.0008	0.0367	0.0104	0.0704	0.0008	0.0707	0.0047
Fraction absorbed (at equilibrium assuming F_{FP}*Ci/Cpl=1, Usansky et al.)	Human	0.14	0.88	0.68	0.93	0.14	0.93	0.48
Clearance hepatic (well stirred) mL/min/kg	Human	0.02	14.77	13.61	0.7	20.4	9.80	13.7
Renal clearance based on glomerular filtration rate (mL/min/kg)	Human	1.4518	0.4318	1.32583	0.7157	0.19873	0.03366	0.5644
Total clearance (mL/min/kg)	Human	1.47	15.20	14.94	1.44	20.60	9.83	14.21
Fraction bioavailable	Human	0.14	0.25	0.23	0.90	0.001	0.49	0.16

Estimated parameters	Specifications	Efavirenz	Cilomilast	Roflumilast	Vildagliptin	Tolbutamide	Rosiglitazone
Human Volume of distribution of rapidly perfused tissue V_c (L)70kg	heart,kidney, liver, lung, spleen, muscles, RBC	23.2	16.9	20.2	33.9	17.18	20.2
Human Volume of distribution V_d (L)70 kg	heart,kidney, liver, lung, spleen, muscles, RBC, Adipose, bone , brain, gut, skin	55.4	20.3	24.1	41.5	21	25.4
Absorption rate constant at equilibrium K_{aeq} (Usansky et al., /min)	Human	0.0436	0.2138	0.1378	0.0055	0.2123	0.0915
Fraction absorbed (at equilibrium assuming $F_{FP}*Ci/Cpl=1$, Usansky et al.)	Human	0.90	0.98	0.96	0.52	0.98	0.95
Clearance hepatic (well stirred) (mL/min/kg)	Human	0.83	0.39	0.27	7.66	0.44	0.24
Renal clearance based on glomerular filtration rate (mL/min/kg)	Human	0.00187	0.0102	0.0068	1.35	0.04	0.00
Total clearance (mL/min/kg)	Human	0.83	0.40	0.28	9.01	0.48	0.24
Fraction bioavailable	Human	0.86	0.96	0.95	0.33	0.96	0.94

Note: As qualifying criteria for plasma protein binding assay, warfarin showed a human protein binding of 99.5%. For intrinsic clearance an internal compound was used with high clearance (> 50 mL/min/kg) to ensure functioning of microsomes. For cacao2 permeability atenolol and propranolol permeability itself were regarded as control.

APPENDIX II: REPRESENTATIVE CHROMATOGRAMS

LC-MS/MS Chromatograms

Atenolol

Metoprolol

Propranolol

Nevirapine

+
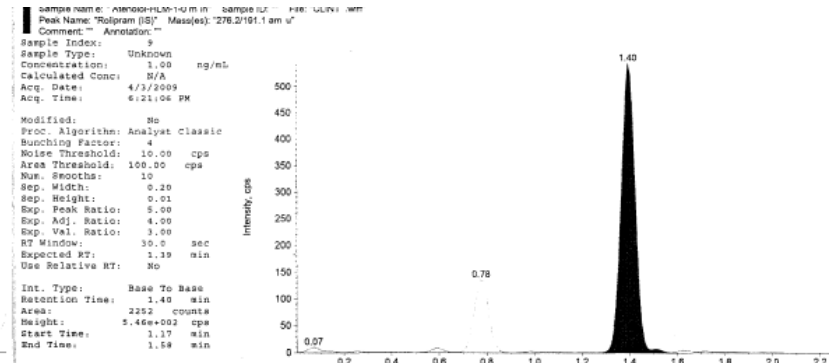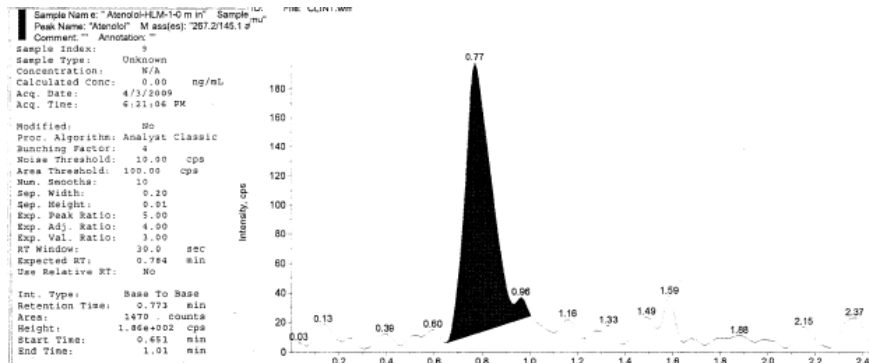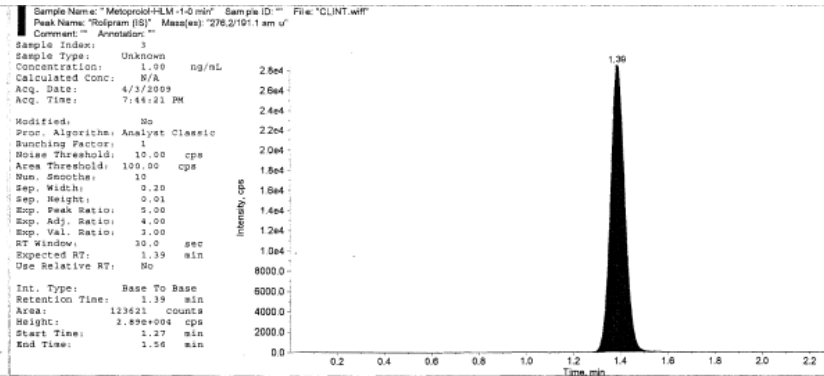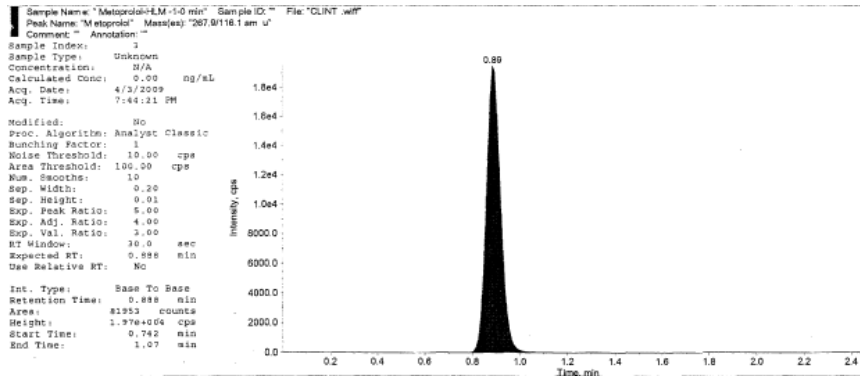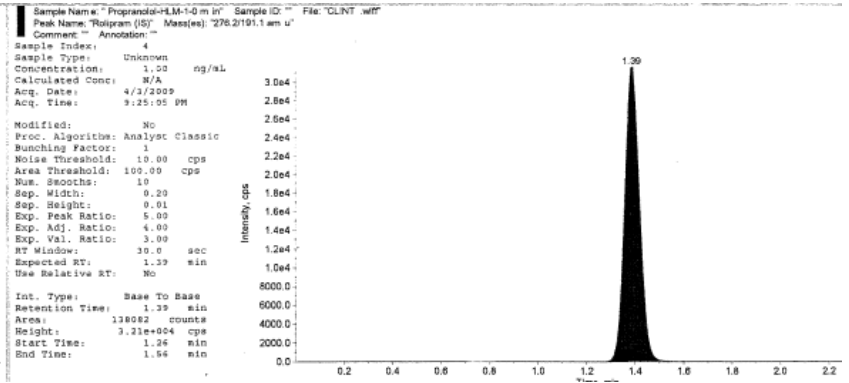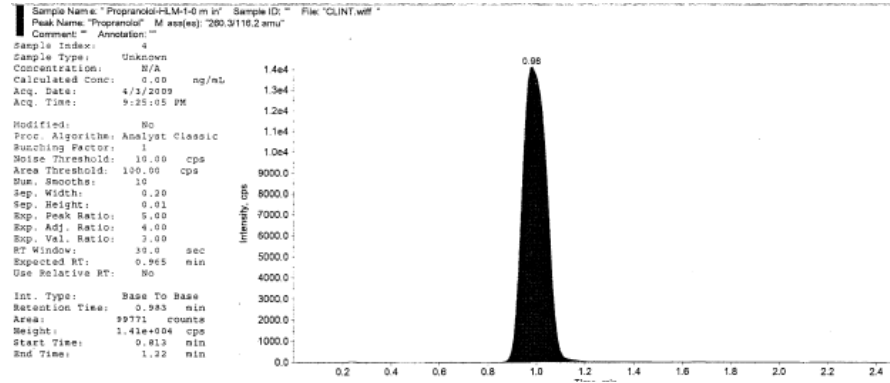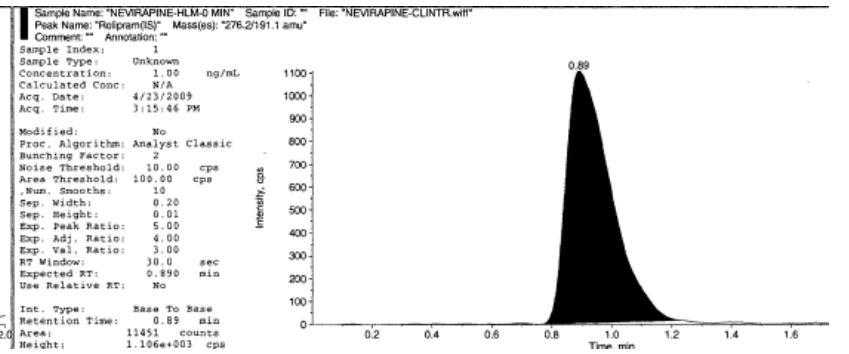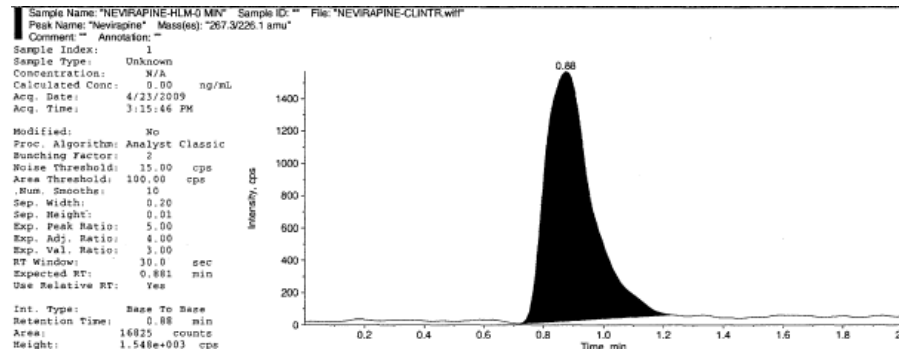
Nelfinavir
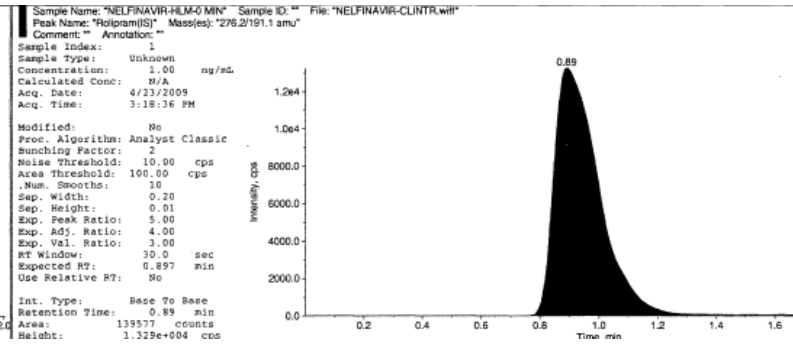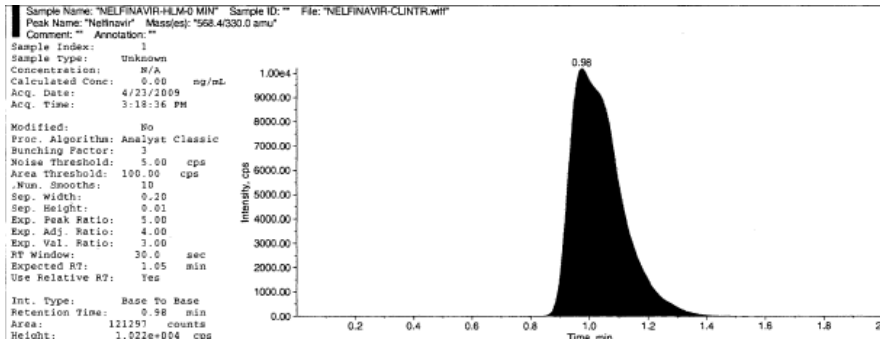
Ritonavir
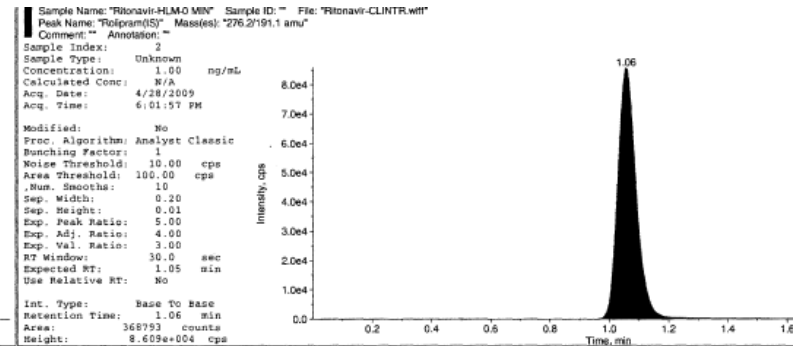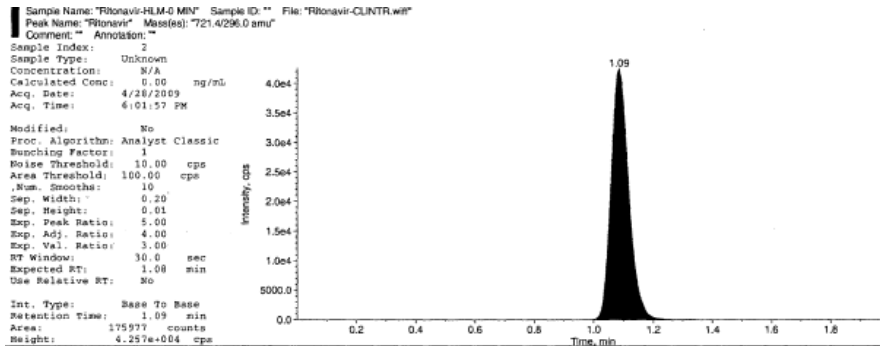
Indinavir

Sample Name: "INDINAVIR_HLM_1MIN"   Sample ID: ""
Peak Name: "Indinavir"   Mass(es): "614.300/421.100 Da"
Comment: ""   Annotation: ""
Sample Index: 9
Sample Type: Unknown
Concentration: N/A
Calculated Conc: 0.00   µM
Acq. Date: 6/6/2012
Acq. Time: 12:27:02 PM

Modified: No
Proc. Algorithm: Specify Parameters - MQ III
Noise Percentage: 50
Base. Sub. Window: 1.00   min
Peak-Split. Factor: 2
Report Largest Peak: Yes
Min. Peak Height: 0.00 cps
Min. Peak Width: 0.00 sec
Smoothing Width: 11   points
RT Window: 30.0   sec
Expected RT: 1.57   min
Use Relative RT: No

Int. Type: Valley
Retention Time: 1.57 min
Area: 360000. counts
Height: 2.31e+005 cps
Start Time: 1.55 min
End Time: 1.65 min
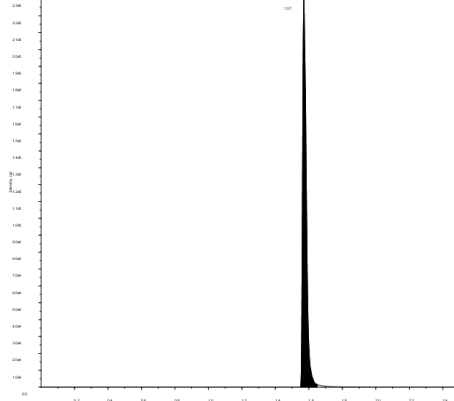
Sample Name: "INDINAVIR_HLM_1MIN"   Sample ID: ""   File: "DATA.wiff"
Peak Name: "Rolipram(IS)"   Mass(es): "276.200/191.000 Da"
Comment: ""   Annotation: ""
Sample Index: 9
Sample Type: Unknown
Concentration: 1.00   µM
Calculated Conc   N/A
Acq. Date: 6/6/2012
Acq. Time: 12:27:02 PM

Modified: No
Proc. Algorithm: Specify Parameters - MQ III
Noise Percentage: 50
Base. Sub. Window: 1.00   min
Peak-Split. Factor: 2
Report Largest Peak: Yes
Min. Peak Height: 0.00 cps
Min. Peak Width: 0.00 sec
Smoothing Width: 11   points
RT Window: 30.0   sec
Expected RT: 1.34   min
Use Relative RT: No

Int. Type: Valley
Retention Time: 1.34 min
Area: 74300. counts
Height: 4.96e+004 cps
Start Time: 1.32 min
End Time: 1.40 min
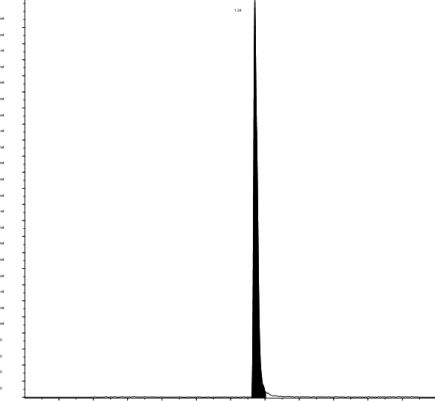
Efavirenz

Sample Name: "EFAVIRENZ_HLM_1MIN"   Sample ID: ""   File: "DATA.wiff"
Peak Name: "Efavirenz"   Mass(es): "316.100/244.100 Da"
Comment: ""   Annotation: ""
Sample Index: 10
Sample Type: Unknown
Concentration: N/A
Calculated Conc   0.00   µM
Acq. Date: 6/6/2012
Acq. Time: 12:30:07 PM

Modified: No
Proc. Algorithm: Specify Parameters - MQ II
Noise Percentage: 50
Base. Sub. Window: 1.00   min
Peak-Split. Factor: 2
Report Largest Peak: Yes
Min. Peak Height: 0.00 cps
Min. Peak Width: 0.00 sec
Smoothing Width: 9   points
RT Window: 30.0   sec
Expected RT: 1.86   min
Use Relative RT: No

Int. Type: Base To Base
Retention Time: 1.86 min
Area: 1010. counts
Height: 8.27e+002 cps
Start Time: 1.84 min
End Time: 1.91 min

Sample Name: "EFAVIRENZ_HLM_1MIN"   Sample ID: ""   File: "DATA.wiff"
Peak Name: "Rolipram(IS)"   Mass(es): "276.200/191.000 Da"
Comment: ""   Annotation: ""
Sample Index: 10
Sample Type: Unknown
Concentration: 1.00   µM
Calculated Conc   N/A
Acq. Date: 6/6/2012
Acq. Time: 12:30:07 PM

Modified: No
Proc. Algorithm: Specify Parameters - MQ III
Noise Percentage: 50
Base. Sub. Window: 1.00   min
Peak-Split. Factor: 2
Report Largest Peak: Yes
Min. Peak Height: 0.00 cps
Min. Peak Width: 0.00 sec
Smoothing Width: 9   points
RT Window: 30.0   sec
Expected RT: 1.34   min
Use Relative RT: No

Int. Type: Valley
Retention Time: 1.34 min
Area: 101000. counts
Height: 6.34e+004 cps
Start Time: 1.32 min
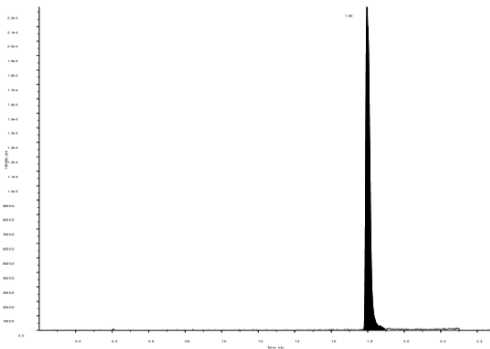End Time: 1.42 min
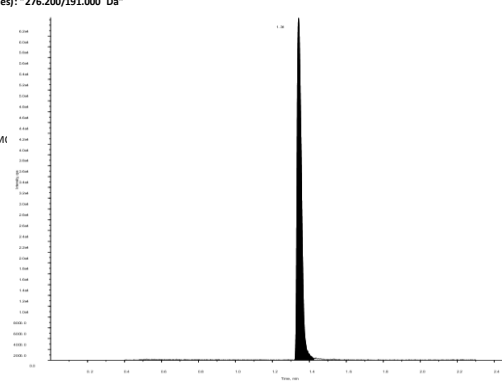
Cilomilast

Sample Name: "CILOMILAST-HLM-0 MIN"   Sample ID: ""   File: "CILOMILAST-CLINTR.wiff"
Peak Name: "Cilomilast"   Mass(es): "342.1/213.9 amu"
Comment: ""   Annotation: ""
Sample Index: 3
Sample Type: Unknown
Concentration: N/A
Calculated Conc: 0.00   ng/mL
Acq. Date: 04/30/2009
Acq. Time: 09:25:32 PM

Modified: No
Proc. Algorithm: Analyst Classic
Bunching Factor: 2
Noise Threshold: 10.00   cps
Area Threshold: 100.00 cps
,Num. Smooths: 10
Sep. Width: 0.20
Sep. Height: 0.01
Exp. Peak Ratio: 5.00
Exp. Adj. Ratio: 4.00
Exp. Val. Ratio: 3.00   RT Window: 30.0   sec
Expected RT: 1.09   min
Use Relative RT: No

Int. Type: Base To Base
Retention Time: 1.09   min
Area: 6934   counts
Height: 1.678e+003 cps
Start Time: 0.991 min
End Time: 1.22   min
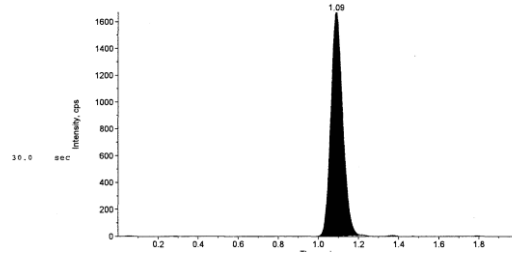
Sample Name: "CILOMILAST-HLM-0 MIN"   Sample ID: ""   File: "CILOMILAST-CLINTR.wiff"
Peak Name: "RBx10017609(IS)"   Mass(es): "473.2/146.0 amu"
Comment: ""   Annotation: ""
Sample Index: 3
Sample Type: Unknown
Concentration: 1.00   ng/mL
Calculated Conc: N/A
Acq. Date: 04/30/2009
Acq. Time: 09:25:32 PM

Modified: No
Proc. Algorithm: Analyst Classic
Bunching Factor: 1
Noise Threshold: 10.00   cps
Area Threshold: 100.00 cps
,Num. Smooths: 10
Sep. Width: 0.20
Sep. Height: 0.01
Exp. Peak Ratio: 5.00
Exp. Adj. Ratio: 4.00
Exp. Val. Ratio: 3.00   RT Window: 30.0   sec
Expected RT: 1.01   min
Use Relative RT: No

Int. Type: Base To Base
Retention Time: 1.02   min
Area: 5816   counts
Height: 1.393e+003 cps
Start Time: 0.916 min
End Time: 1.12   min
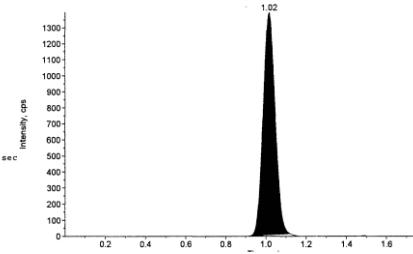
Roflumilast

Sample Name: "ROFLUMILAST_HLM_1MIN"   Sample ID: ""   File: "DATA.wiff"
Peak Name: "Roflumilast"   Mass(es): "405.200/187.000 Da"
Comment: ""   Annotation: ""
Sample Index: 12
Sample Type: Unknown
Concentration: N/A
Calculated Conc: 0.00   µM
Acq. Date: 6/6/2012
Acq. Time: 12:36:19 PM

Modified: No
Proc. Algorithm: Specify Parameters - MQ III
Noise Percentage: 50
Base. Sub. Window: 1.00 min
Peak-Split. Factor: 2
Report Largest Peak: Yes
Min. Peak Height: 0.00 cps
Min. Peak Width: 0.00 sec
Smoothing Width: 9   points
RT Window: 30.0 sec
Expected RT: 1.80 min
Use Relative RT: No

Int. Type: Valley
Retention Time: 1.80 min
Area: 33600. counts
Height: 2.24e+004 cps
Start Time: 1.77 min
End Time: 1.89 min

Sample Name: "ROFLUMILAST_HLM_1MIN"   Sample ID: ""   File: "DATA.wiff"
Peak Name: "Rolipram(IS)"   Mass(es): "276.200/191.000 Da"
Comment: ""   Annotation: ""
Sample Index: 12
Sample Type: Unknown
Concentration: 1.00   µM
Calculated Conc: N/A
Acq. Date: 6/6/2012
Acq. Time: 12:36:19 PM

Modified: No
Proc. Algorithm: Specify Parameters - MQ III
Noise Percentage: 50
Base. Sub. Window: 1.00 min
Peak-Split. Factor: 2
Report Largest Peak: Yes
Min. Peak Height: 0.00 cps
Min. Peak Width: 0.00 sec
Smoothing Width: 9   points
RT Window: 30.0 sec
Expected RT: 1.34 min
Use Relative RT: No

Int. Type: Valley
Retention Time: 1.34 min
Area: 106000. counts
Height: 6.91e+004 cps
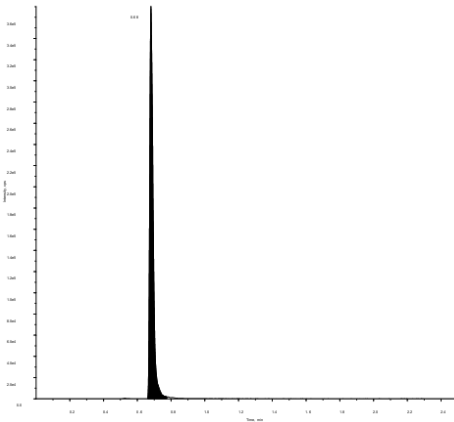Start Time: 1.32 min
End Time: 1.41 min
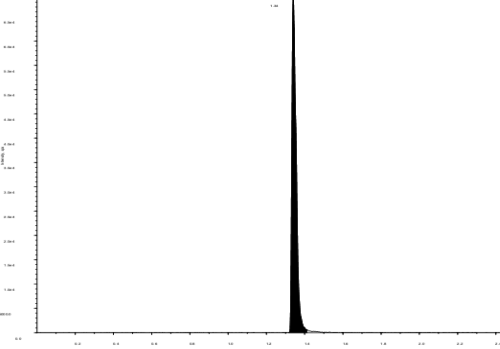
Vildagliptin (LAF237)

Sample Name: "LAF237_HLM_1MIN"   Sample ID: ""   File: "DATA.wiff"
Peak Name: "efa"   Mass(es): "304.500/154.000 Da"
Comment: ""   Annotation: ""

Sample Index:	11
Sample Type:	Unknown
Concentration:	N/A
Calculated Conc:	0.00 µM
Acq. Date:	6/6/2012
Acq. Time:	12:33:11 PM
Modified:	No

Proc. Algorithm: Specify Parameters - MQ III
Noise Percentage: 50
Base. Sub. Window: 1.00   min
Peak-Split. Factor: 2
Report Largest Peak: Yes
Min. Peak Height: 0.00   cps
Min. Peak Width: 0.00   sec
Smoothing Width: 9   points
RT Window: 30.0   sec
Expected RT: 0.680   min
Use Relative RT: No

Int. Type: Valley
Retention Time: 0.680   min
Area: 503000. counts
Height: 3.70e+005 cps
Start Time: 0.662   min
End Time: 0.775   min

Sample Name: "LAF237_HLM_1MIN"   Sample ID: ""   File: "DATA.wiff"
Peak Name: "Rolipram(IS)"   Mass(es): "276.200/191.000 Da"
Comment: ""   Annotation: ""

Sample Index:	11
Sample Type:	Unknown
Concentration:	1.00 µM
Calculated Conc:	N/A
Acq. Date:	6/6/2012
Acq. Time:	12:33:11 PM
Modified:	No

Proc. Algorithm: Specify Parameters - MQ III
Noise Percentage: 50
Base. Sub. Window: 1.00   min
Peak-Split. Factor: 2
Report Largest Peak: Yes
Min. Peak Height: 0.00   cps
Min. Peak Width: 0.00   sec
Smoothing Width: 9   points
RT Window: 30.0   sec
Expected RT: 1.34   min
Use Relative RT: No

Int. Type: Valley
Retention Time: 1.34   min
Area: 106000. counts
Height: 6.82e+004 cps
Start Time: 1.32   min
End Time: 1.44   min
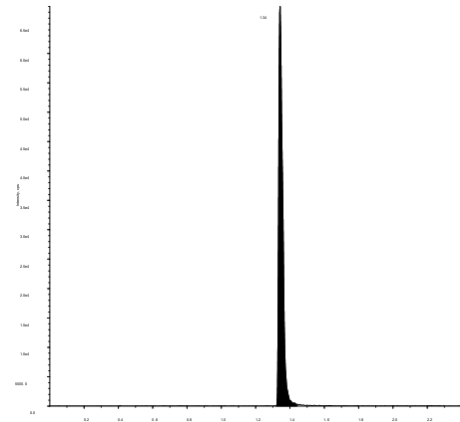
Tolbutamide

Sample Name: "TOLBUTAMIDE_HLM_1MIN"   Sample ID: ""   File: "DATA.
Peak Name: "Tolbutamide"   Mass(es): "271.100/91.100 Da"
Comment: ""   Annotation: ""

Sample Index:	17
Sample Type:	Unknown
Concentration:	N/A
Calculated Conc:	0.00 µM
Acq. Date:	6/6/2012
Acq. Time:	1:07:03 PM
Modified:	No

Proc. Algorithm: Specify Parameters - MQ III
Noise Percentage: 50
Base. Sub. Window: 1.00   min
Peak-Split. Factor: 2
Report Largest Peak: Yes
Min. Peak Height: 0.00   cps
Min. Peak Width: 0.00   sec
Smoothing Width: 9   points
RT Window: 30.0   sec
Expected RT: 1.26   min
Use Relative RT: No

Int. Type: Valley
Retention Time: 1.26   min
Area: 63900. counts
Height: 3.91e+004 cps
Start Time: 1.24   min
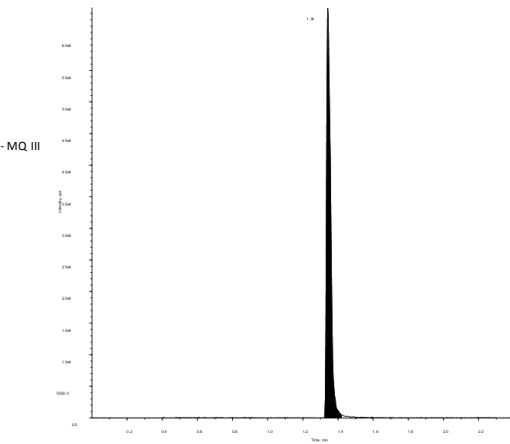End Time: 1.33   min
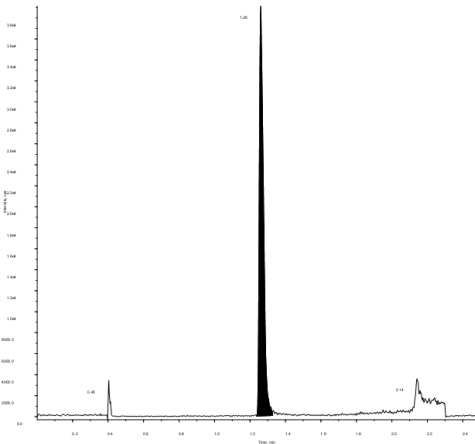
Sample Name: "TOLBUTAMIDE_HLM_1MIN"   Sample ID: ""   File: "DATA.wiff"
Peak Name: "Rolipram(IS)"   Mass(es): "276.200/191.000 Da"
Comment: ""   Annotation: ""

Sample Index:	17
Sample Type:	Unknown
Concentration:	1.00 µM
Calculated Conc:	N/A
Acq. Date:	6/6/2012
Acq. Time:	1:07:03 PM
Modified:	No

Proc. Algorithm: Specify Parameters - MQ III
Noise Percentage: 50
Base. Sub. Window: 1.00   min
Peak-Split. Factor: 2
Report Largest Peak: Yes
Min. Peak Height: 0.00   cps
Min. Peak Width: 0.00   sec
Smoothing Width: 9   points
RT Window: 30.0   sec
Expected RT: 1.34   min
Use Relative RT: No

Int. Type: Valley
Retention Time: 1.34   min
Area: 103000. counts
Height: 6.51e+004 cps
Start Time: 1.32   min
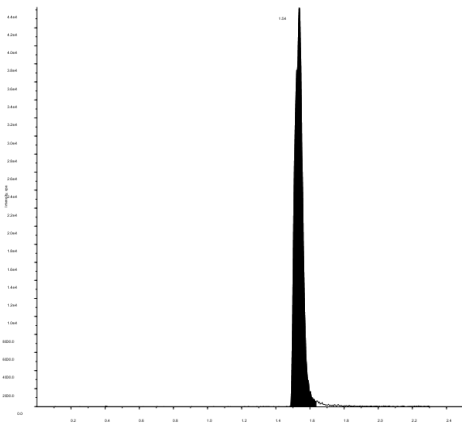End Time: 1.42   min

160

Rosiglitazone

Sample Name: "Rosiglitazone_HLM_1MIN"   Sample ID: ""   File: "DATA.wiff"
Peak Name: "Rosiglitazone"   Mass(es): "358.000/135.000 Da"
Comment: ""   Annotation: ""

Sample Index: 19
Sample Type: Unknown
Concentration: N/A
Calculated Conc: 0.00   µM
Acq. Date: 6/6/2012
Acq. Time: 1:40:23 PM

Modified: No
Proc. Algorithm: Specify Parameters - MQ III
Noise Percentage: 50
Base. Sub. Window: 1.00   min
Peak-Split. Factor: 2
Report Largest Peak: Yes
Min. Peak Height: 0.00   cps
Min. Peak Width: 0.00   sec
Smoothing Width: 9   points
RT Window: 30.0   sec
Expected RT: 1.54   min
Use Relative RT: No

Int. Type: Valley
Retention Time: 1.54   min
Area: 141000.   counts
Height: 4.43e+004 cps
Start Time: 1.48   min
End Time: 1.64   min

Sample Name: "Rosiglitazone_HLM_1MIN"   Sample ID: ""   File: "DATA.wiff"
Peak Name: "Rolipram(IS)"   Mass(es): "276.200/191.000 Da"
Comment: ""   Annotation: ""

Sample Index: 19
Sample Type: Unknown
Concentration: 1.00   µM
Calculated Conc: N/A
Acq. Date: 6/6/2012
Acq. Time: 1:40:23 PM

Modified: No
Proc. Algorithm: Specify Parameters - MQ III
Noise Percentage: 50
Base. Sub. Window: 1.00   min
Peak-Split. Factor: 2
Report Largest Peak: Yes
Min. Peak Height: 0.00   cps
Min. Peak Width: 0.00   sec
Smoothing Width: 9   points
RT Window: 30.0   sec
Expected RT: 1.34   min
Use Relative RT: No

Int. Type: Valley
Retention Time: 1.34   min
Area: 1280000.   counts
Height: 6.97e+005 cps
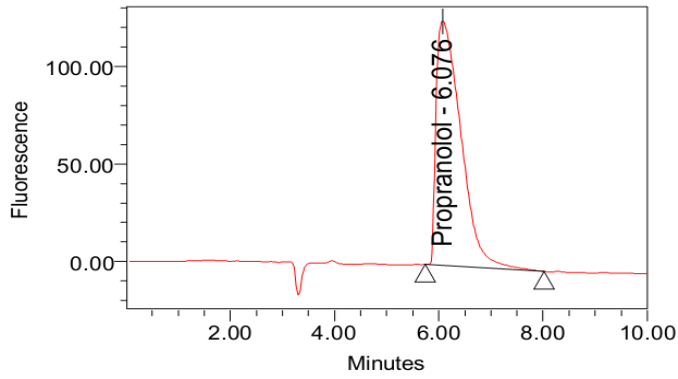Start Time: 1.30   min
End Time: 1.43   min
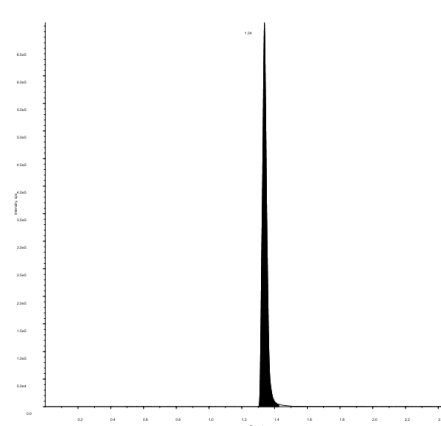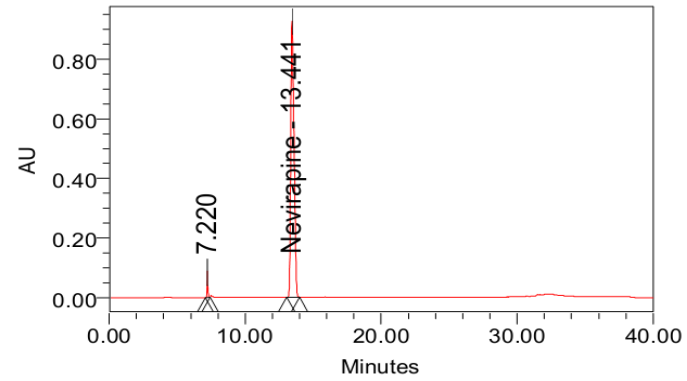
HPLC Chromatograms
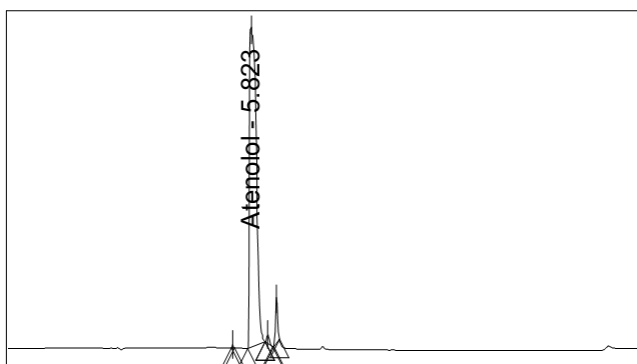
Sample Name: Aten pH 1.8 sample;   Date Acquired: 2/25/2010 8:25:46 PM;   Vial: 5; Injection: 1; Processed Channel Descr. PDA 229.0 nm
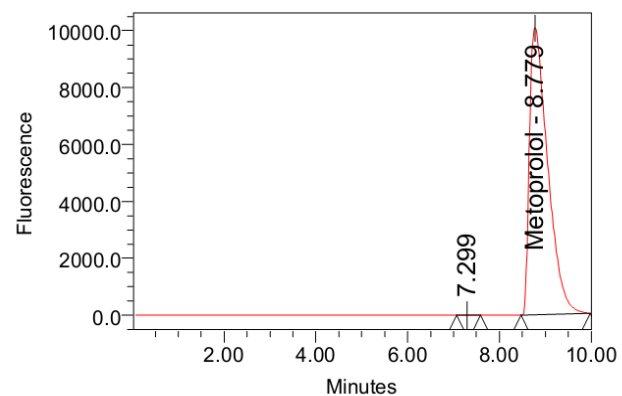
Sample Name: Metoprolol PH 1.8;   Date Acquired: 11/19/2008 9:26:44 PM;   Vial: 35; Injection: 1
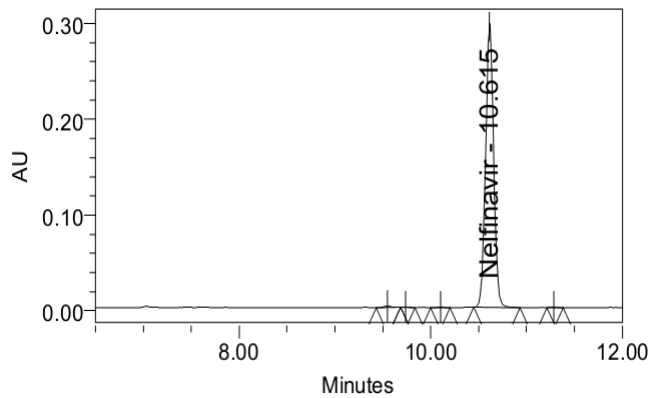
161

Sample Name: Propranolol PH 3.0; Date Acquired: 11/19/2008 11:54:59 PM; Vial: 46; Injection: 1
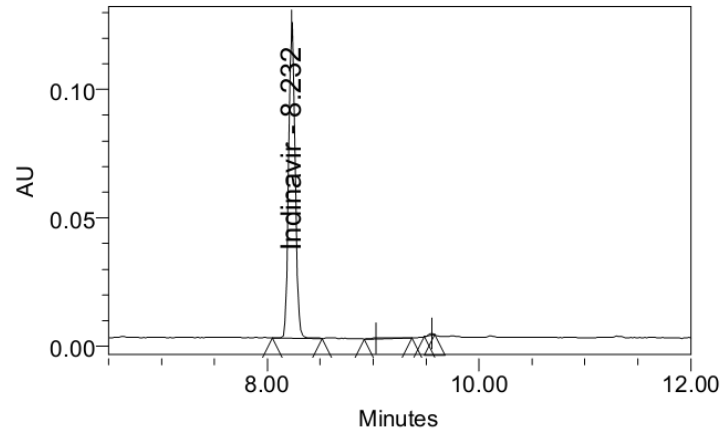
Sample Name: Nevirapine 10µg on column; Date Acquired: 11/10/2008 7:14:10 PM; Vial: 25; Injection: 1
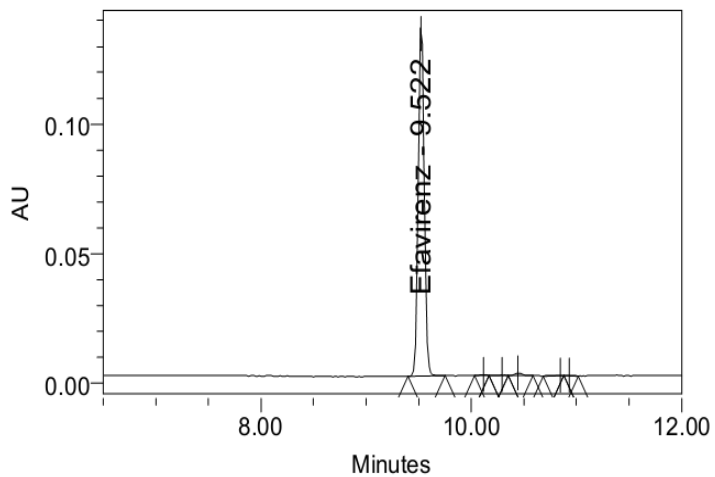
Project Name: Training2010_13

Project Name: Training2010_13

Sample Name: Nelfinavir 0.5 mg/mL; Date Acquired: 1/24/2010 4:29:30 PM; Vial: 25; Injection: 1; Processed Channel Descr. PDA 255.0 nm
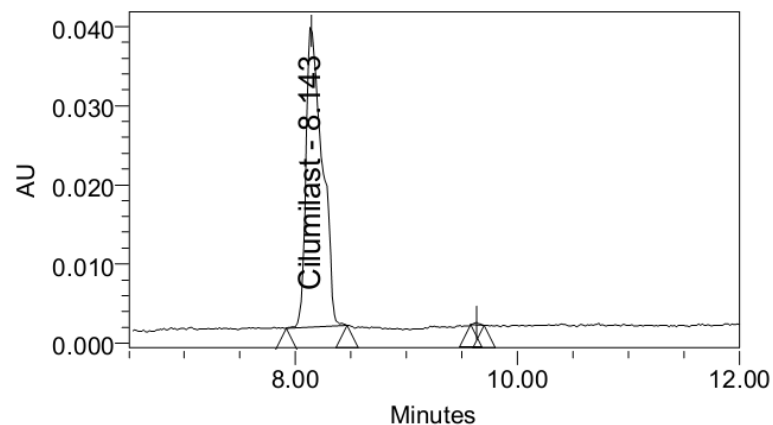
Sample Name: Ind 0.5 mg/mL; Date Acquired: 1/23/2010 7:12:09 PM; Vial: 97; Injection: 1; Processed Channel Descr. PDA 261.0 nm
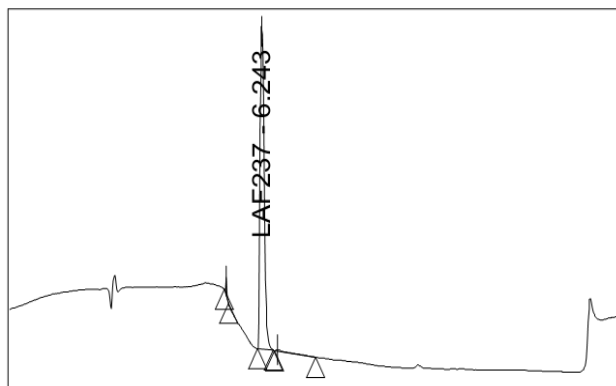
Project Name: Training2010_13

Sample Name: efa 0.5 mg/mL; Date Acquired: 1/23/2010 8:17:01 PM; Vial: 98; Injection: 1; Processed Channel Descr. PDA 284.4 nm
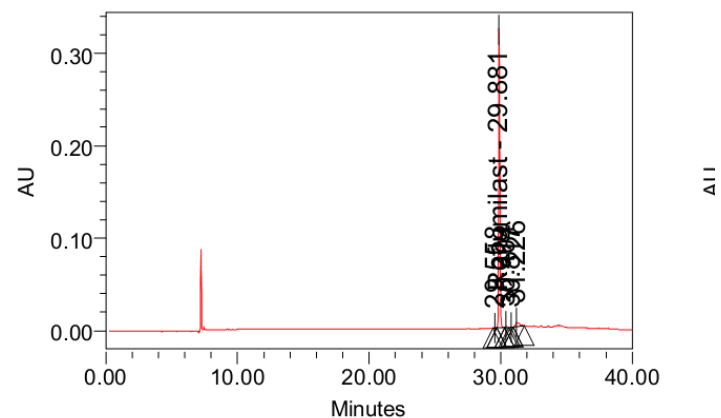

Project Name: Training2010_13

Sample Name: Cilomilast 0.5 mg/mL; Date Acquired: 2/25/2010 7:04:22 PM; Vial: 4; Injection: 2; Processed Channel Descr. PDA 280.0 nm
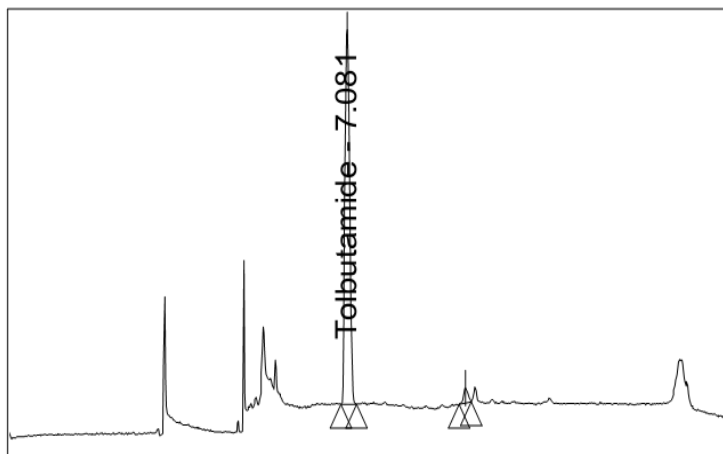

Sample Name: LAF pH 1.8 sample; Date Acquired: 2/25/2010 11:38:23 PM; Vial: 10; Injection: 1; Processed Channel Descr. PDA 209.8 nm
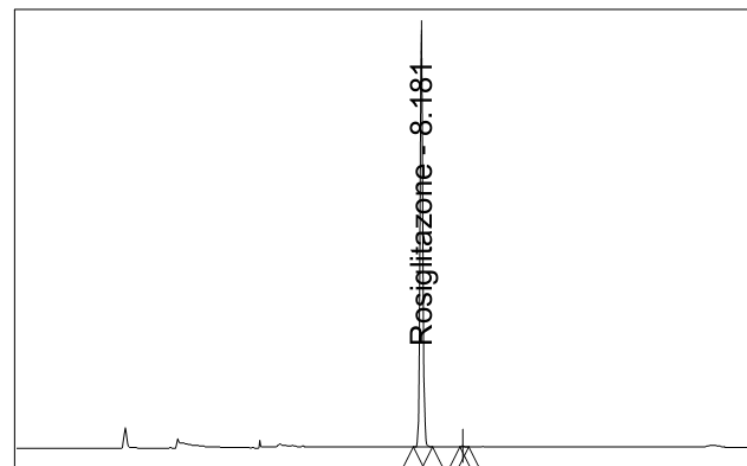

Sample Name: Roflumilast 2µg on column ; Date Acquired: 11/15/2008 1:56:46 AM; Vial: 34; Injection: 1

163

Project Name: Training2010_13

Tolbutamide - 7.081

Sample Name: Tolbutamide 0.5 mg/mL;   Date Acquired: 1/24/2010 6:40:05 PM;   Vial: 27; Injection: 1; Processed Channel Descr. PDA 260.0 nm

Project Name: Training2010_13

Rosiglitazone - 8.181

Sample Name: Rosi 0.5 mg/mL;   Date Acquired: 1/23/2010 9:22:01 PM;   Vial: 99; Injection: 1; Processed Channel Descr. PDA 250.0 nm

APPENDIX III: LIST OF PUBLICATIONS AND POSTER PRESENTATIONS

Related to Thesis

1) Integration of physicochemical and pharmacokinetic parameters in lead optimization: A physiological pharmacokinetic model based approach, Current Drug Discovery Technologies, 2010, 7: 143-153

2) Metabolic interaction potential of arterolane (RBx 11160), a new anti-malarial compound with rifampicin and antiretroviral agents. Poster presentation at IPS December 2007

3) The Relevance of Pharmacokinetic Modeling and Optimization in Drug Discovery Screening: Integration of *In vitro* ADME Data, poster presentation, National conference on emerging trends in life sciences research. March. 6-7, 2009, BITS, Pilani.

4) The observed correlation between in vivo clinical pharmacokinetic parameters and in vitro potency of VEGFR2 inhibitors-Can this be used as a prospective guide for development of novel compounds? Arzneimittelforschung, 2012, 62(4):194-201.

Other Publications

5) A-drug-drug interaction study of everolimus (an mTOR inhibitor) and JI-101, an orally active inhibitor of VEGF 2, PDGF and EphB4 receptors, in patients with advanced urologic tumors, 2011, ASCO general Meeting (abstract e 15077)

6) Approaches towards the development of a chimeric DPP4/ACE inhibitor for treating metabolic syndrome. Seventeenth Annual Symposium, New Delhi, February 2011, Ranbaxy Science Foundation

7) RBx-0597, a potent, selective and slow-binding inhibitor of dipeptidyl peptidase –IV for the treatment of type II diabetes, European Journal of Pharmacology 2011, 652:157-163

8) Identification of Novel Orally Active Dipeptidyl Peptidase IV Inhibitor 7E8E80B, Equipotent and Equi-efficaceous to Januvia^{TM}, poster presentation IPS 2008

9) MNR 88281: A novel, potent and sage PDE4 inhibitor, Poster presentation, Gordon Research Conference 2008

10) Enhanced expression of recombinant proteins utilizing a modified baculovirus expression vector, Molecular Biotechnology 2010, 46: 80-89.

11) HPLC method for determination of rosiglitazone in human plasma and its application in a clinical pharmacokinetic study, Drug Research 2002, 52: 560-564.

12) Simple Method for the determination of Rosiglitazone in human plasma using a commercially available internal standard, biomedical chromatography 2003 17: 417-420

13) Open access generic method for continous determination of major human CYP 450 probe substrates metabolites and its application in drug metabolism studies. Xenobiotica, 2003, 12: 1233-1245.

APPENDIX IV: BRIEF BIOGRAPHY OF SUPERVISOR

Dr. Nuggehally R Srinivas, a trained pharmacist and clinical pharmacologist, is a drug development specialist with over two decades of pharmaceutical industry experience. Dr. Srinivas obtained his Ph.D in the field of stereoselective pharmacokinetics and pharmacodynamics from University of Saskatchewan, Canada. Dr. Srinivas spent over a decade working at Bristol Myers Squibb, USA engaged in leading a group in drug development across multi therapeutic areas. After his tenure in the USA, Dr Srinivas took a position at Dr. Reddy's Laboratories (Hyderabad, India) to strategize and operationalize global drug development for the various key discovery programs for over seven years. At Dr. Reddy's, his group was responsible for not only clinical candidate selection but creating a target product profile needed for product differentiation and carrying out clinical development to confirm human proof of concept in relevant patient population. In his current position as the Chief Executive of Vanthys, he is leading a diverse group of drug development specialists whose mission is to enable the attainment of proof of concept for some important assets in the chosen disease areas such as diabetes, oncology, pain/inflammation, lipid disorders etc. Dr. Srinivas has published over 175 research articles in international peer reviewed journals. He serves on the editorial boards of journals such as Journal of Clinical Pharmacology, Biomedical Chromatography, Bioanalysis and Current Pharmaceutical Analysis. His outstanding contribution in the field of clinical pharmacology has fetched him a nomination of Fellow of Clinical Pharmacology (FCP) from the prestigious American College of Clinical Pharmacology.

APPENDIX V: BRIEF BIOGRAPHY OF THE CANDIDATE

Biju Benjamin has basic training in Pharmaceutical Sciences from Dr. MGR medical University, Chennai and higher specialization in Pharmacology (M.Pharm) from College of Pharmaceutical Sciences, Manipal.

Biju Benjamin has 13 years of experience in working with Pharmaceutical research. Initial research experience was with Vimta Labs, Hyderabad with focus on Bioanalyis and clinical sample analysis as well as drug product analysis. Subsequently the exposure to drug discovery research was obtained in Dr. Reddy's Research Laboratories. As part of M.Pharm program, Biju specialized in animal experimentation and preclinical models on diabetes, some areas of inflammation and CNS disorders, as well as statistical analytical techniques. Considerable experimental skills and theoretical background was developed during the tenure in Dr. Reddy's in *in vitro* and *in vivo* pharmacokinetic studies and bioanalysis. Subsequently the role was broadened being part of the research team in Ranbaxy Research Laboratories with involvement with multidisciplinary discovery teams for seven years. Key focus areas included drug discovery screens with high end automation (robotic screening systems, automated sample clean up, centralized data integration and analysis) specialized cell based assays including primary cells, integration with pharmacological data as well as interfacing with medicinal chemists. Additionally there was some focus on early developmental assessments and drug interaction studies. In his current position at Vanthys Pharmaceutical Development, Biju has further widened his research interests in developability assessments of clinical candidates, development of PK-PD models with preclinical pharmacology and pharmacokinetic data, prediction of human doses and PK profiles from preclinical data as well as clinical PK-PD analysis using phase I and phase II data. Biju has 8 international publications and 5 posters published during his tenure. Biju has received formal training in PK-PD modeling at the intermediate level (WinNonlin training, Pharsight Corporation). Major research interests include pharmacokinetic-pharmacodynamic modeling, physiological based pharmacokinetic models and integrated approach to drug discovery and early drug development.